Millimeter Wave Photonics: Design, Integration and Application

Dennis Prather, Professor

Department of Electrical and Computer Engineering

Outline

- Overview of RF imaging
- Optical phase modulators
- Ultra-wideband frequency synthesis
- RF photonic module integration
- Silicon Nanomembranes for 3D RF signal routing
- Summary

RF Imaging

Imaging Across the EM Spectrum

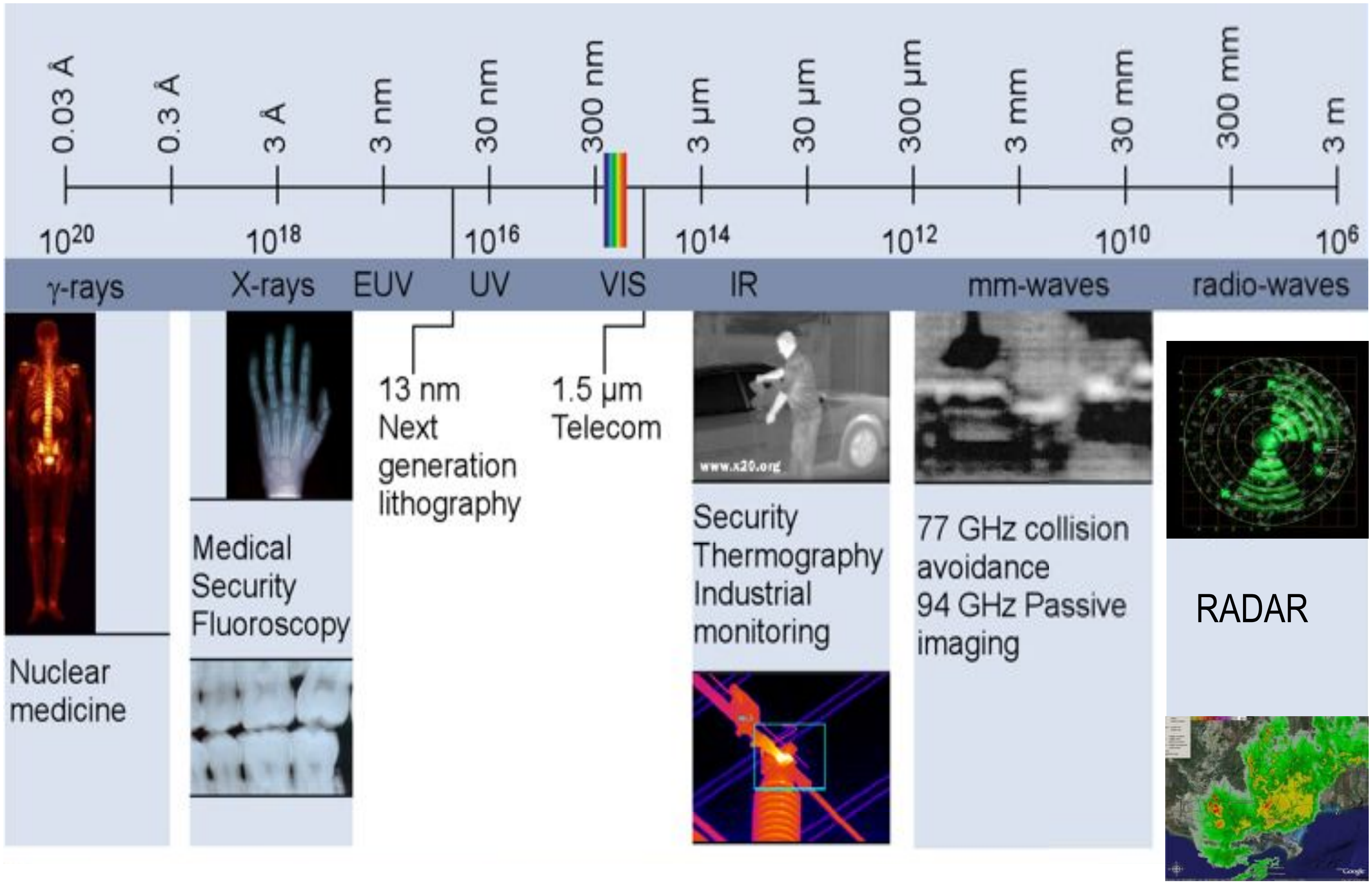

Advantages of Passive mmW Imaging



- Provides *all-weather, day/night imaging* including cloud, fog, smoke, and dust penetration.
- "Cold" sky delivers *high effective contrast* for many man-made targets independent of most camouflage.
- Systems operate using passive detection enabling *covert operation*.
- *Blowing dust/sand has minimal impact* on "passive" mmW for brownout distance scales.
- Imagery is *easily interpreted* by operator as it is similar to FLIR .


Atmospheric Attenuation in the EM Spectrum

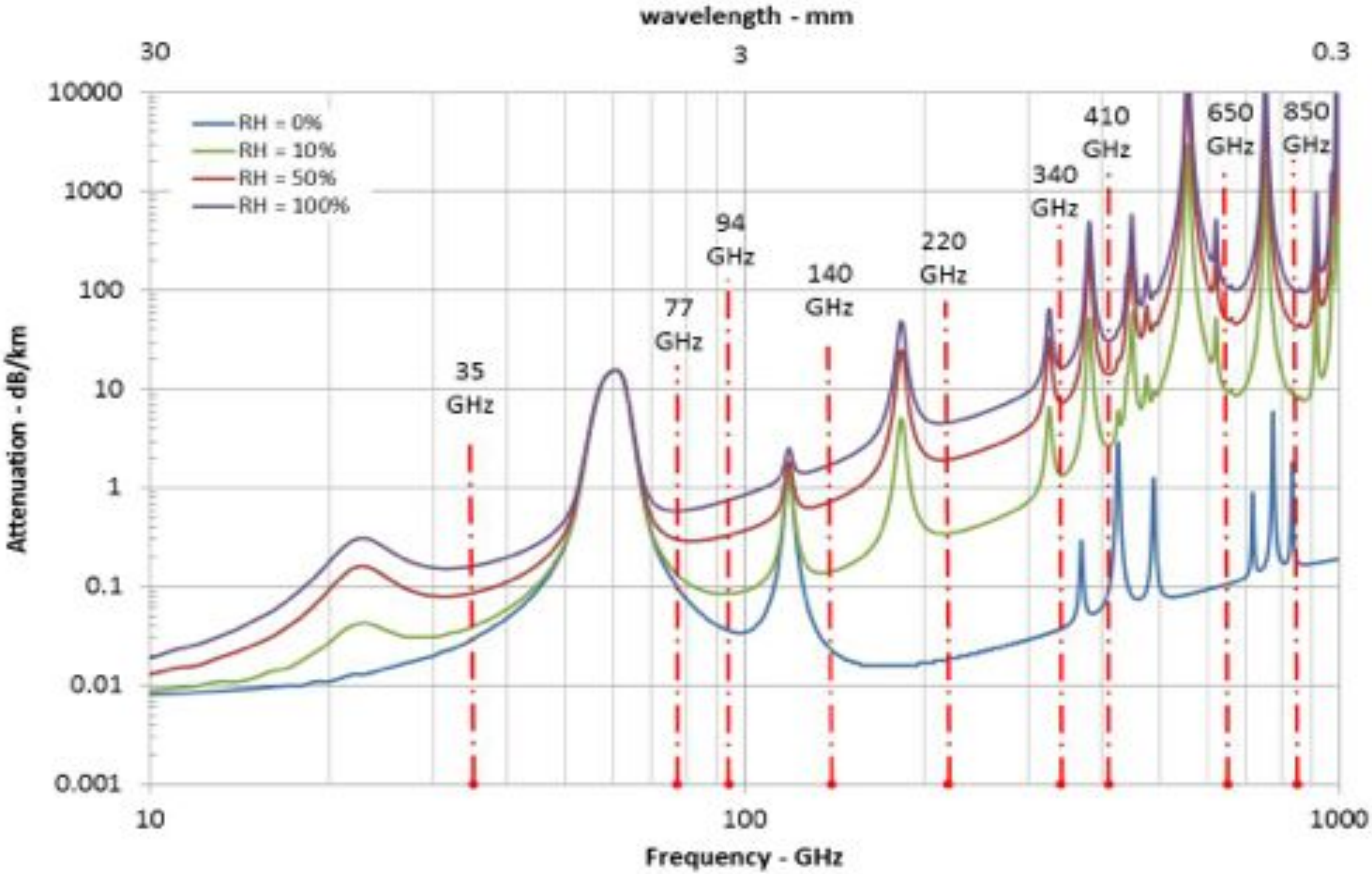

Limitations of Real Imagers

- Maximum resolution of **ANY** imaging system is proportional to the wavelength over maximum aperture diameter.

35-GHz image (60 cm aperture)

95-GHz image (60 cm aperture)

Visible image (2 cm aperture)

$$\theta \sim \frac{\lambda}{D}$$

Increasing frequency/ enhanced resolution →

For "see-through" operation, achievable resolution will be limited by the practical size of aperture that can be found on platform.

Primary Technology Barriers

- Sensitivity:
  - Eight orders of magnitude less power emitted at mmW than in IR wavelengths.
  - Currently requires a large degree of up front gain (LNA's), cryogenic cooling, or long averaging times. (*high cost per element*)
- Resolution:
  - Physical limitations imposes severe resolution constraints for aperture sizes feasible in most applications.
  - Most imager designs require volumetric scaling to increase resolution and require contiguous space for placement. (*very large SWaP*)

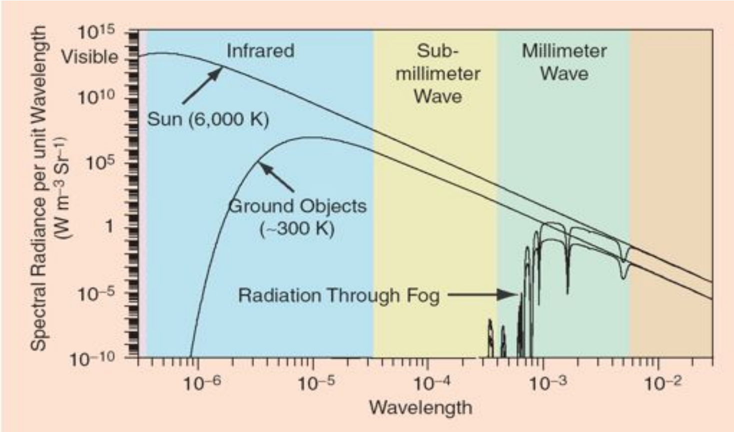

[Yujiri et al. IEEE Mic. Mag. , Sep. 2003]

Northrop-Grumman (TRW) MMW imaging camera
Weight: 600 lbs, for 0.5 m aperture (~0.5° resolution)

Our design uses optical enabled, distributed aperture to minimize part count and greatly reduce size and weight.

2D vs 3D Scaling Technology

We use a distributed aperture imaging (DAI) approach over a standard focal plane array (FPA). An FPA requires a lens, larger volume, and an expensive mmW detector for each pixel.

Advantages of DAI:

- increased resolution without a lens and the volumetric scaling of size and weight
- field amplitude and phase is captured at discrete points
- enables a flat or conformal, high resolution imaging system
- lower number of millimeter wave components needed

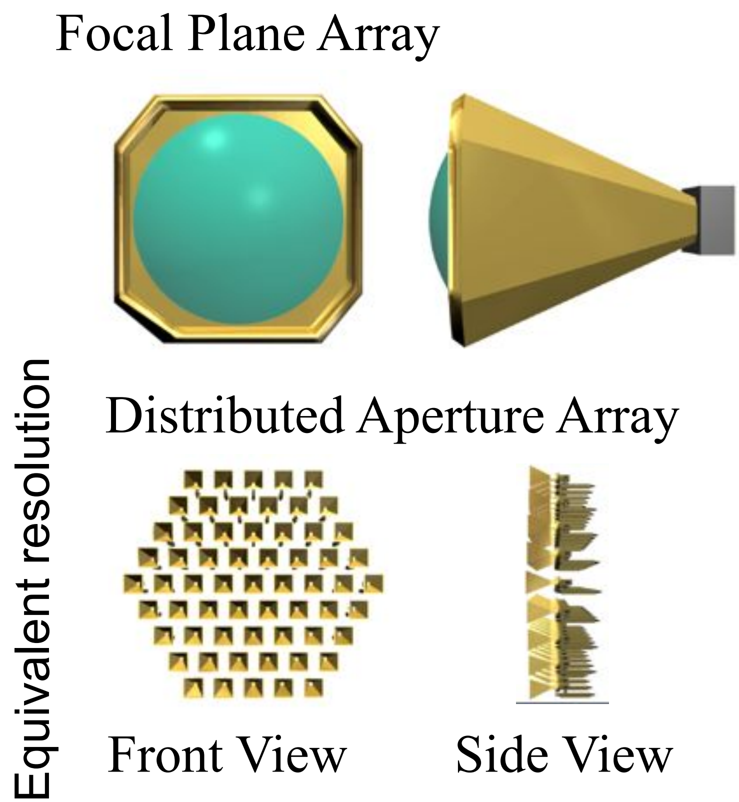

Optical Upconversion Phase Preservation

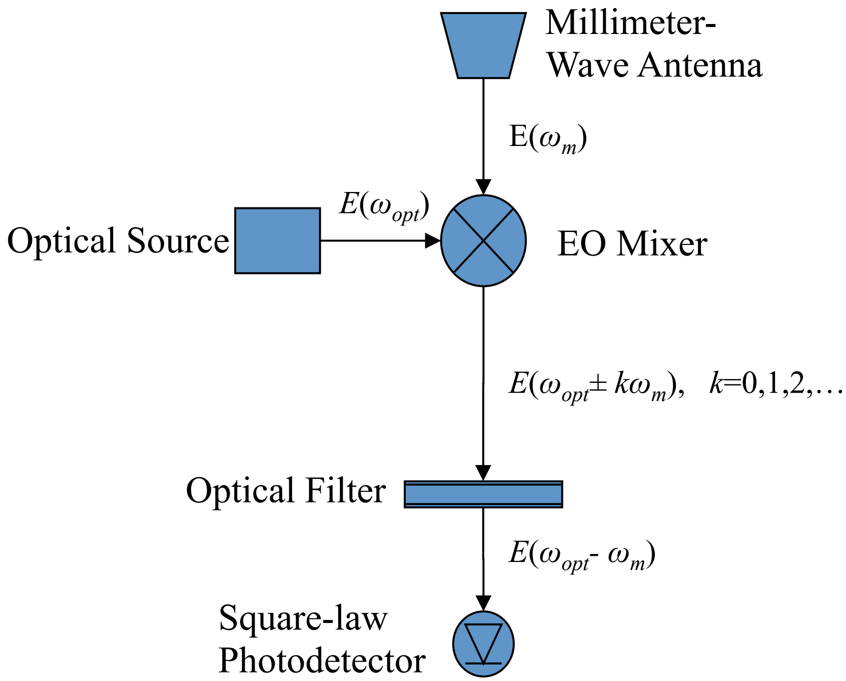

Incident millimeter-wave field

$$E_m \cos\left(\omega_m t + \phi_m\right)$$

Induced phase change in optical field

$$\Delta\phi = mE_m \cos\left(\omega_m t + \phi_m\right)$$

Optical field at modulator output

$$E_o = E_{opt}\, \mathrm{e}^{j\omega_{opt}t + j\Delta\phi} = E_{opt}\, \mathrm{e}^{j\omega_{opt}t + jmE_m\cos(\omega_m t + \phi_m) + j\phi_{opt}}$$

First sideband of optical field

$$E_{o,FSB} = jE_{opt}\, \mathrm{e}^{j\omega_{opt}t} J_1\left(mE_m\right)\mathrm{e}^{j\left(\omega_m t + \phi_m + \phi_{opt}\right)}$$

Small signal approximation yields

$$E_{o,FSB} = \frac{jmE_{opt}}{2} E_m \left(\mathrm{e}^{j\left(\omega_{opt} + \omega_m\right)t + j\phi_m + j\phi_{opt}}\right)$$

Amplitude Scaling — Frequency Scaling — Millimeter-wave Phase

The optical field is proportional to the incident complex millimeter-wave field scaled in amplitude and frequency.

mmW Detection: Optical Upconversion

- Mapping mmW signals onto optical carriers using an EO modulator enables optical photodetection.
- Technique has demonstrated sub-picowatt noise-equivalent powers without cooling or low-noise
- Phase preservation allows for interferometric (or distributed-aperture) imaging.
- Phased array enables electronically controlled focusing and scanning.

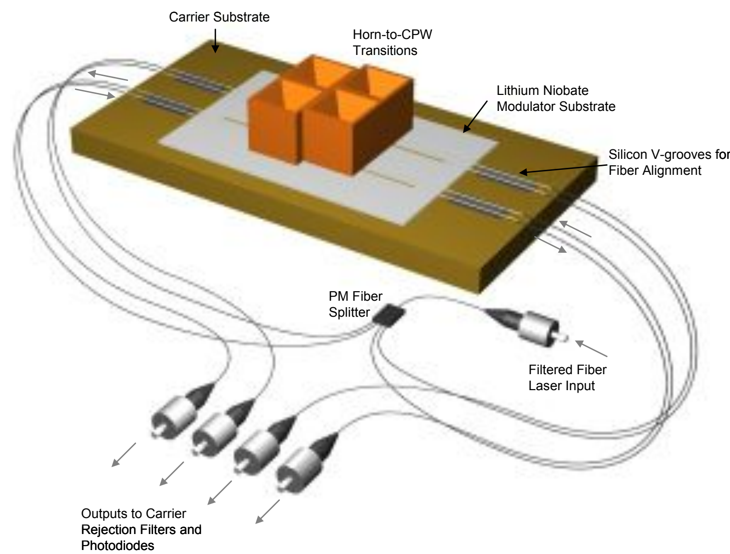

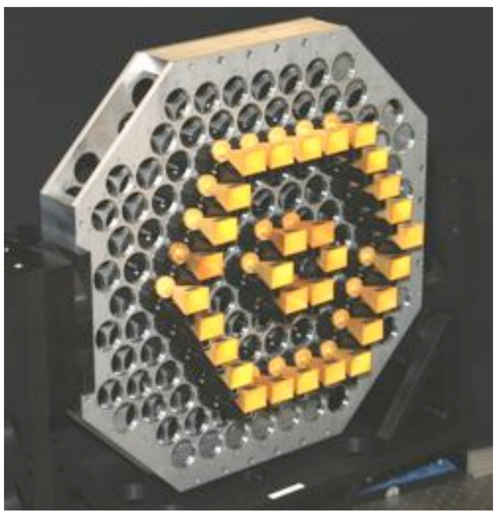

Interferometric imaging reduces size and allows for conformal mount

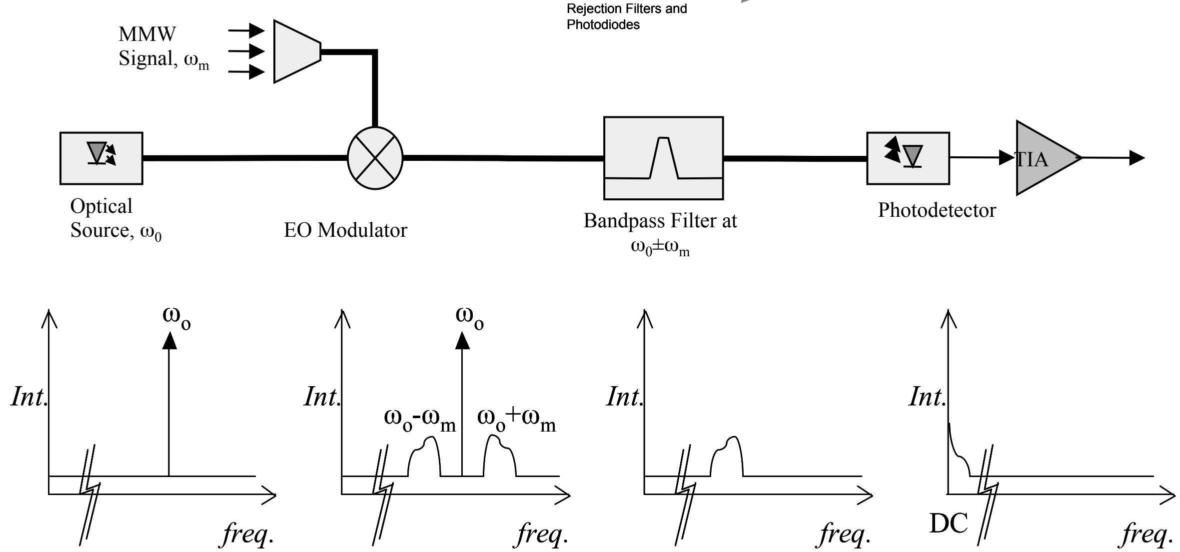

Optical Upconversion Phased Array

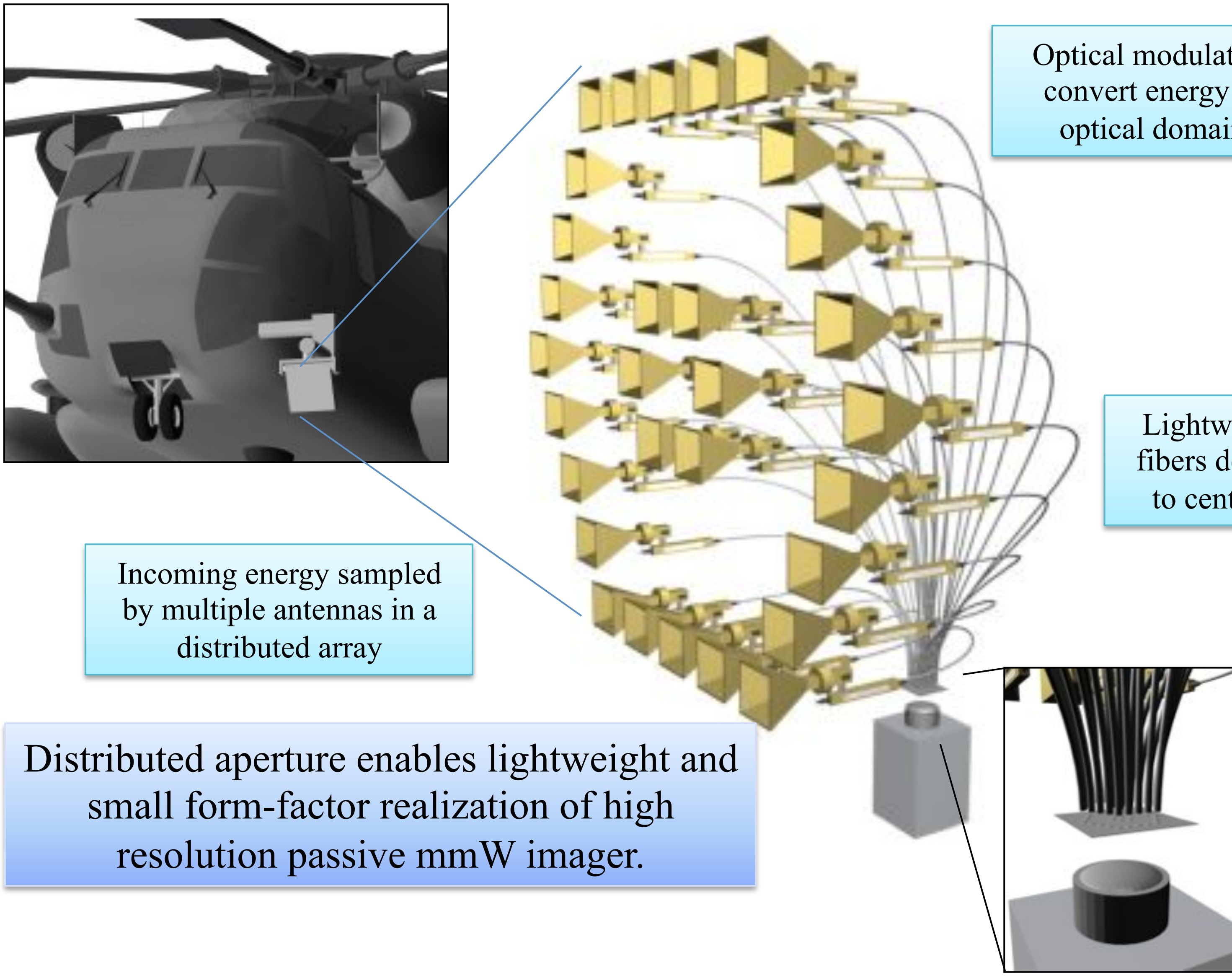

Distributed aperture enables lightweight and small form-factor realization of high resolution passive mmW imager.

Optical Upconversion Flow

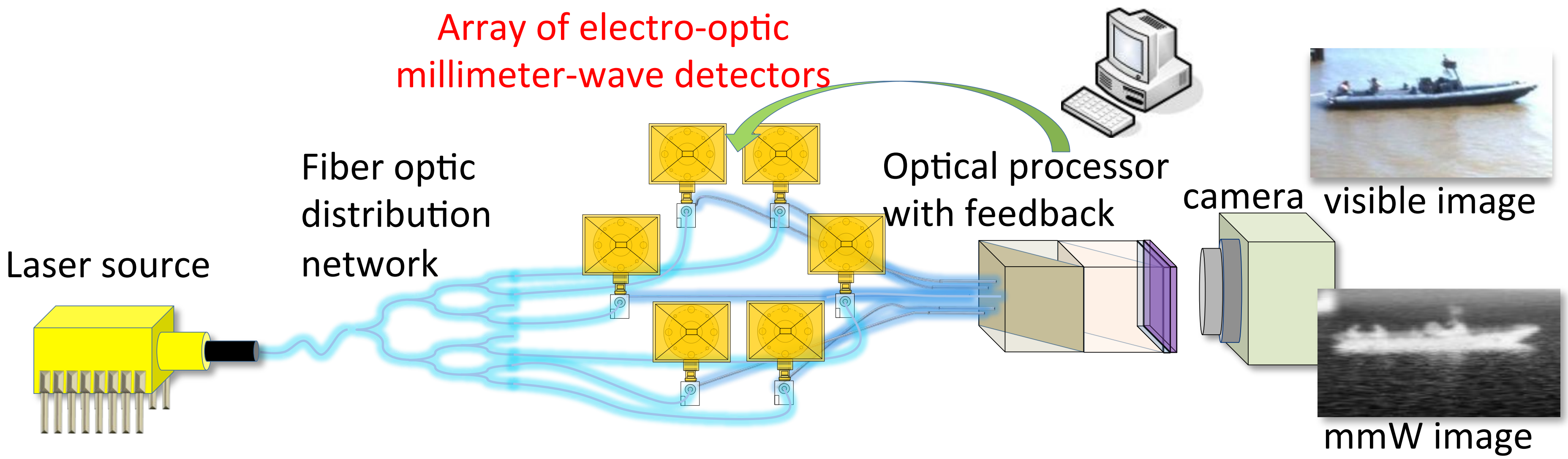

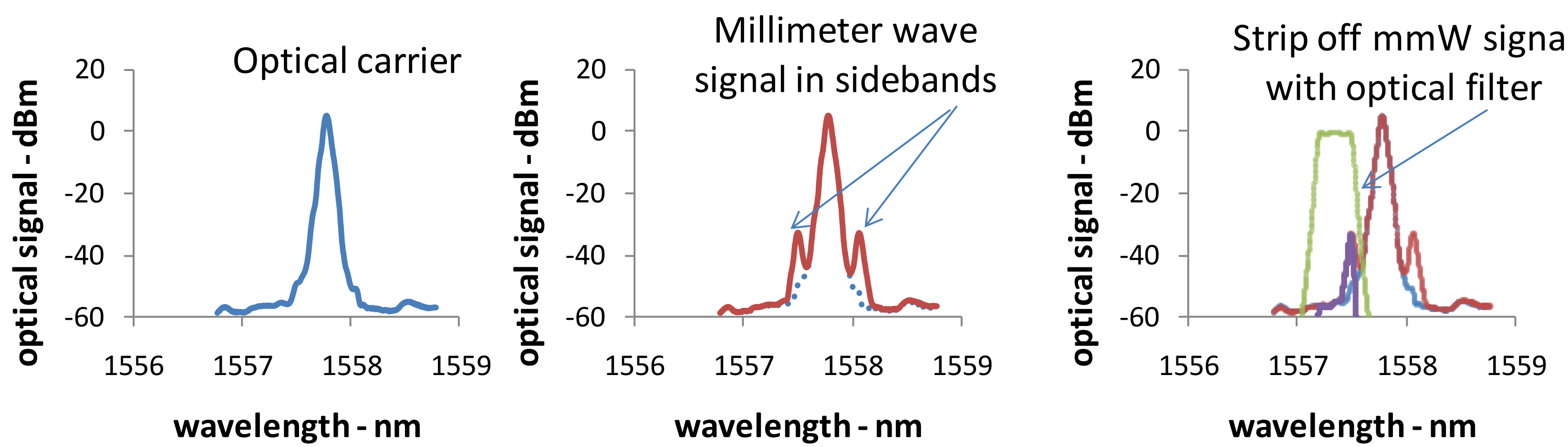

Optical processor stabilizes phase of each channel and enables electronic image enhancement techniques such as electronic focus/steering and super-resolution.

Passive mmW Phased Array Imager

We have demonstrated a video rate (15 fps) 35 GHz passive imaging system

Visible mmW image

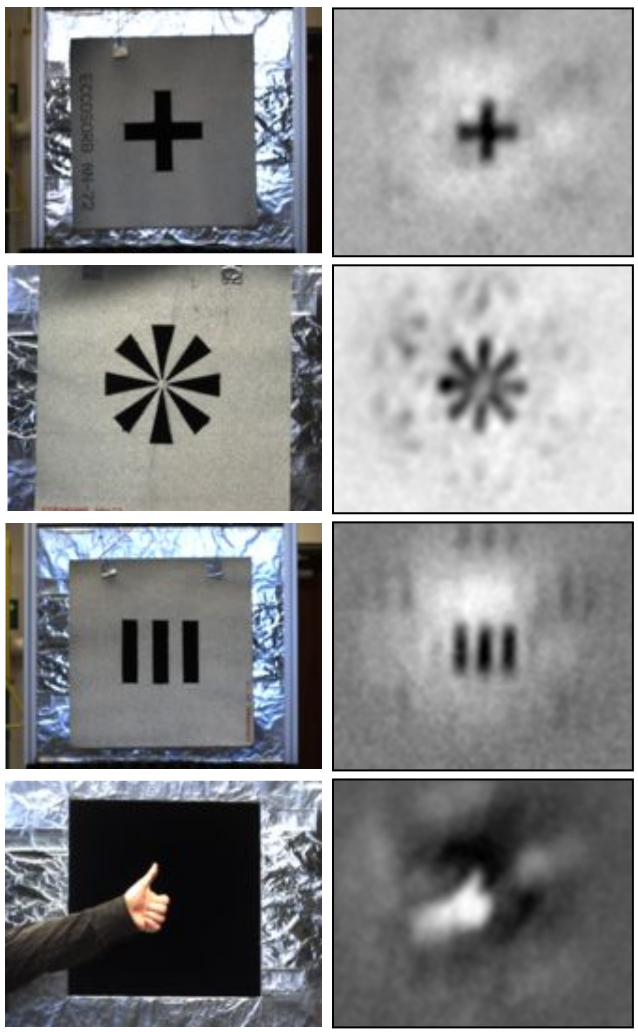

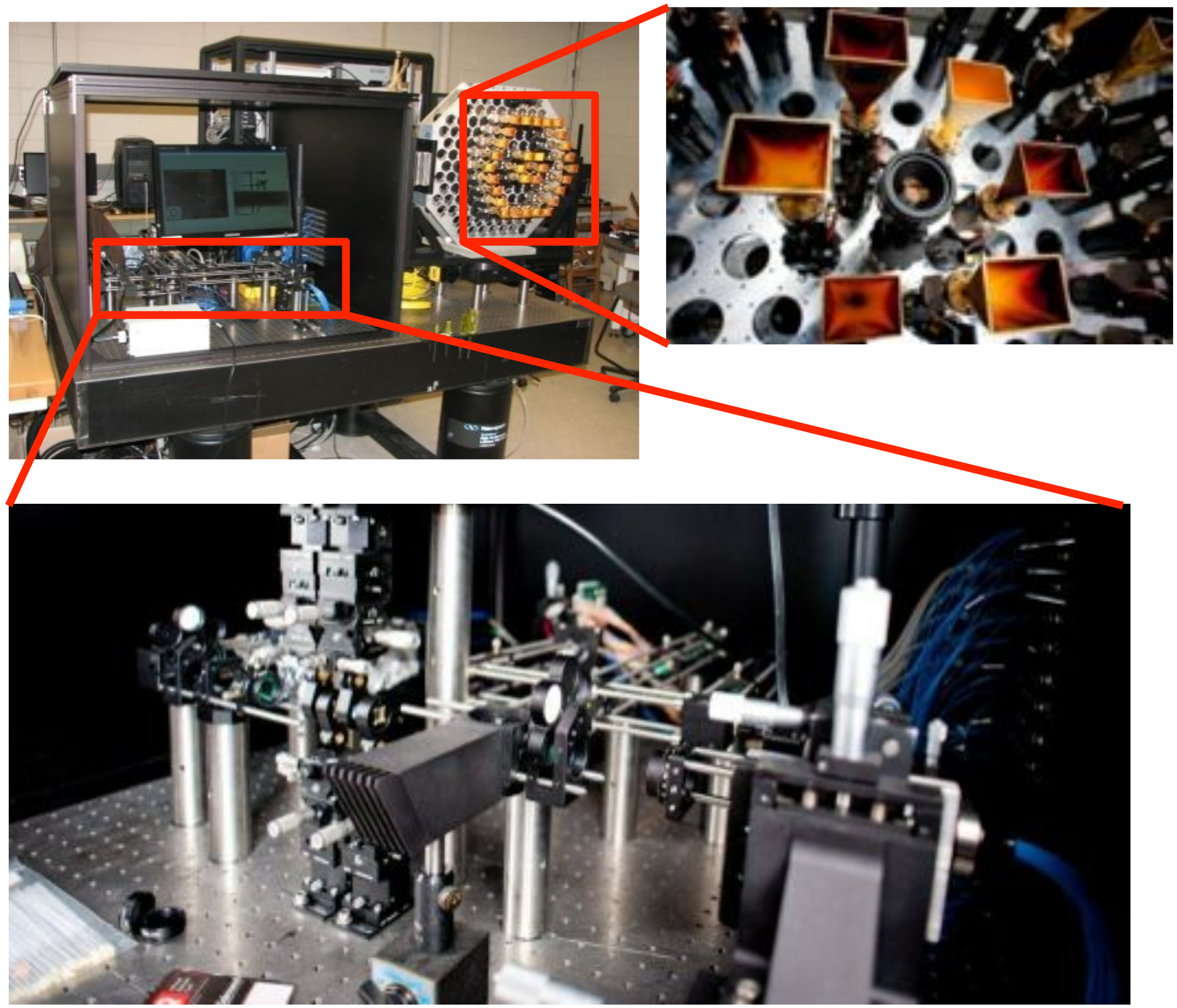

Hand Passive Video

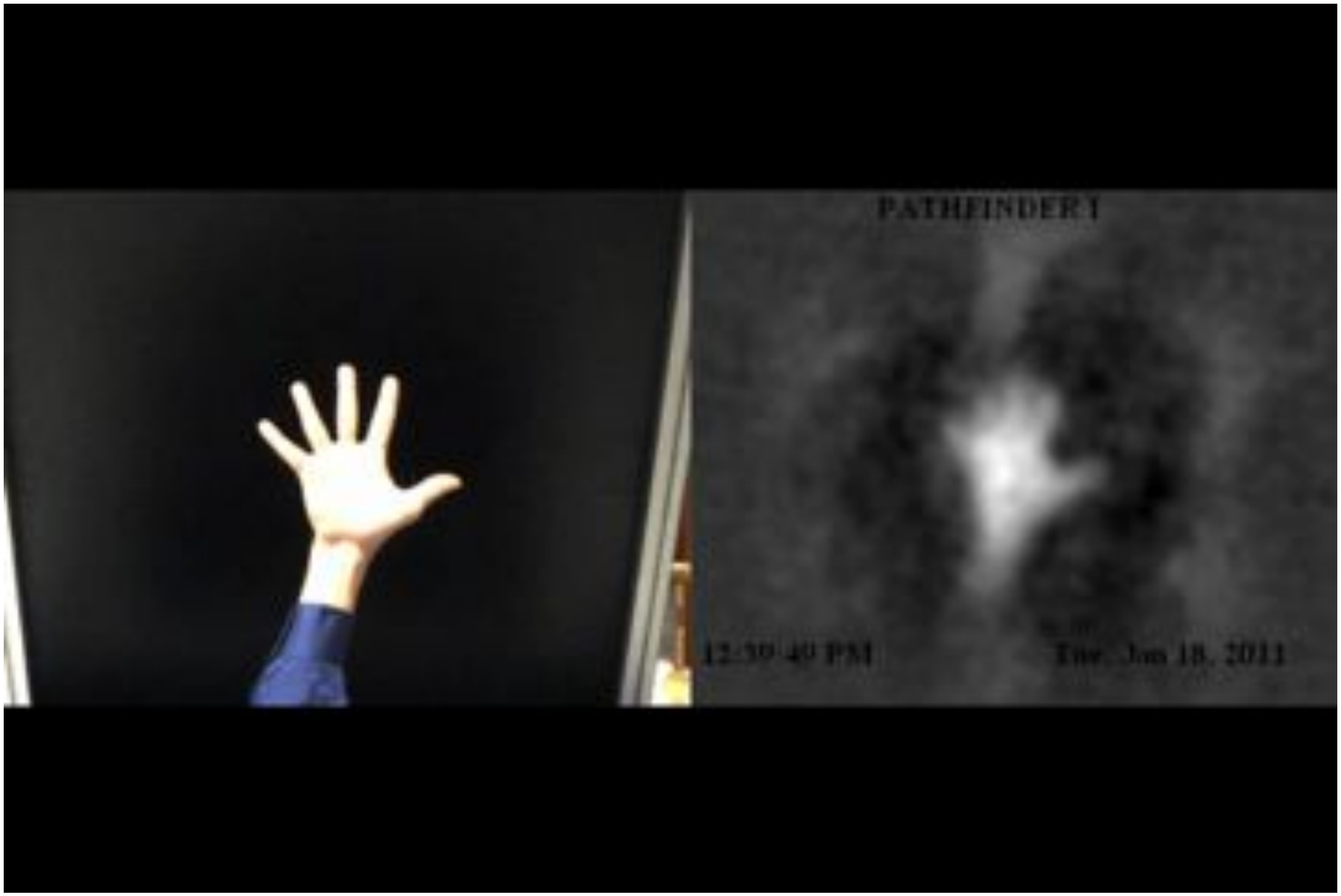

Resolution Target Passive Video

Passive W-Band Field Test Images

Scanning Imaging System

- Single-pixel scanning cart based on optical upconversion.
- Operational frequency ~95GHz.
- Noise equivalent temperature resolution of 2K.
- Diffraction-limited spatial resolution.
- Utilized for a variety of phenomenology studies, e.g., desert imaging

System Schematic

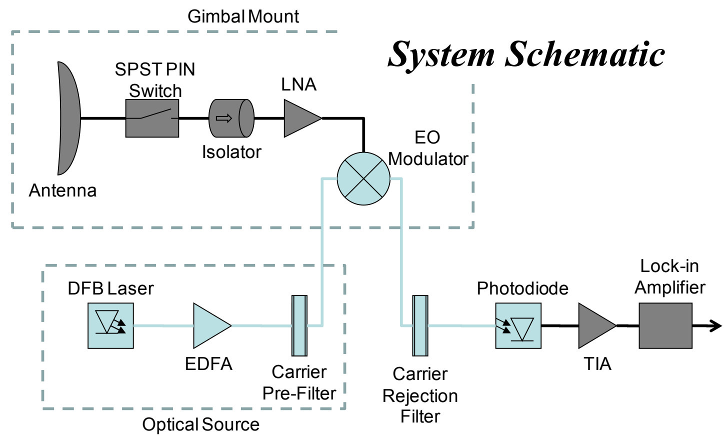

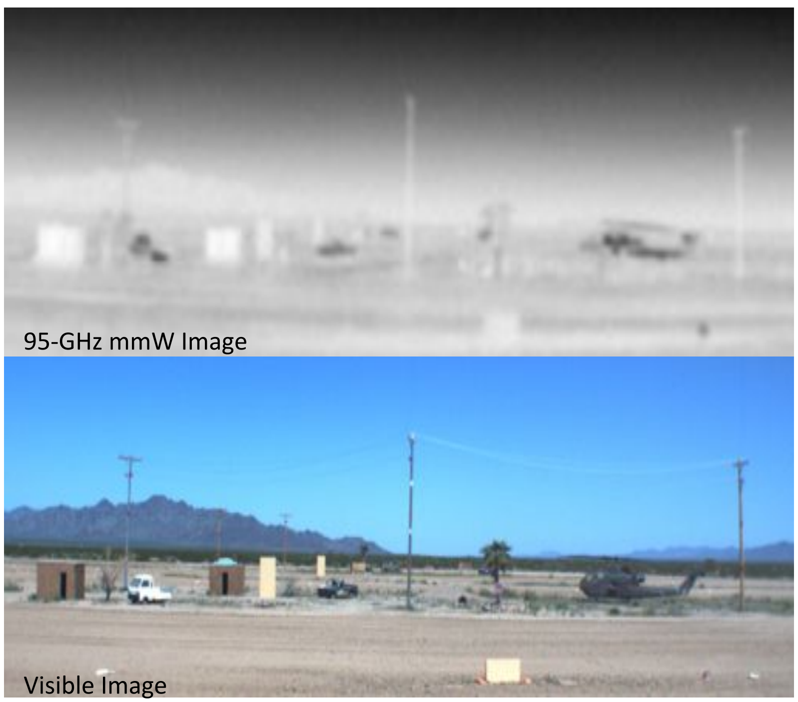

Imagery of Yuma, AZ

mmW (95GHz) and visible images

See through the hull of boats

Foot prints in the sand and cell phone in pocket

Field Measured Obstacles

Visible | mmW (W-band)

Pickup Truck

AH-1 Helicopter

Field Measured Obstacles

Visible | mmW (W-band)

2' Diameter Holes

Rock on dirt

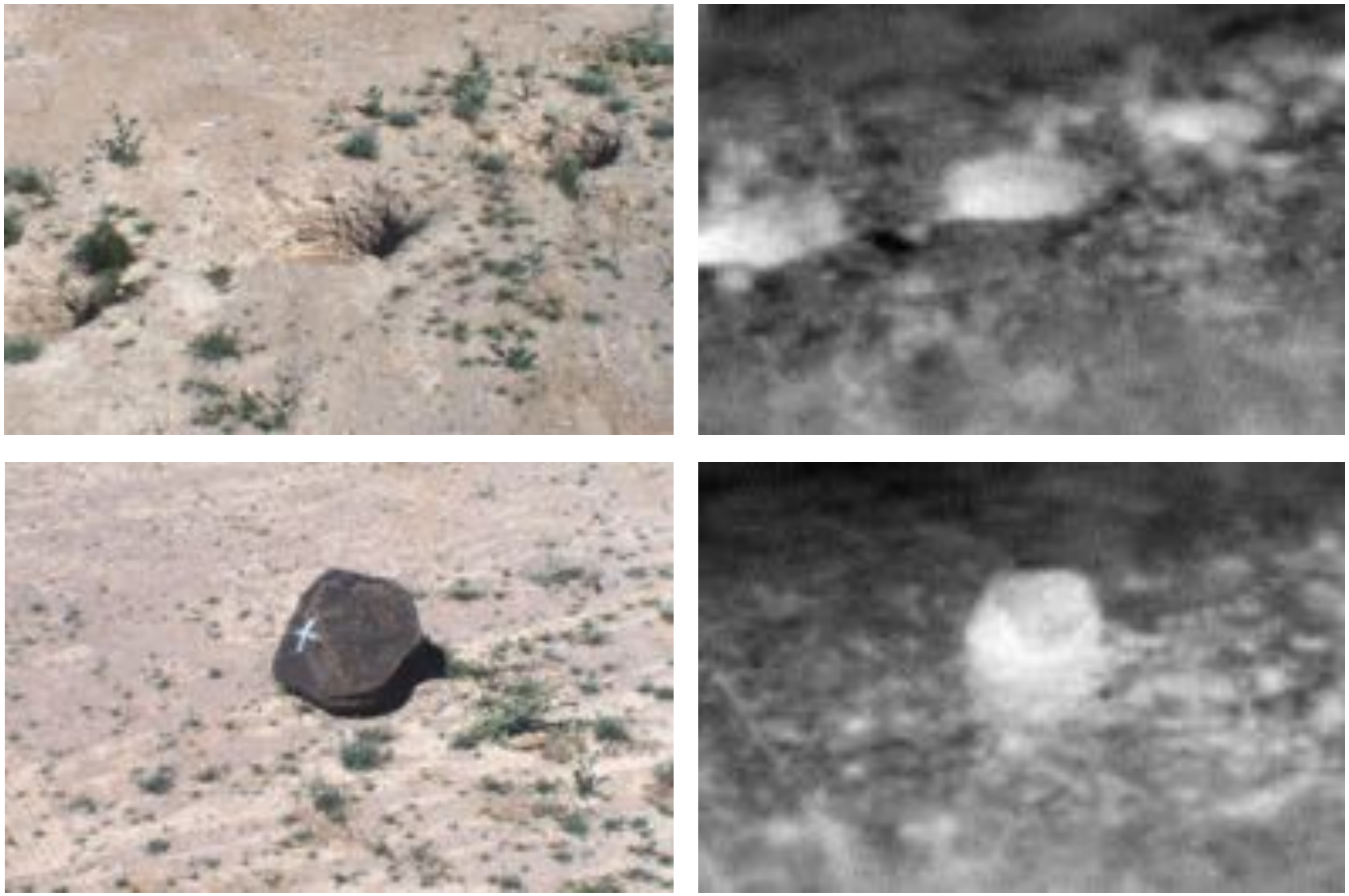

Field Measured Obstacles

	Visible	mmW (W-band)
6” Brick		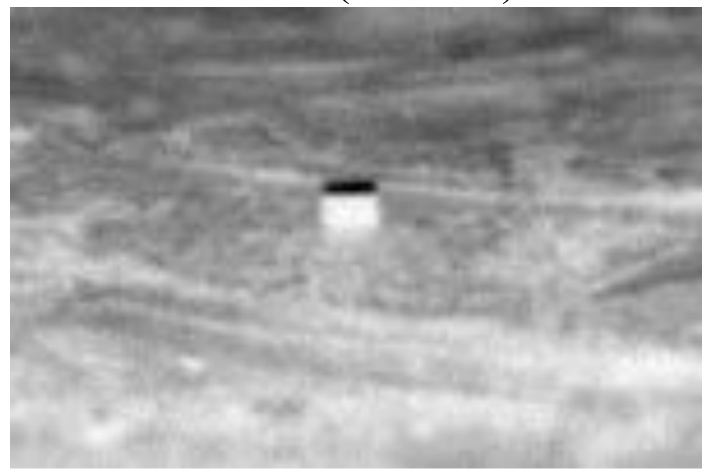
Stack of bricks		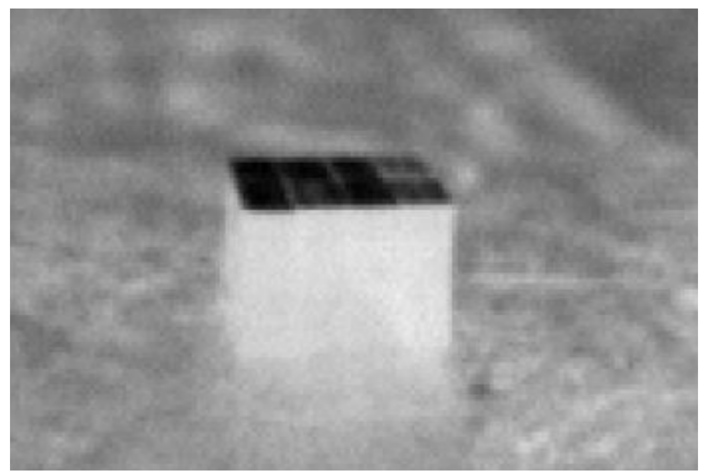

Field Measured Obstacles

Visible | mmW (W-band)

Person with caulking gun

Concrete Telephone Pole

Field Measured Obstacles

Visible | mmW (W-band)

Wooden Posts with Wire

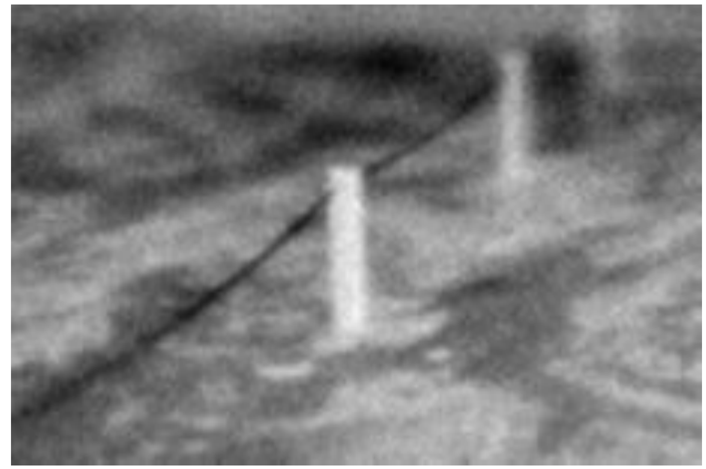

3/8” and 1” Wire

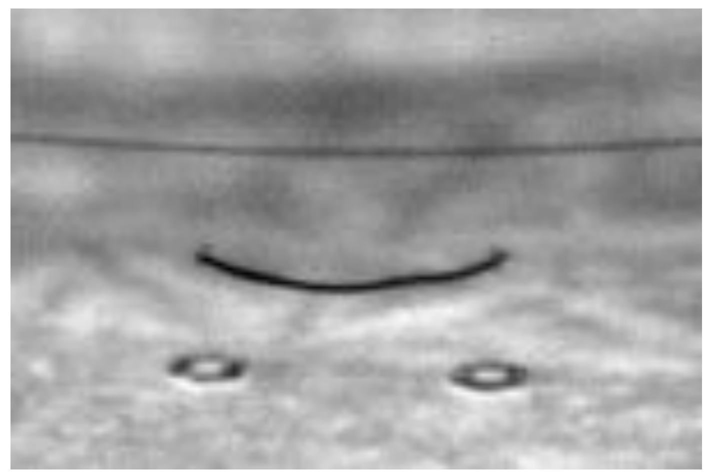

Field Measured Obstacles

	Visible	mmW (W-band)
Adobe Hut		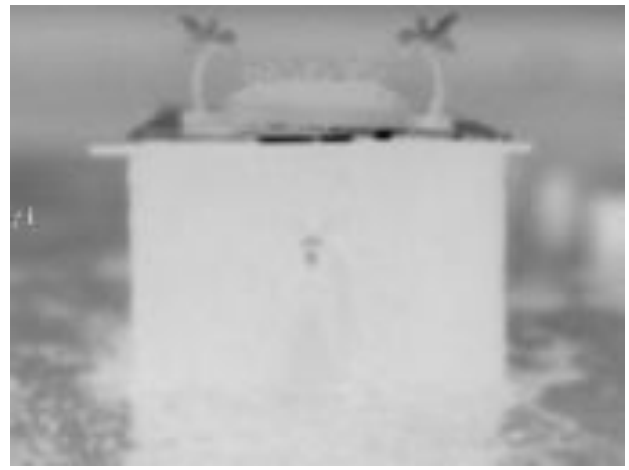
Brick building		

Field Measured Obstacles

Visible

mmW (W-band)

Field Measured Obstacles

Visible

mmW (W-band)

Field Measured Obstacles

Visible | mmW (W-band)

Field Measured Obstacles

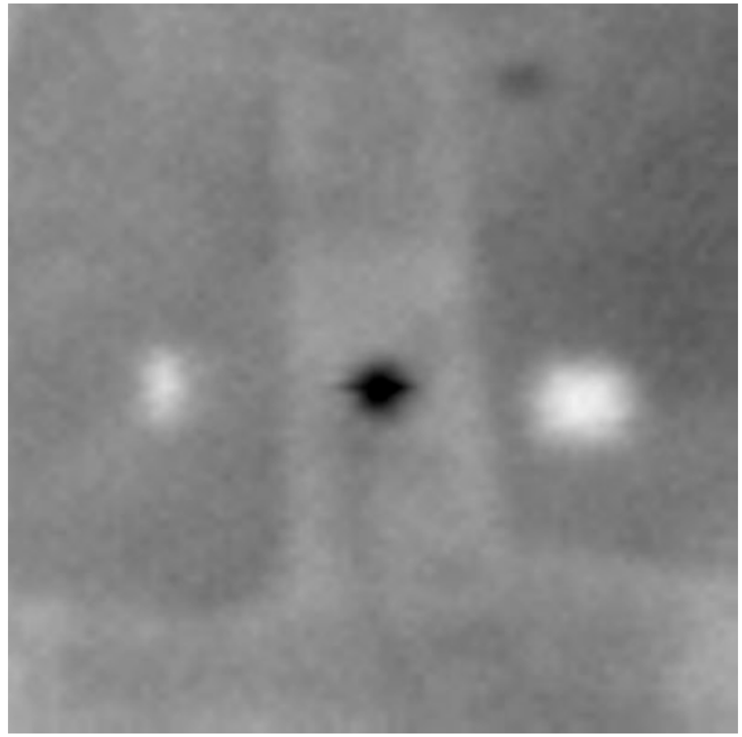

Range of 100 feet at a declination angle of 27°
Image of three targets on pavement:

- Pair of bricks on end presenting ~7”x6” target (left)
- 6” square aluminum plate (center)
- Cinderblock (right)

Can mmW's Penetrate Brownout?

UNIVERSITY OF DELAWARE 1743

UNIVERSITY OF DELAWARE

Imaging Through Obscurants

H-53 Helicopter at the
Yuma Proving Grounds

Dynamic Test Setup

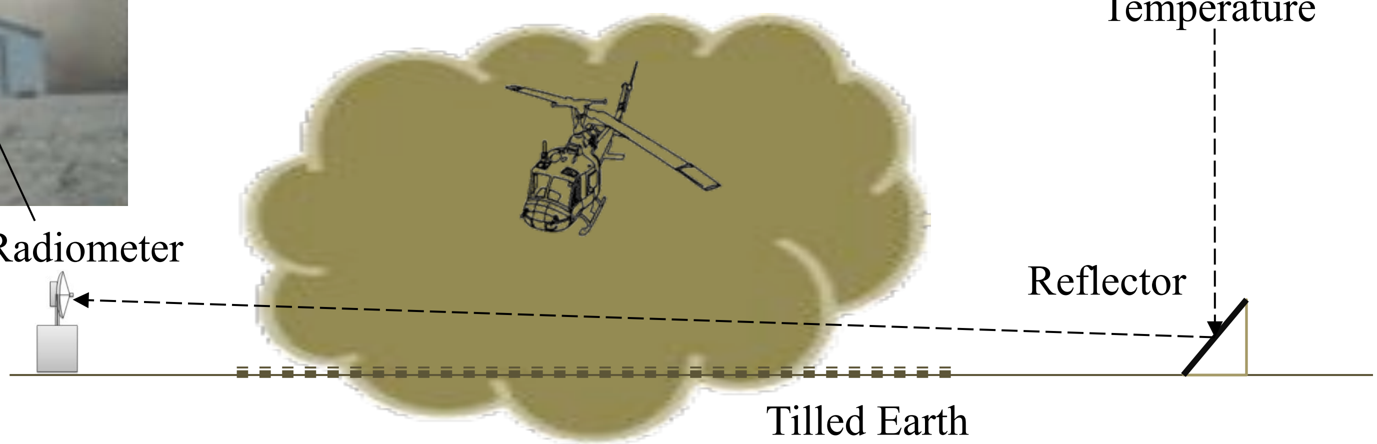

- Data consists of temporal recording of passive detector staring at cold sky reflector during several helicopter passes directly over view path
- Average height of view path ~1.5 m at a distance of 270’
- Both V and H polarizations recorded

Geometry of test provides higher losses than helicopter-mounted sensor will see.

The Problem - Video

IR and Visible Images in Brownout

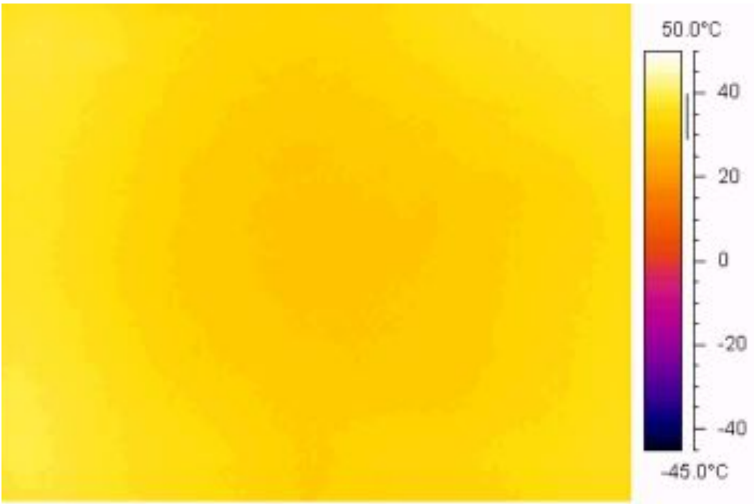

IR Image in Dust

Visible Image in Dust

Brownout Field Testing Results

mmW and visible images of 2' boulder, 2' diameter holes, and person in Oasis LZ

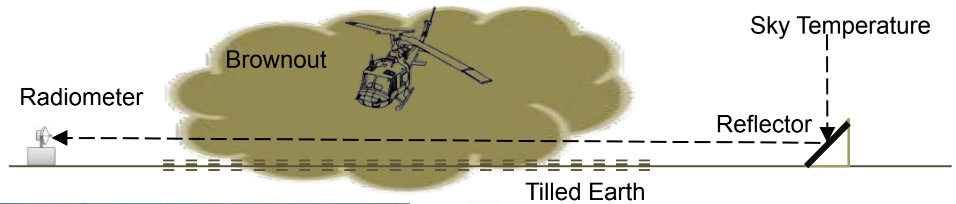

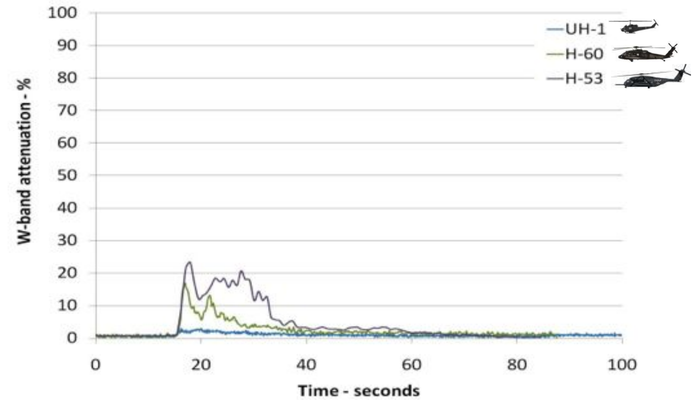

Flyover testing demonstrates less than 20% contrast reduction for H-53 brownout at target operational range of 150'.

- **Landing zone obstacles are clearly visible in mmW** for all measured obstacles
  - Average contrast on the order of 15°C for H-polarization for ground targets tested
- mmW **losses are low under all brownout conditions tested**
  - Average maximum values of loss during all flyover tests: 1% for UH-1, 8% for H-60, 20% for H-53 over 150' path

*Passive mmW presents **sufficient contrast** in desert environments and impact of even worst case **brownout attenuation is minimal**.*

How The Technology Works

mmW Detection: Optical Upconversion

- Mapping mmW signals onto optical carriers using an EO modulator enables optical photodetection.
- Technique has demonstrated sub-picowatt noise-equivalent powers without cooling or low-noise
- Phase preservation allows for interferometric (or distributed-aperture) imaging.
- Phased array enables electronically controlled focusing and scanning.

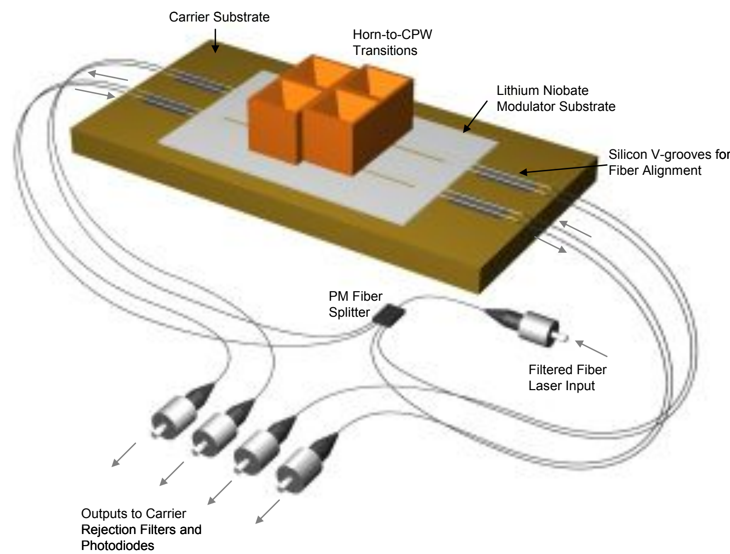

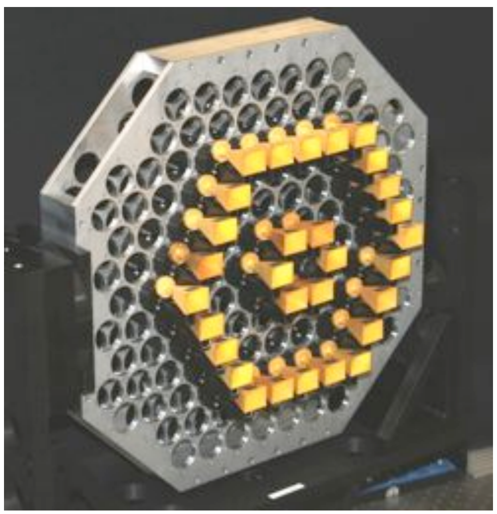

Interferometric imaging reduces size and allows for conformal mount

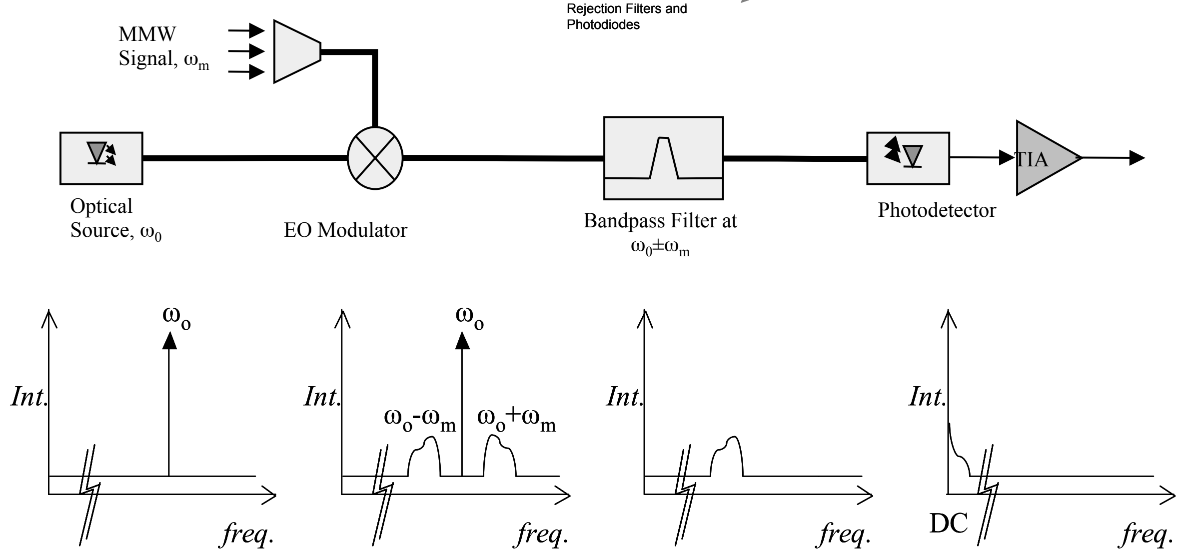

Antenna Array Fabrication

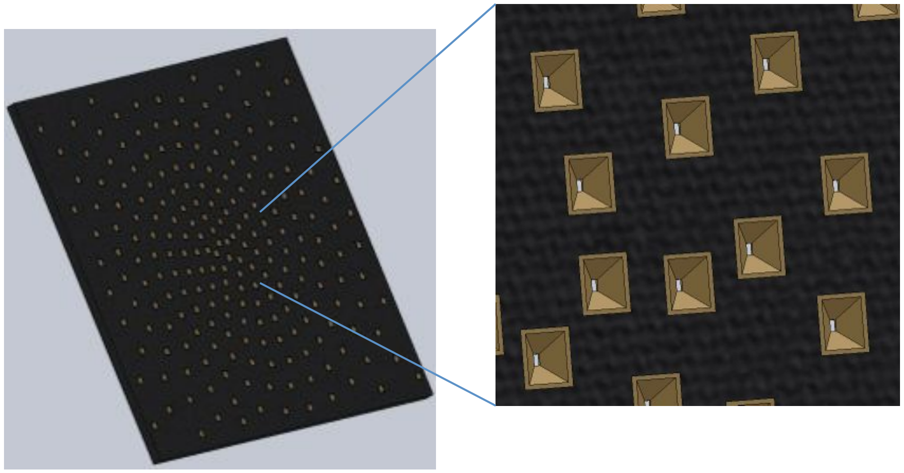

Antenna plate overview

- Antenna array fabricated from COTS horn elements embedded in carbon fiber, foam composite.
- Horn element backed by machined flange to mate to upconversion element.

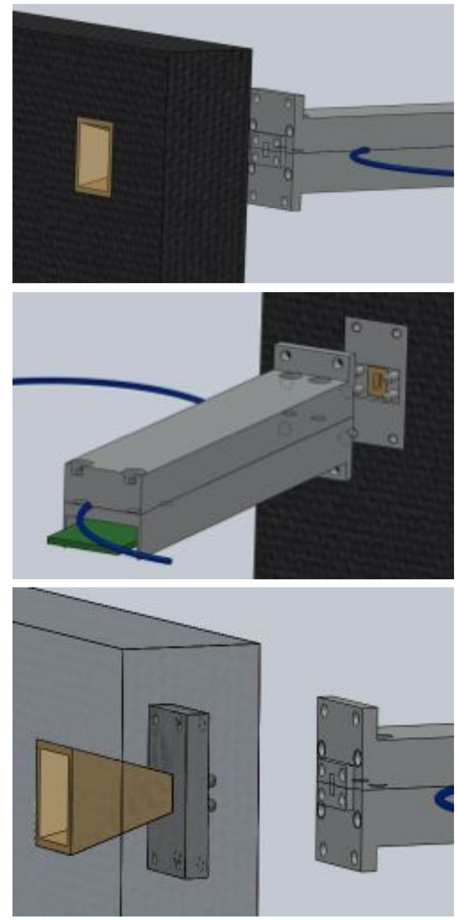

Upconversion module mating details

RF Modules

CPW to Modulator

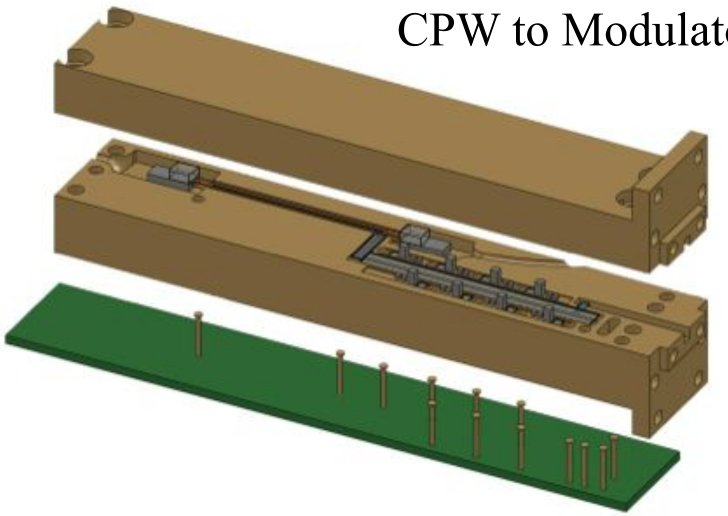

Front Gain Stage

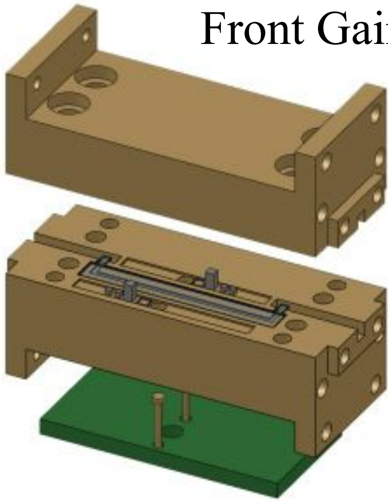

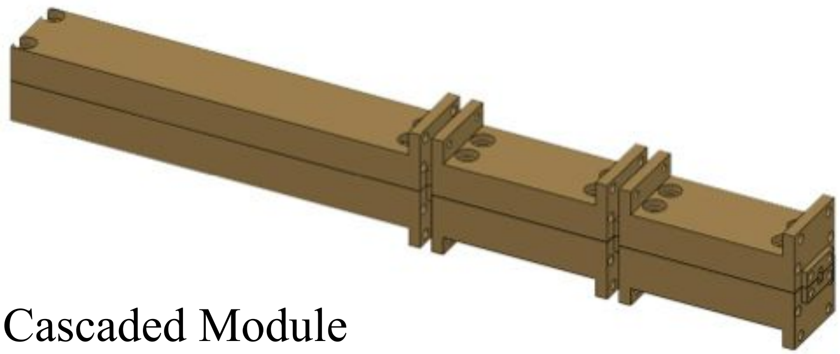

Cascaded Module

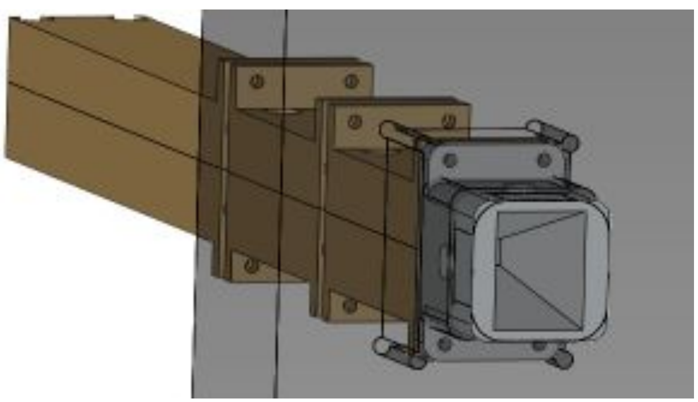

W-band antenna integration

mmW Module Integration

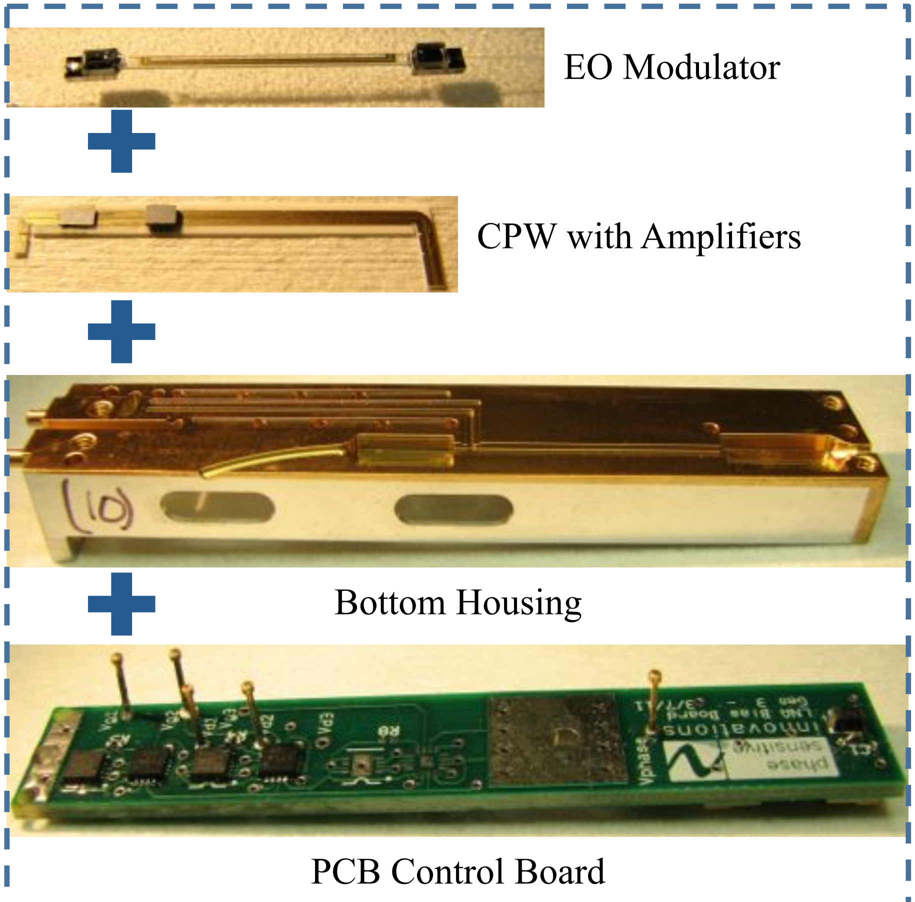

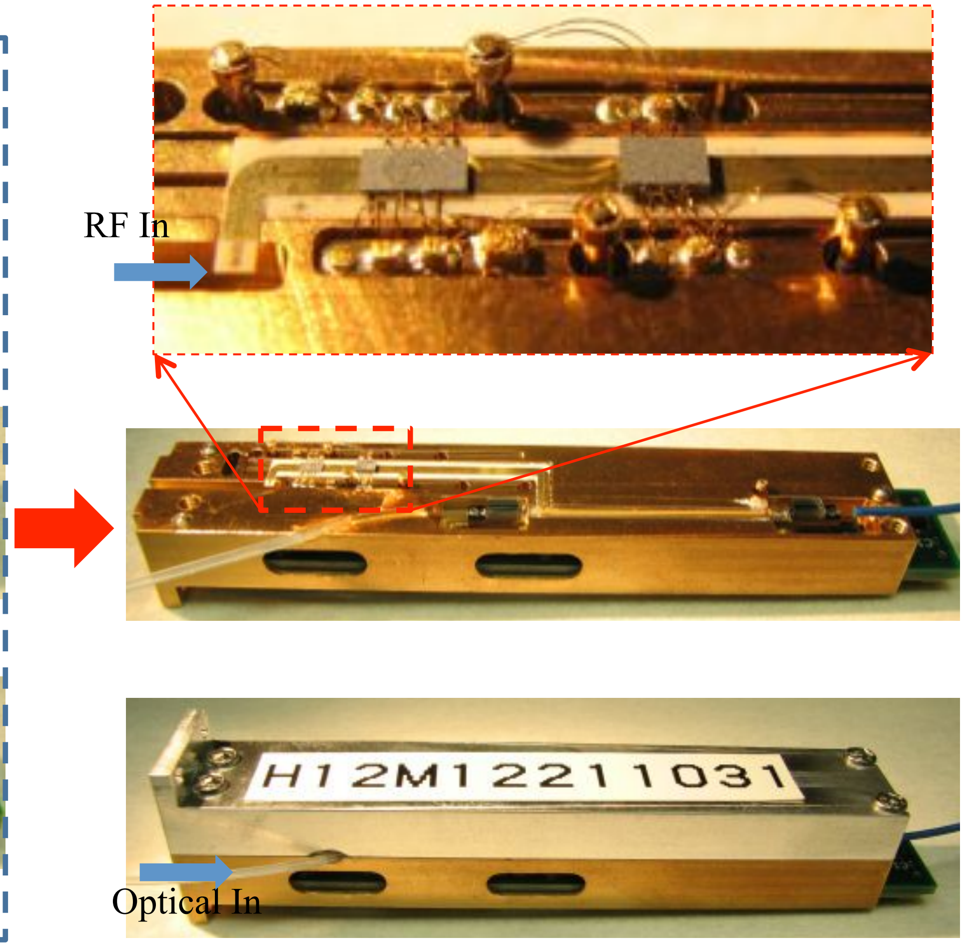

Detector module consists of metal housings, patterned alumina substrate, amplifiers, high speed EO modulator and PCB control board.

Fully integrated module with RF absorber filled top housing.

Integrated Detector Module

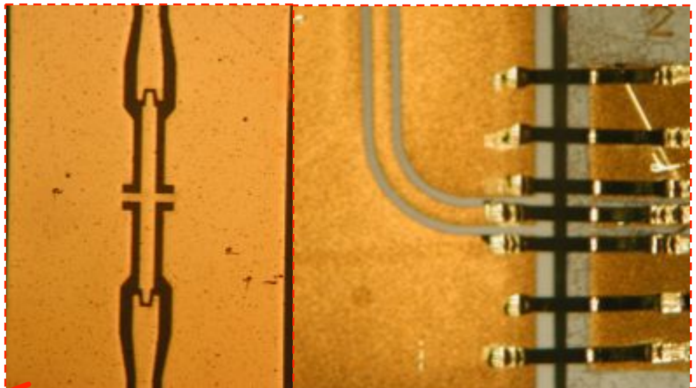

Wire bond transition and filter

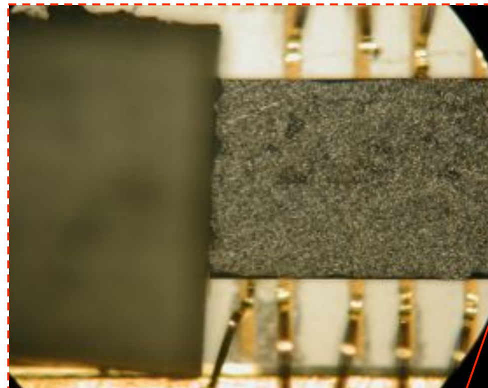

LNA and absorber chain

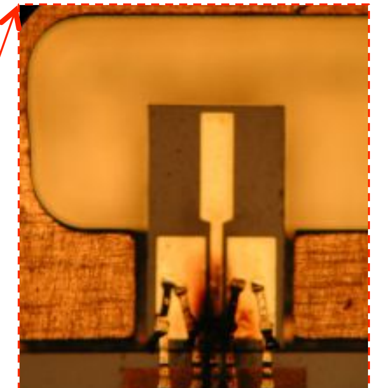

<1.3dB Probe/WG transition

DC bias control board

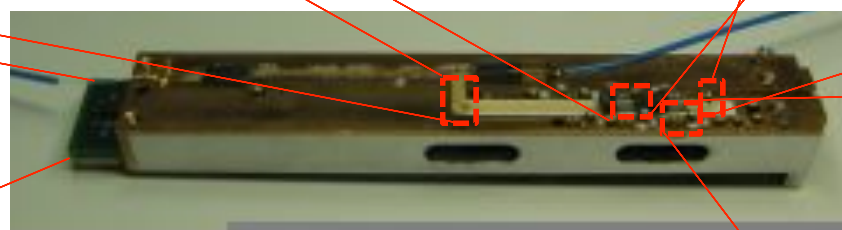

Bottom of an integrated detector module

DC biasing network

A full module that is under testing

High Bandwidth Modulators

Design of a Traveling-Wave Modulator

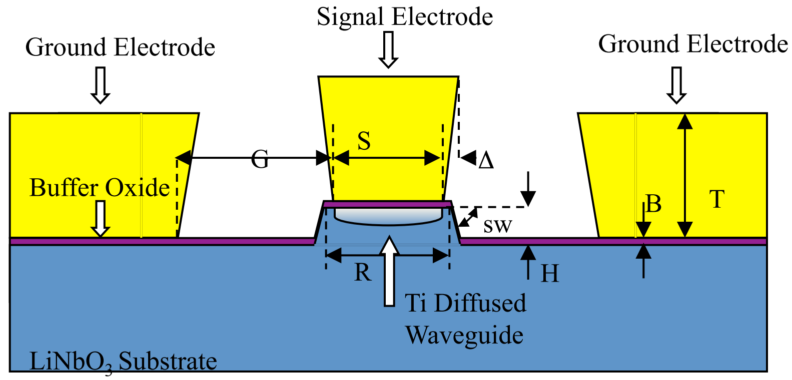

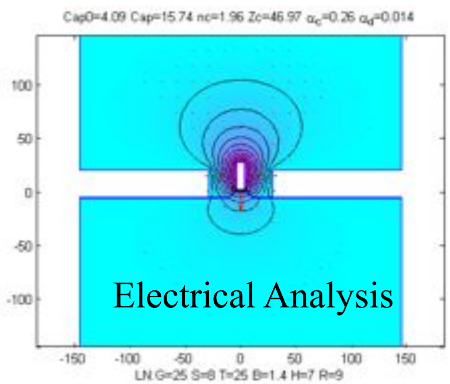

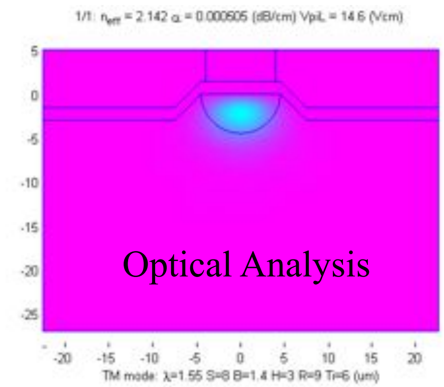

Cross section geometry
G, S, B, T, H, R, sw, Δ

Index, losses, and impedance
n_m, a_d, a_c, and Z_m

⊕

Interaction length
L

⊕

Modulation depth
m(f)

⊕

DC half wave voltage
$V_\pi(0)$

$$\eta_{mod} = \frac{\pi^2 Z_g}{2V_\pi^2(f)}$$

To maximize η_{mod} at high frequency, we need:

1. $n_m = n_o = 2.15$
2. $Z_m = Z_g = 50\ \Omega$
3. a_d, a_c = min
4. $V_\pi(0)$ = min

Other important parameters include

Modulation Efficiency Calculation

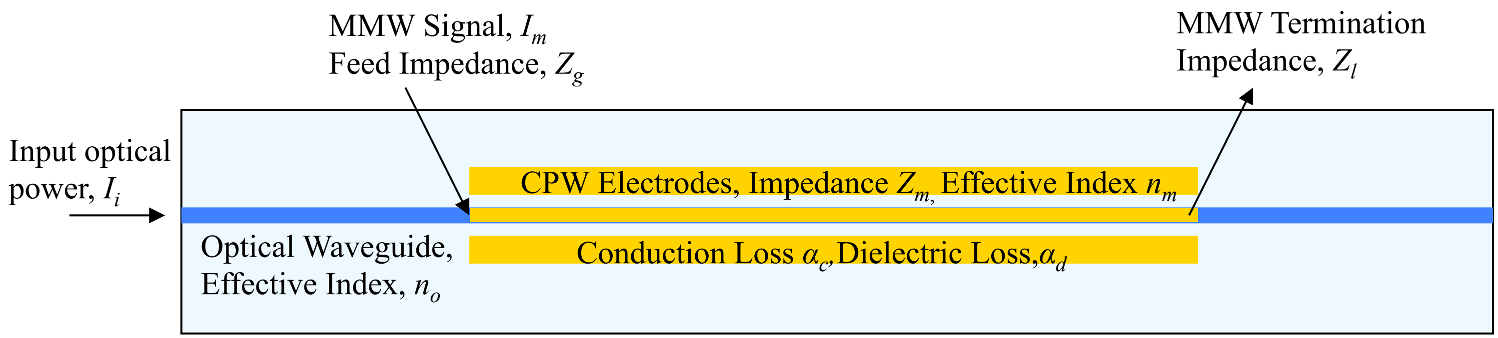

- Voltage on a traveling-wave modulator imposes phase change:

$$\Delta\phi = \left(\frac{1}{2}\right) n^3 r \vec{E} \left(\frac{2\pi L}{\lambda}\right) = \left(\frac{\pi n^3 r}{\lambda}\right)\int_0^L \vec{E}(x)\,dx = \left(\frac{\pi n^3 r}{\lambda}\right)\int_0^L \frac{V(x)}{d}\,dx$$

- $V_\pi(f)$: voltage for $\Delta\phi = \pi$
- Using transmission line theory:

$$\eta_{\mathrm{mod}}(f) = \left(\frac{\pi^2 Z_{\mathrm{m}}}{2V_{\pi,f}^2}\right) = \left(\frac{\pi^2 Z_{\mathrm{m}}}{2\left(V_{\pi,DC}\cdot m(f)\right)^2}\right)\left(\frac{1}{Watts}\right)$$

Dependends on Z_m, $|n_{\mathrm{o}} - n_{\mathrm{m}}|$, α_{c}, and α_{d}

Bandwidth Limiting Mechanisms

- Slight index mismatch, $\Delta_n = |n_o - n_m|$, is primary contributor to the roll-off in frequency response
- The effective index difference should be less than 0.05 for 95 GHz operation for 2 cm modulator length.

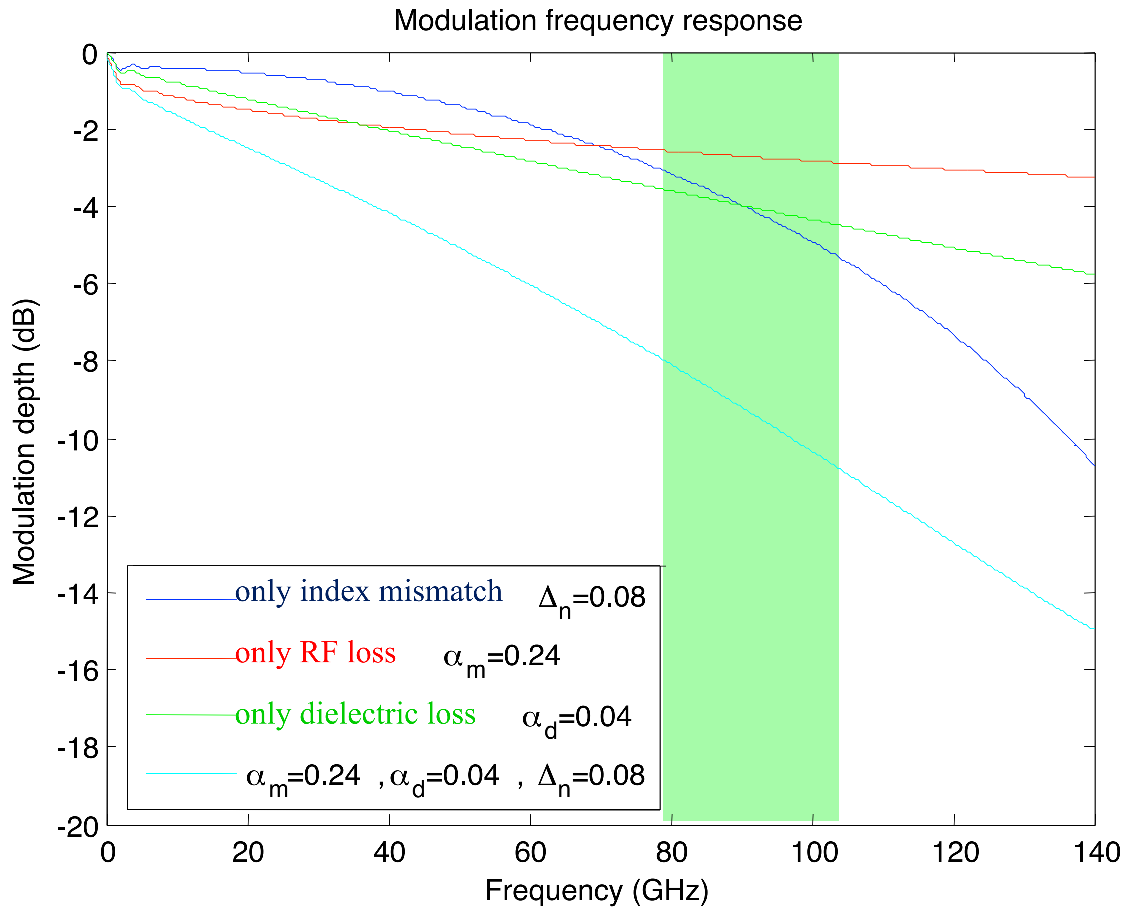

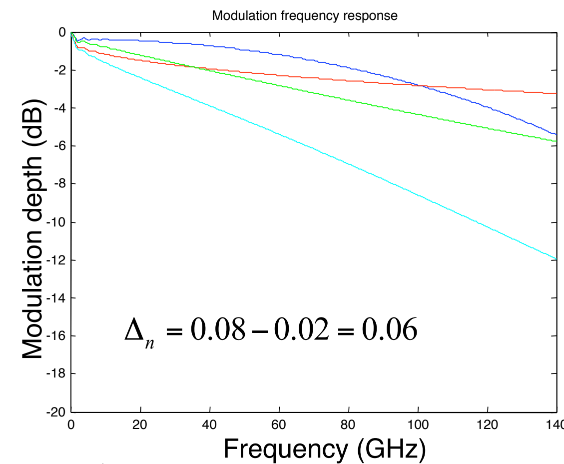

Change RF Index by ±0.02

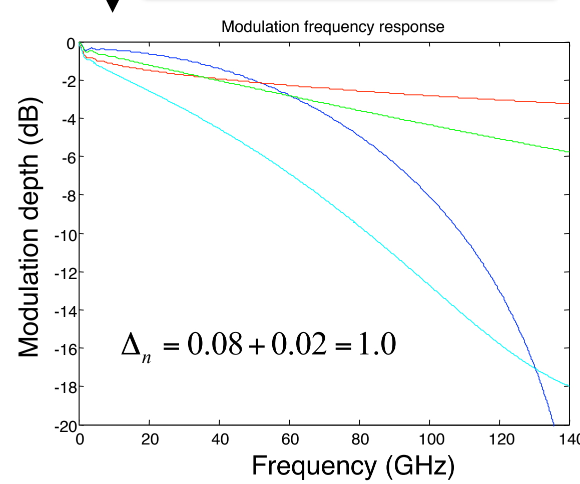

Overview of Fabrication Process

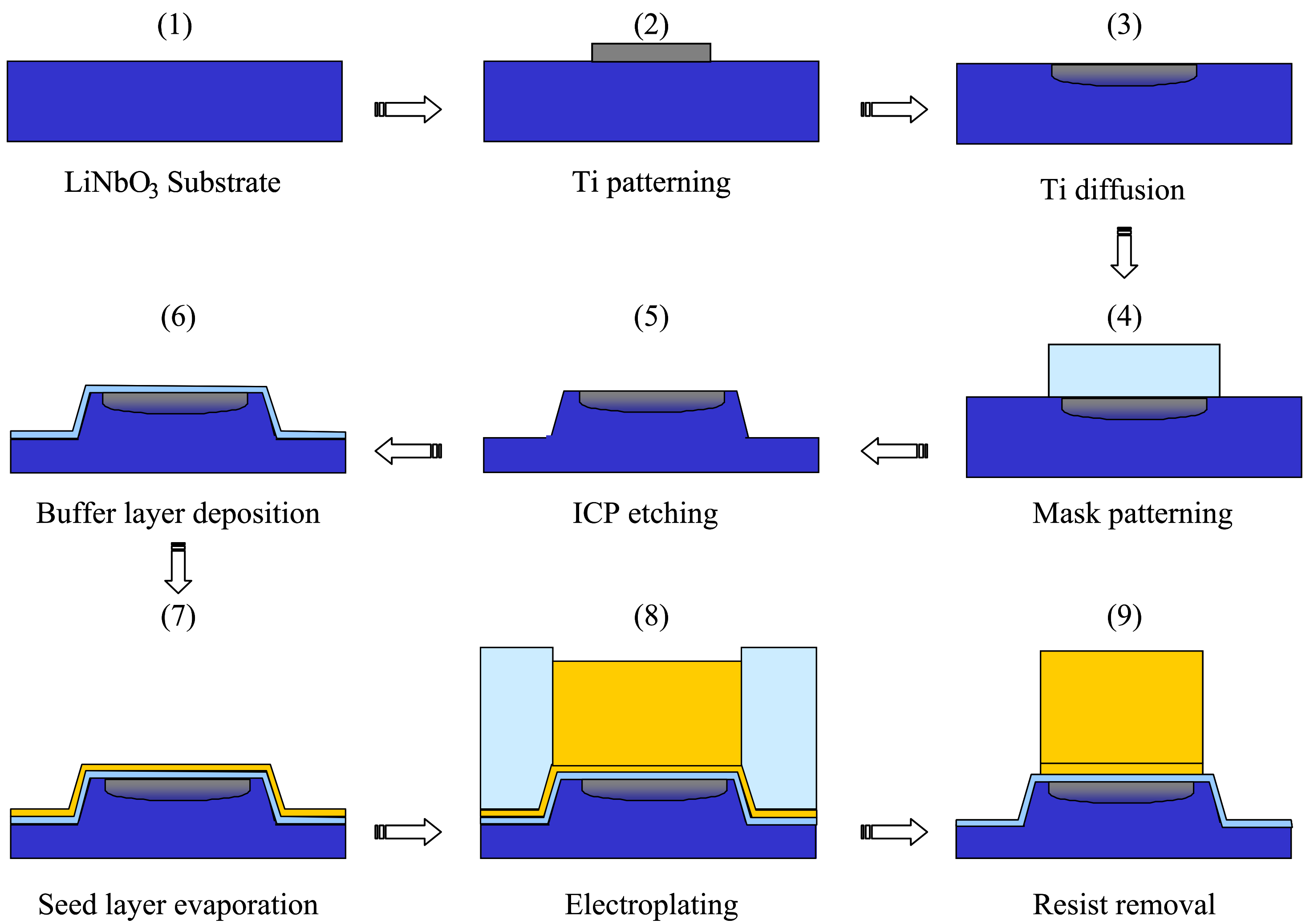

Fabrication process

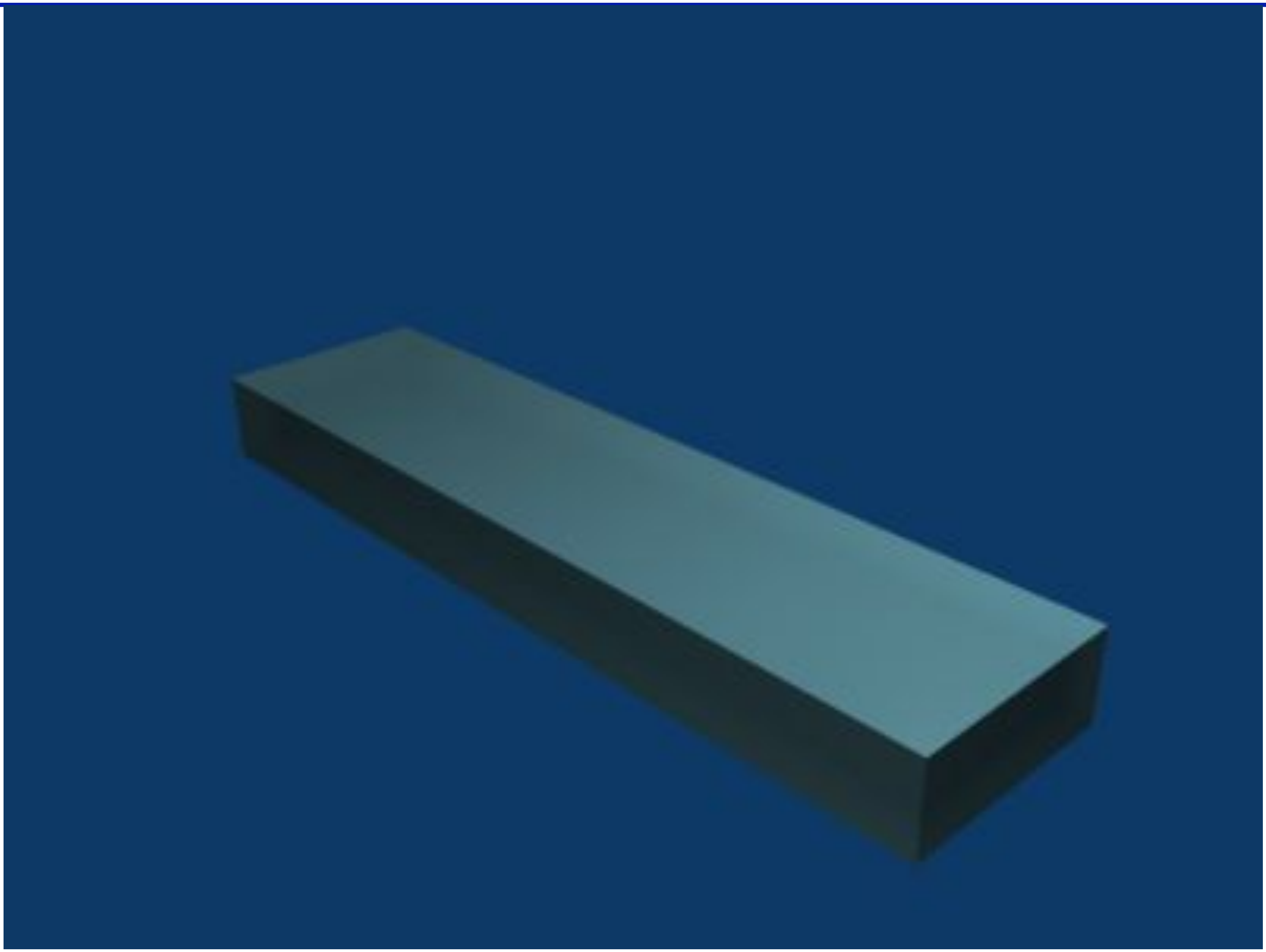

Formation of Ti strip

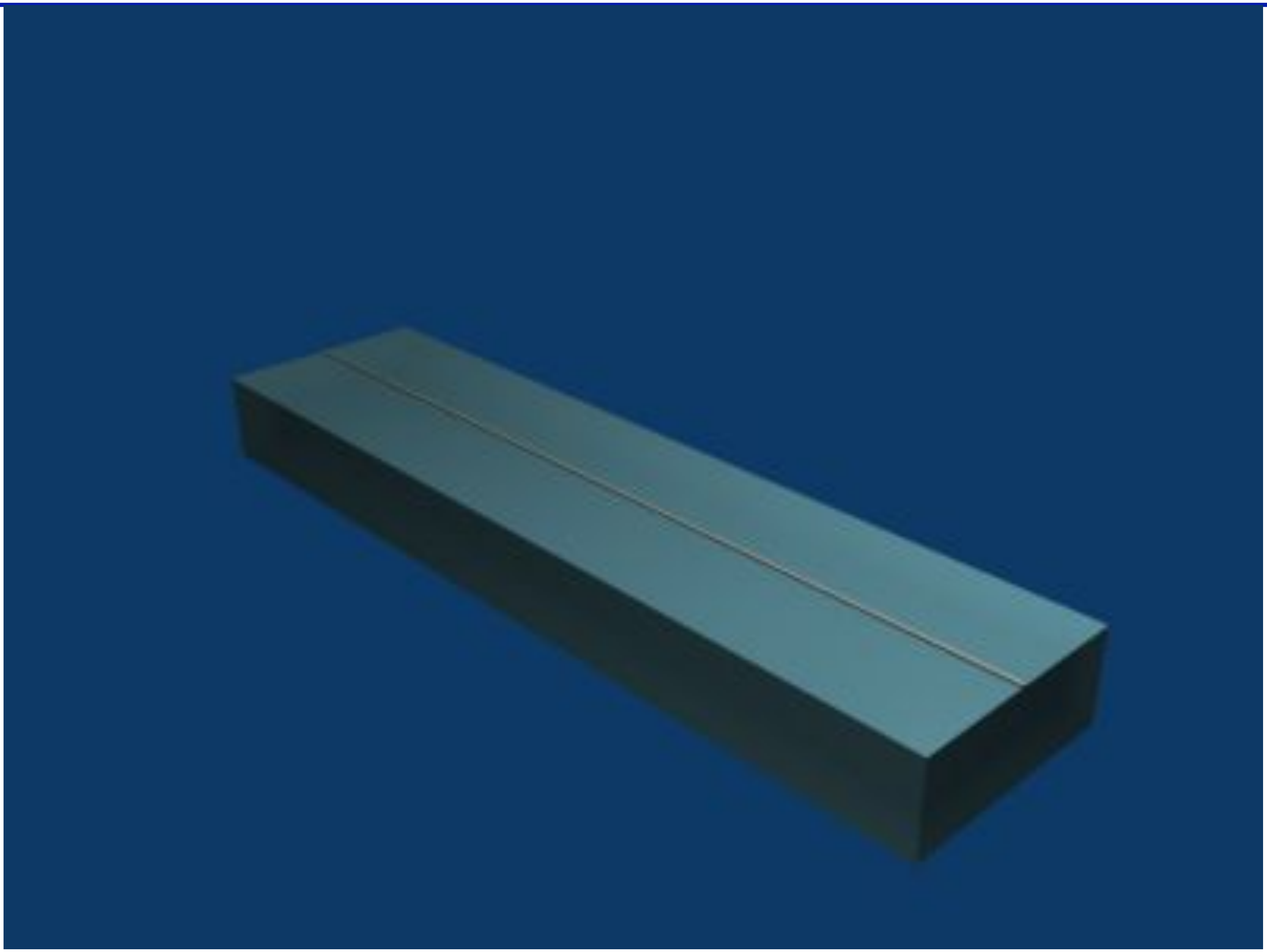

Ti in-diffusion

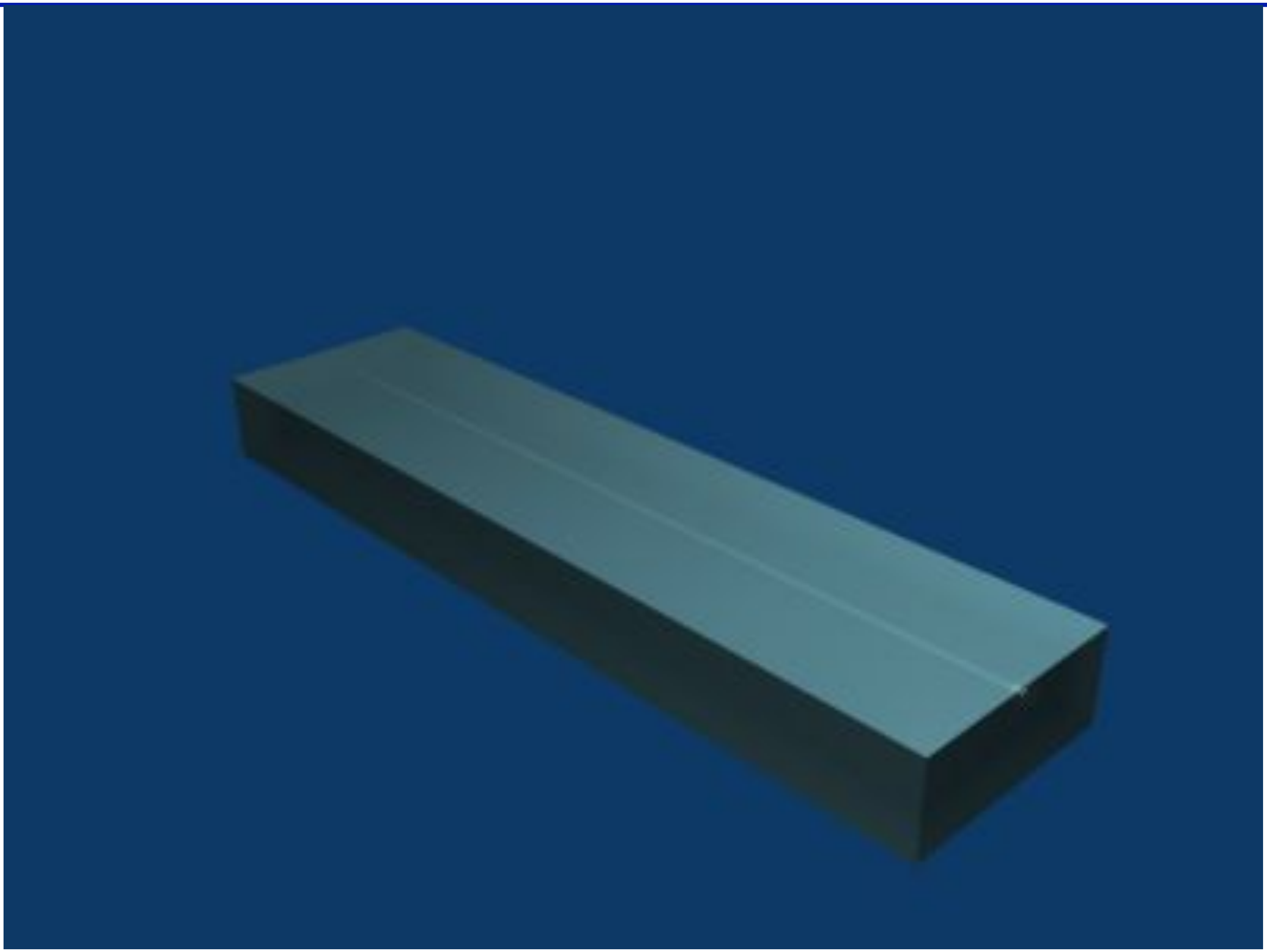

Ridge etching

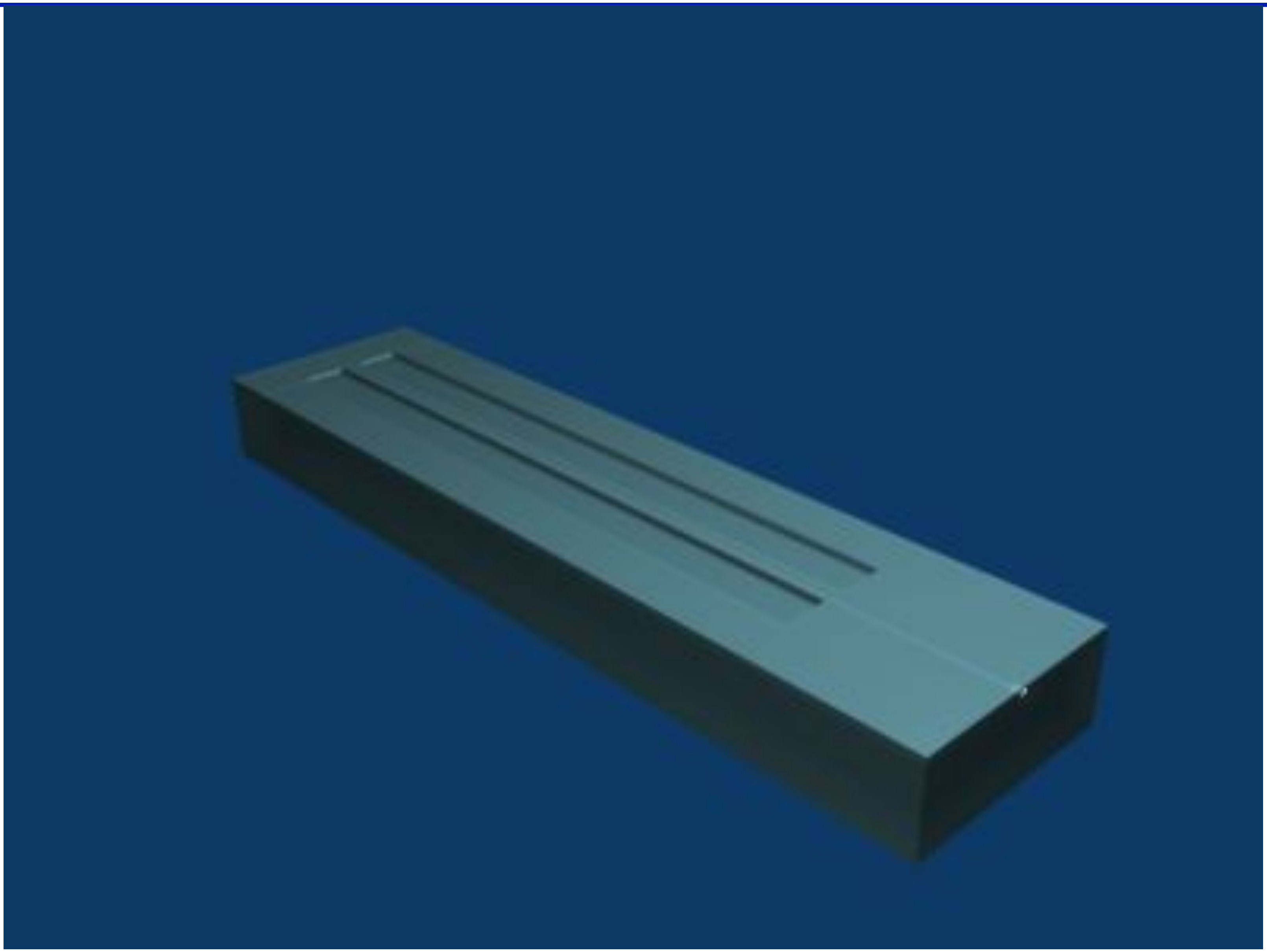

Oxide layer deposition

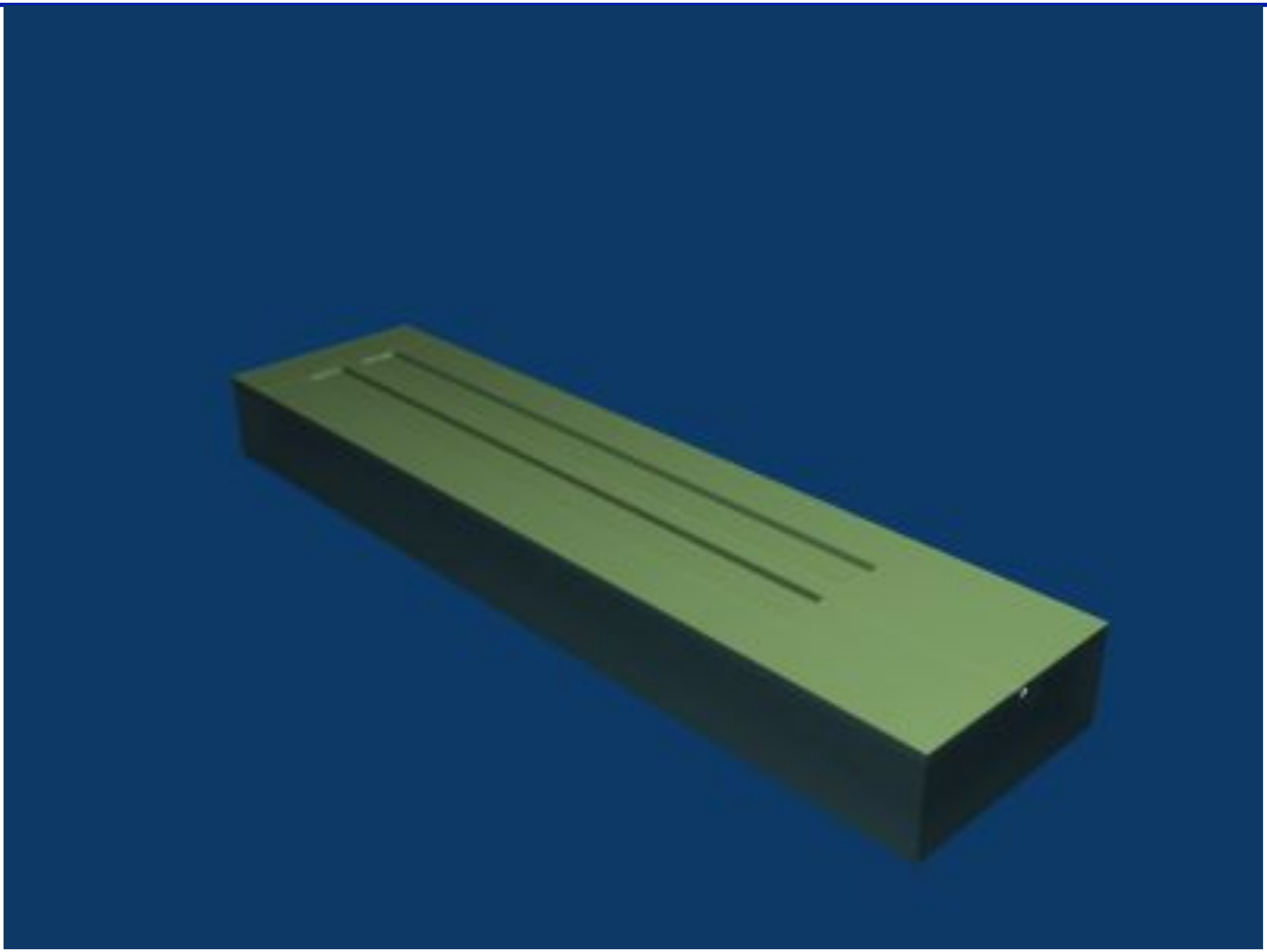

Seed layer deposition

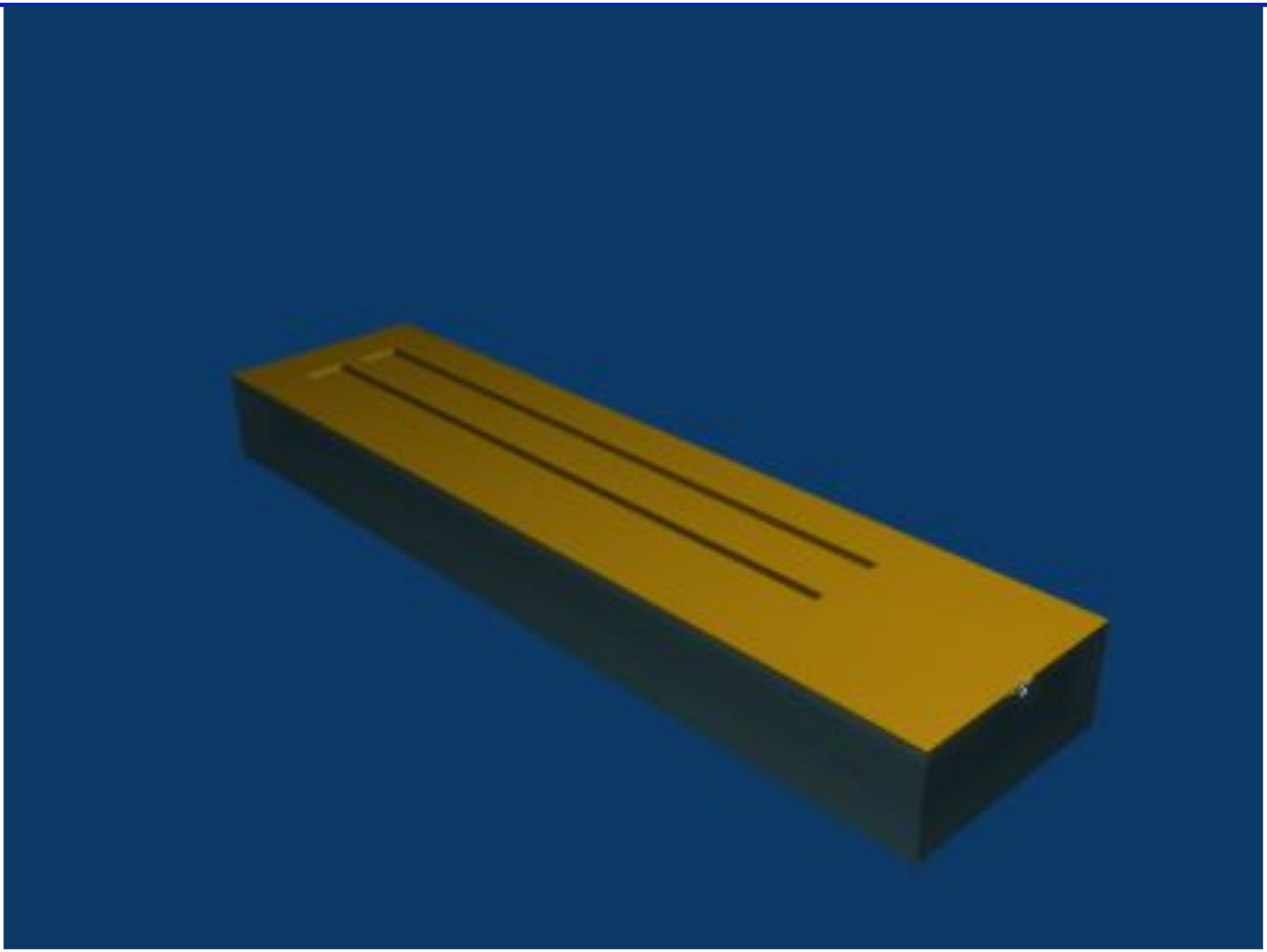

Thick resist lithography

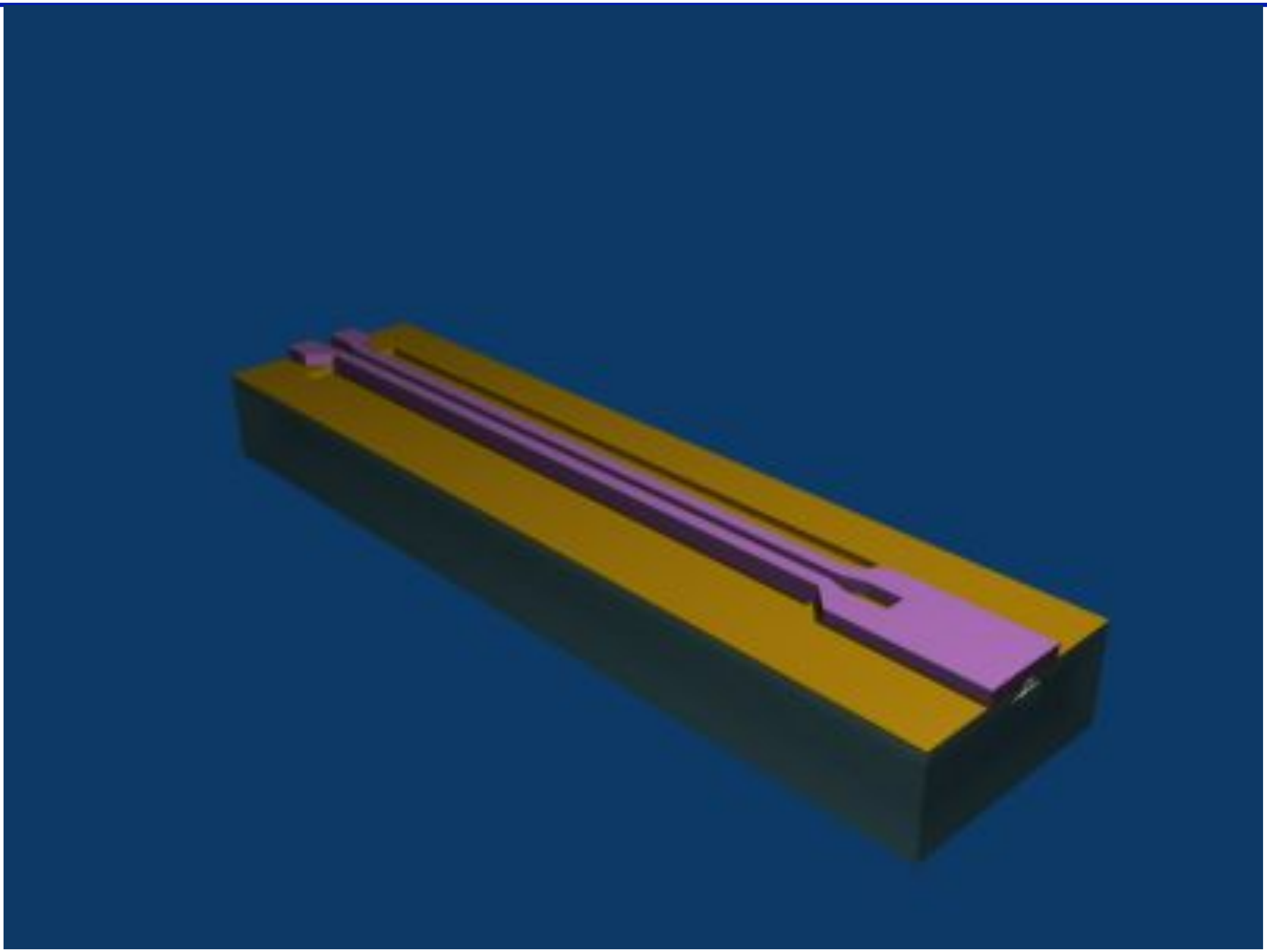

Electroplating of gold electrodes

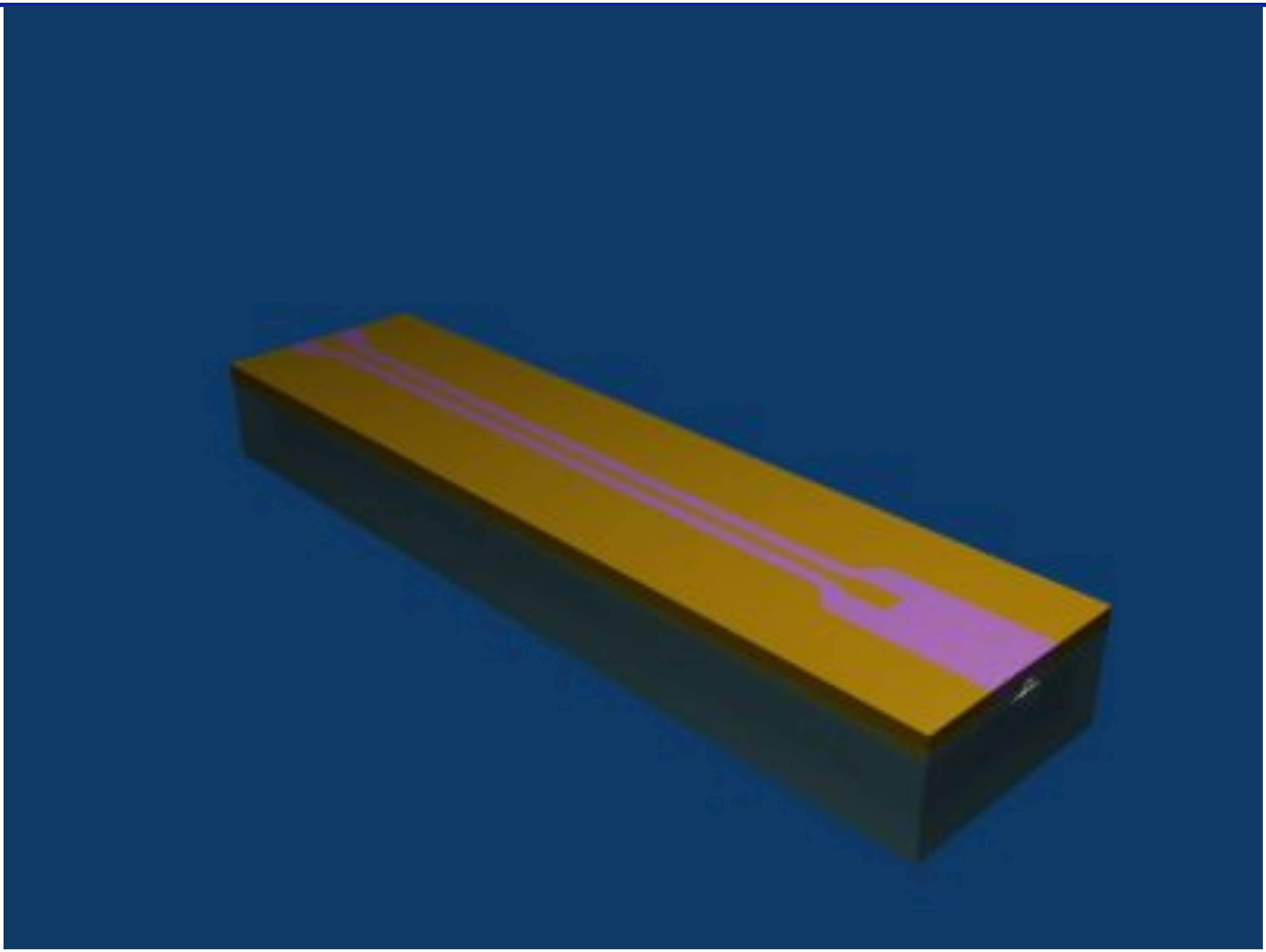

Striping of seed layer

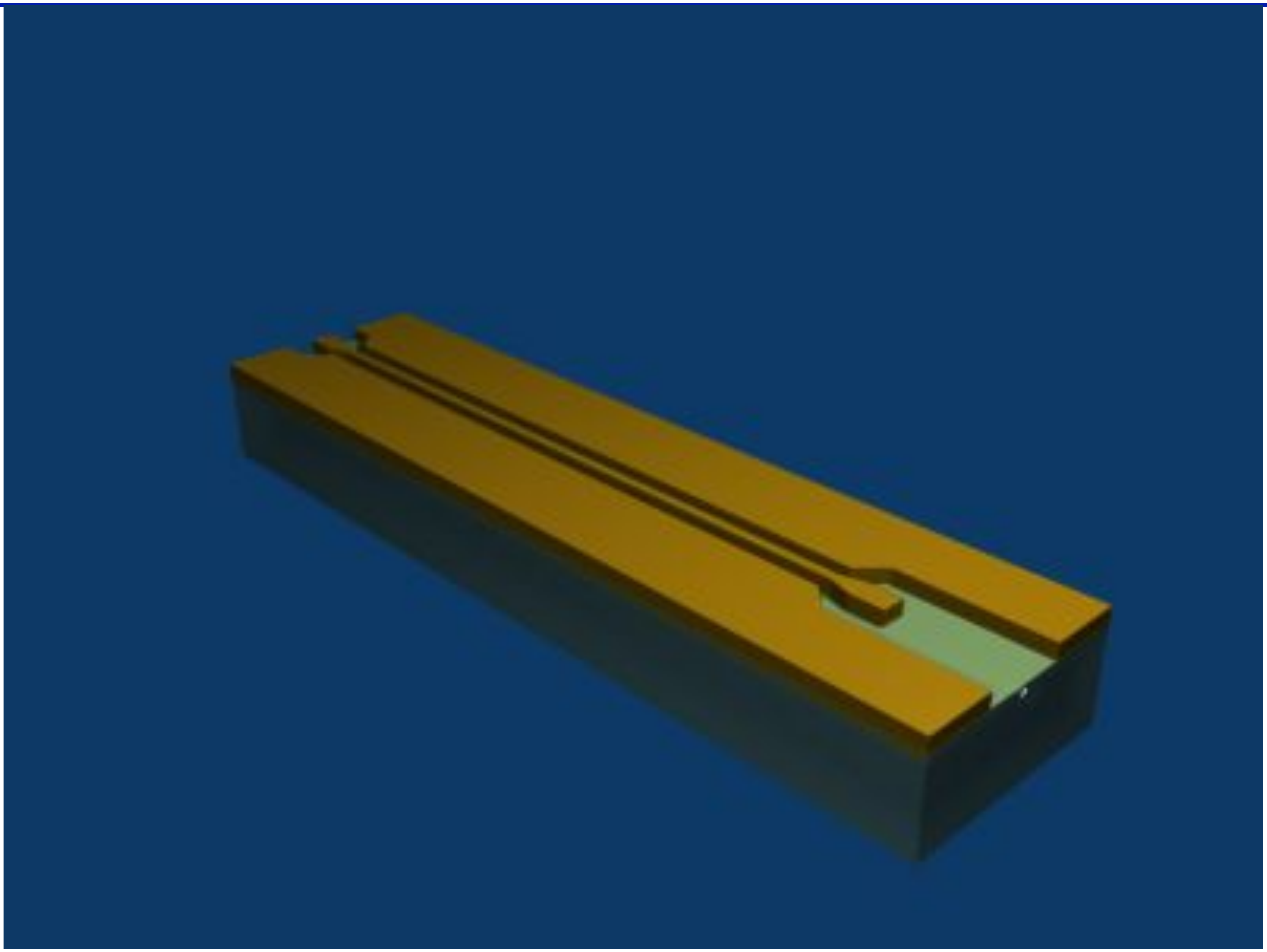

Fabricated High Frequency Modulator

Modulator array

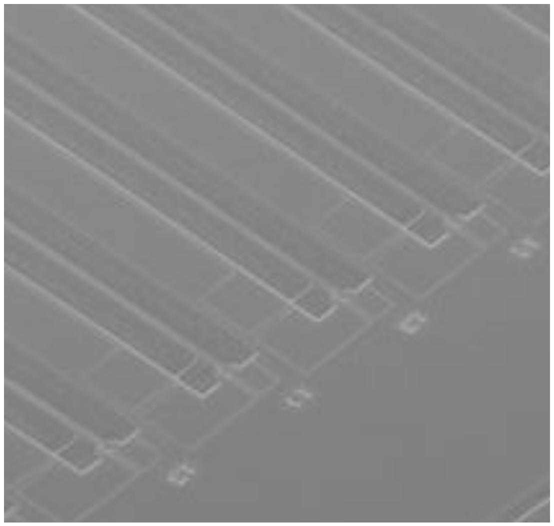

Modulator feed

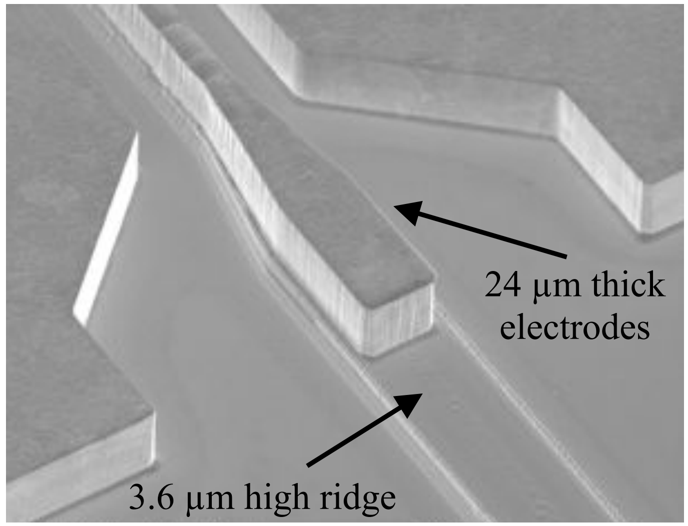

Close view of modulator

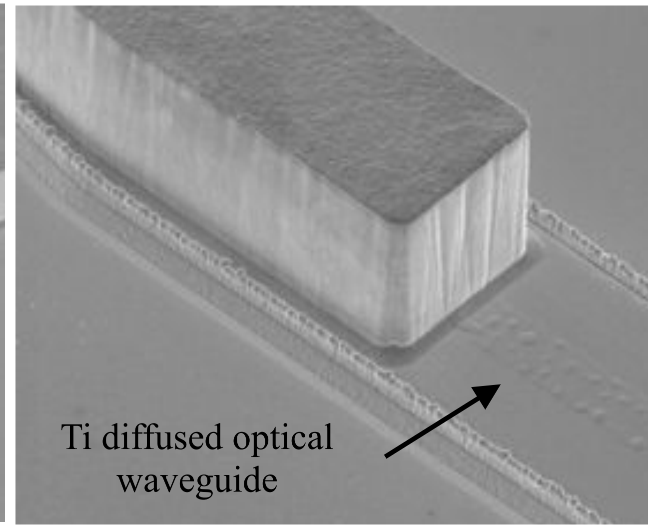

Substrate thinning to eliminate substrate mode

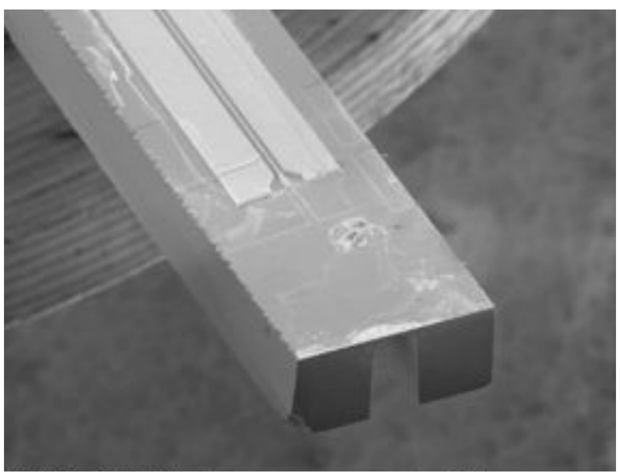

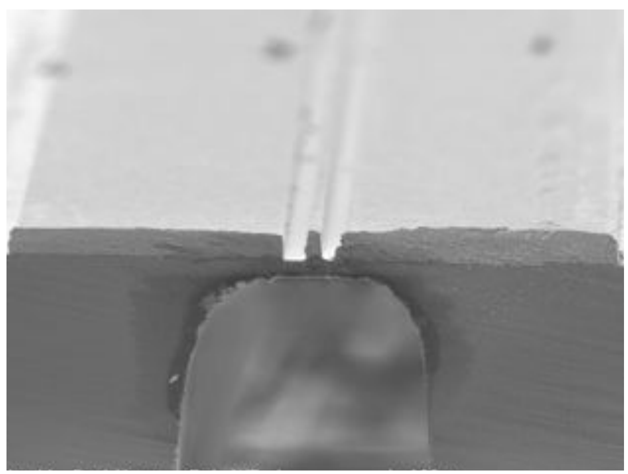

To mitigate the substrate mode, particularly at high frequencies (>50 GHz), the 500um thick $LiNbO_3$ wafer was thinned on the backside of device. A trench with a width of 200um and depth of 450um is formed, thereby leaving a 50um thick device layer.

High Frequency Up-conversion Modulators

Fully developed simulation tools

Industrial leading high power ICPs

Uniform electro-plating

Efficient design for low mmW loss

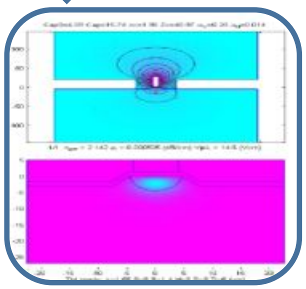

Design, simulation, optimization

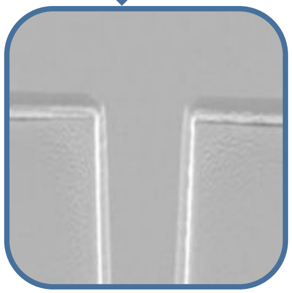

Ridge and buffer layer for index matching

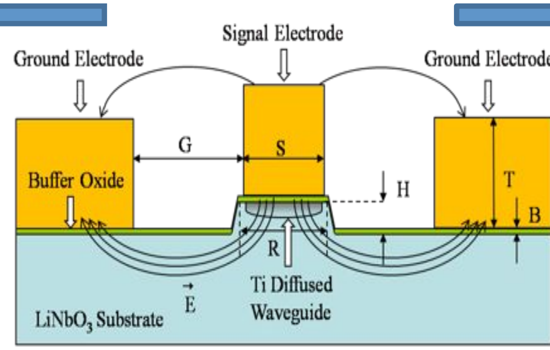

Cross-section of designed modulator structure

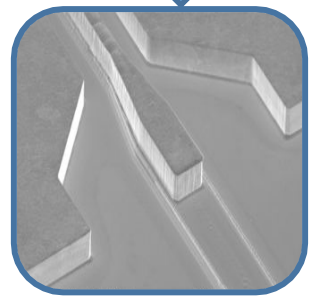

High aspect-ratio electrodes for low conduction loss

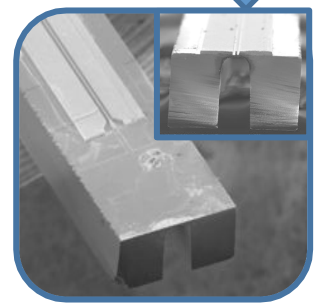

Eliminate substrate modes via trench

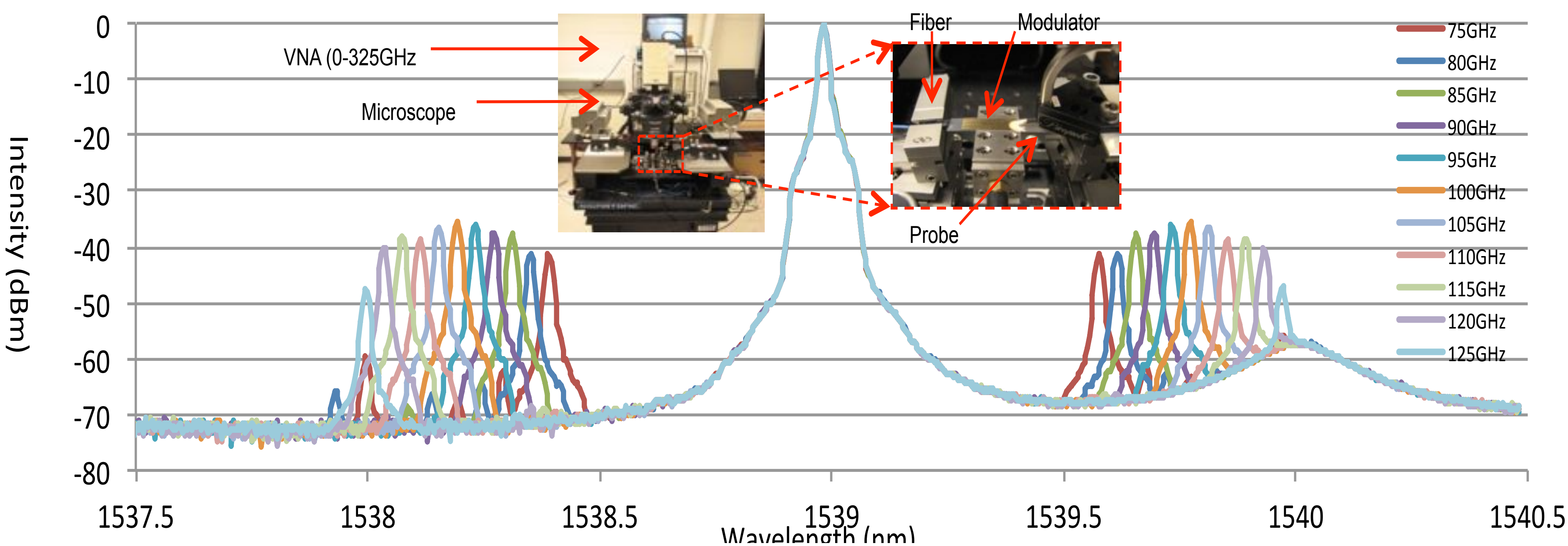

Modulator Processing and Packaging

Wafer level micro-fabrication includes optical waveguide diffusion, ridge etching, buffer layer deposition and electroplating.

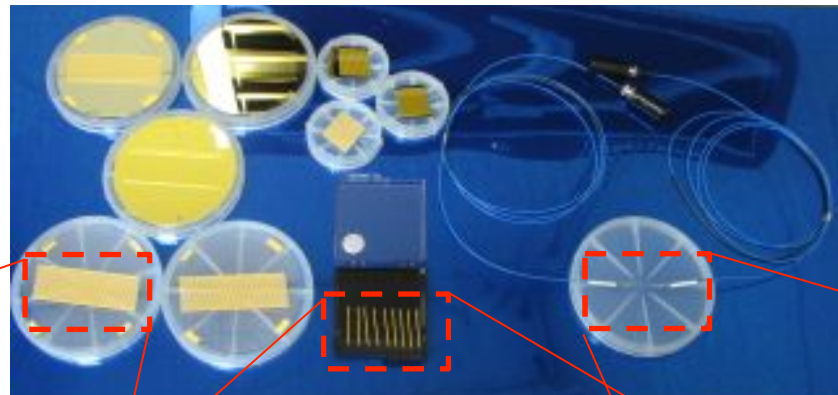

Post-processing and packaging includes dicing, polishing, annealing, index tuning and optical bonding.

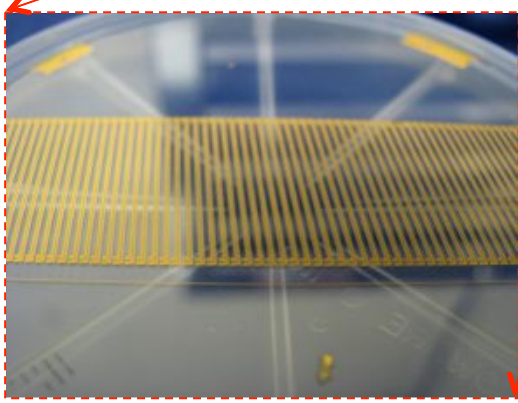

Modulator wafer after micro-fabrication. 61 modulators on each wafer.

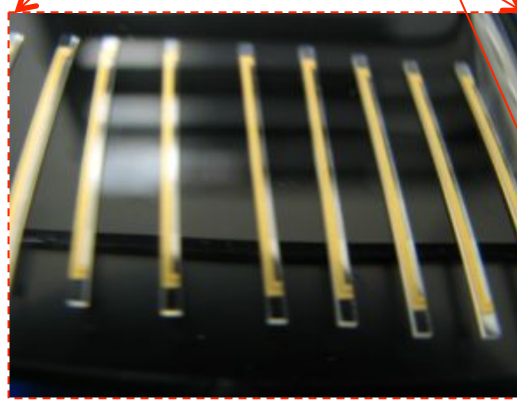

Individual modulator chip after dicing, polishing and index tuning.

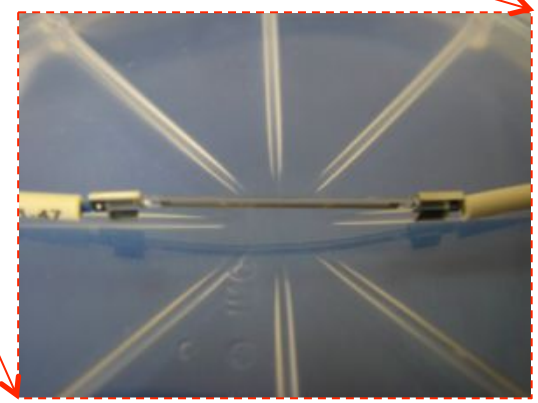

Modulator is optically integrated to PM fiber through V-groove bonding.

Measurements at 110 GHz

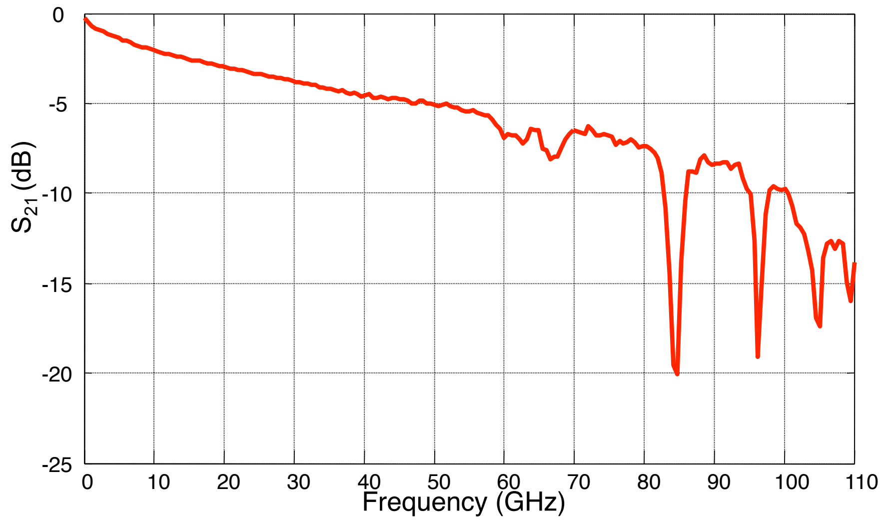

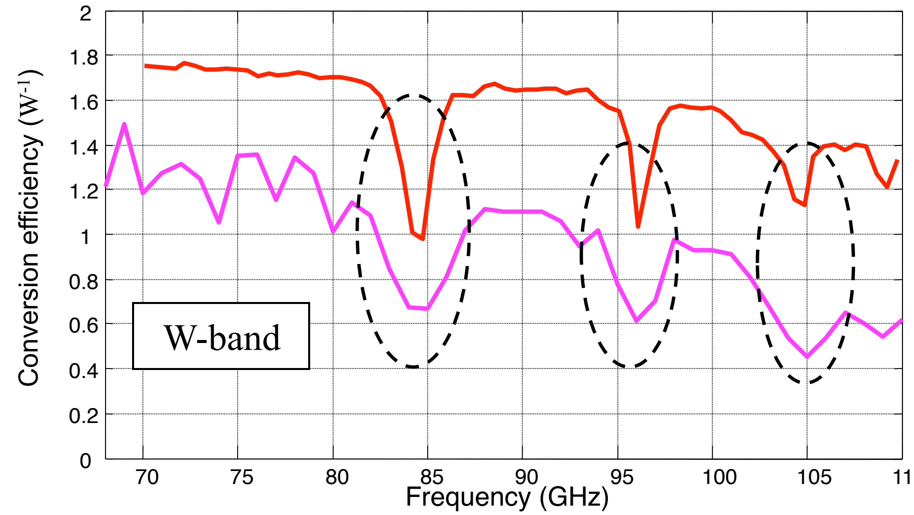

Conduction loss: α_m = 0.28 dB/(cm.GHz$^{1/2}$)

Dielectric loss: α_d = 0.01 dB/(cm.GHz)

Input Impedance: Z_m = 46.4 Ω

Effective index: **n_{eff} = 2.19**

Optical loss: L_{opt}= 3.0 dB

Substrate modes negatively impact the performances of the device in W-band

Measurements at 110 GHz

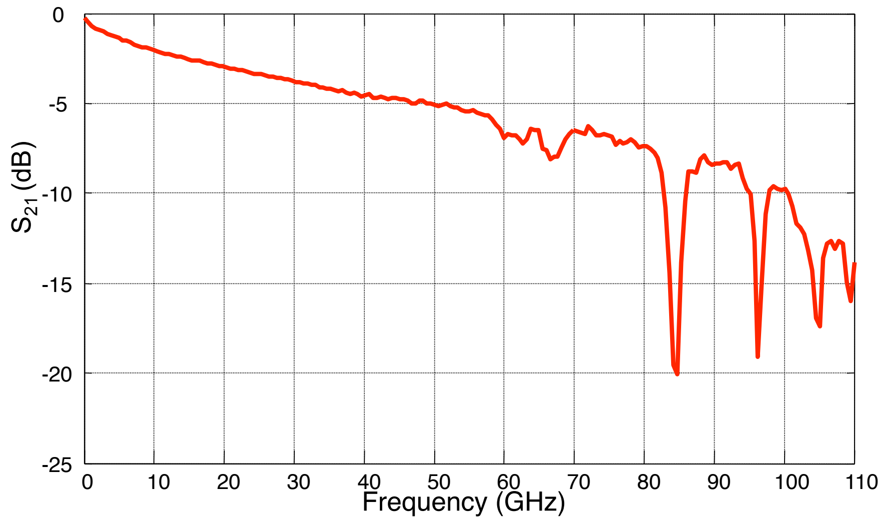

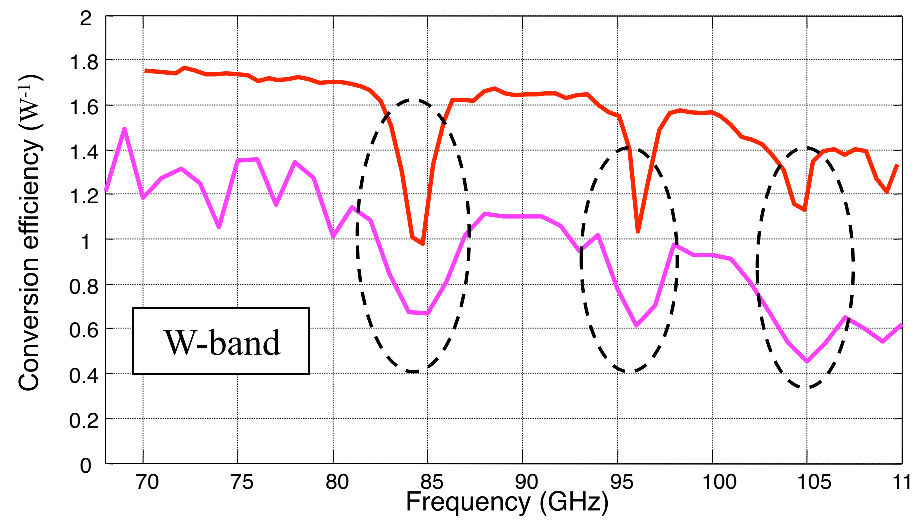

Conduction loss: $\alpha_m = 0.28$ dB/(cm.GHz$^{1/2}$)

Dielectric loss: $\alpha_d = 0.01$ dB/(cm.GHz)

Input Impedance: $Z_m = 46.4\ \Omega$

Effective index: **$n_{eff} = 2.19$**

Optical loss: $L_{opt} = 3.0$ dB

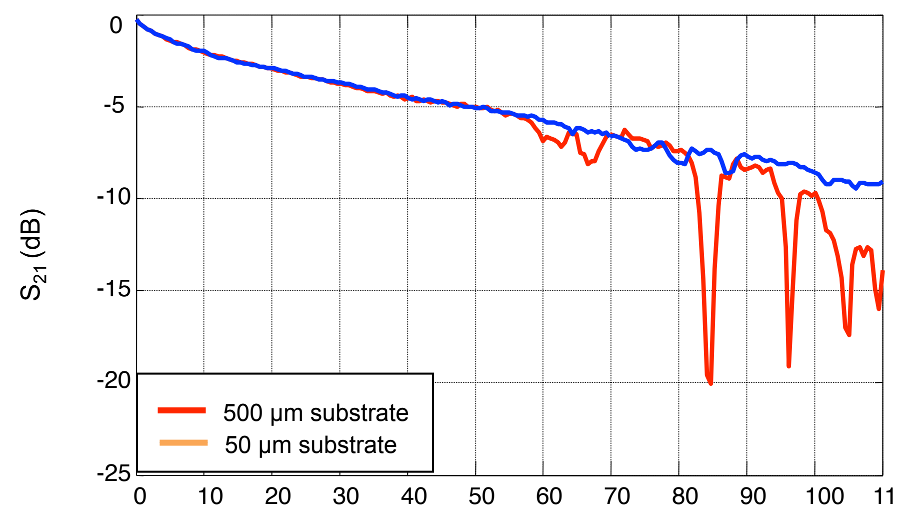

Substrate modes negatively impact the performances of the device in W-band

Substrate Modes Suppression

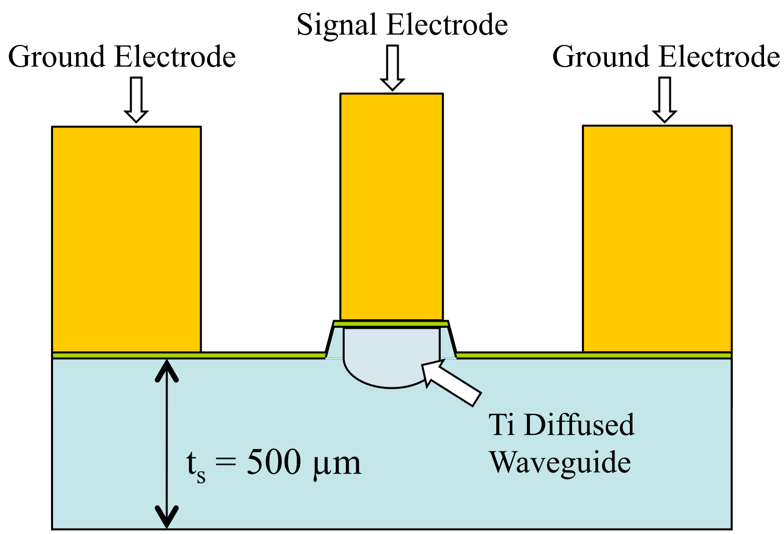

Modulator profile before machining

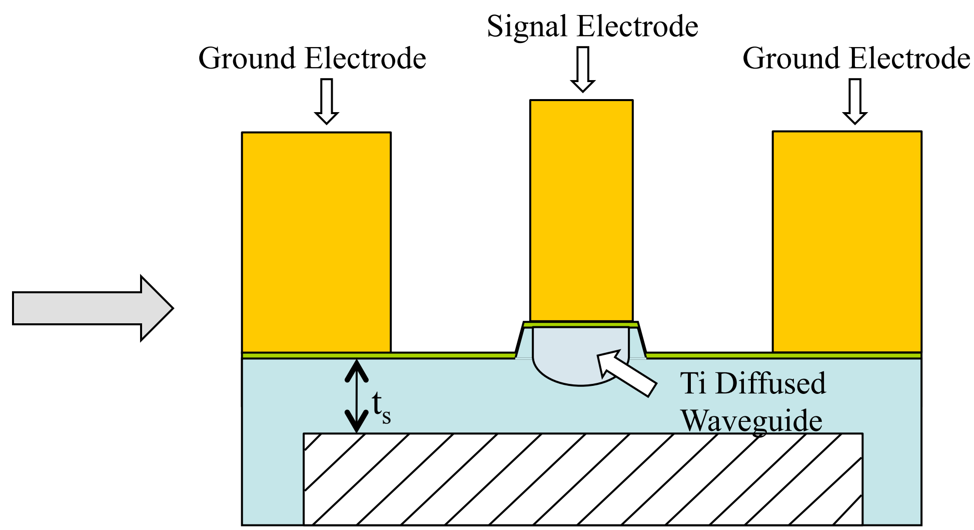

Modulator profile after machining

Substrate modes frequency cut-off [1]:

$$f_c\,(\text{GHz}) = \frac{11.9}{t_s\,(\text{mm})}$$

- 100 GHz: t_s = 120 μm
- 200 GHz: t_s = 60 μm

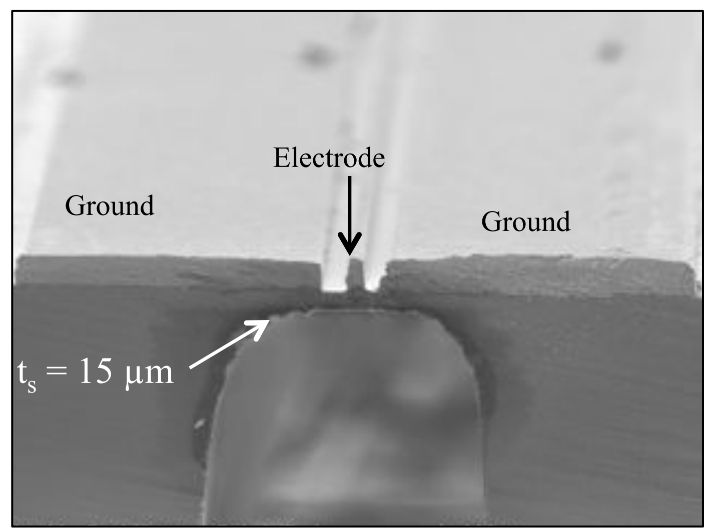

[1] Y. Shi, "Micromachined Wide-Band Lithium-Niobate Electrooptic Modulators," IEEE Trans. Microw. Theory Tech., vol. 54, no. 2, pp 0810-815, Feb. 2006.

High Bandwidth Operation

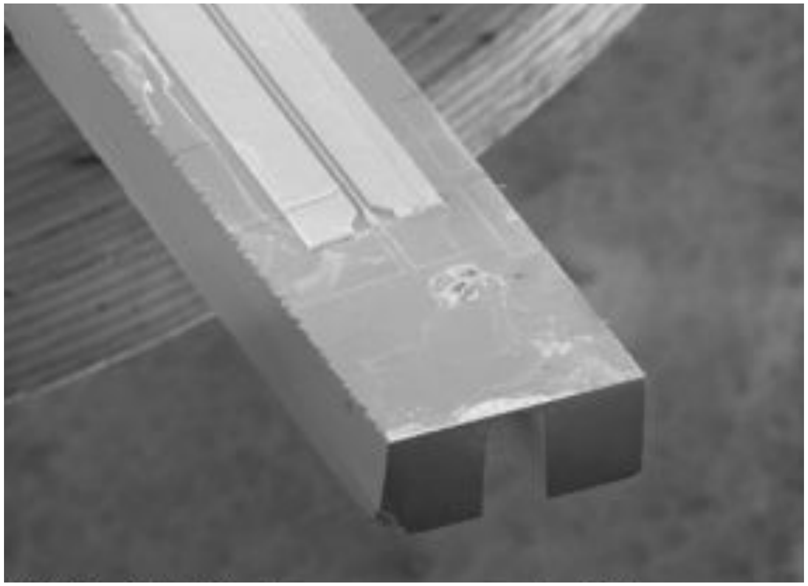

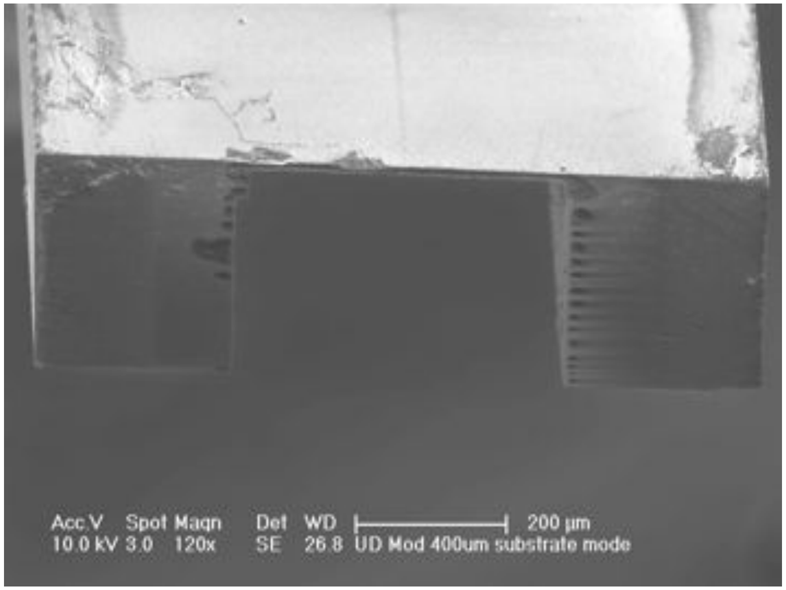

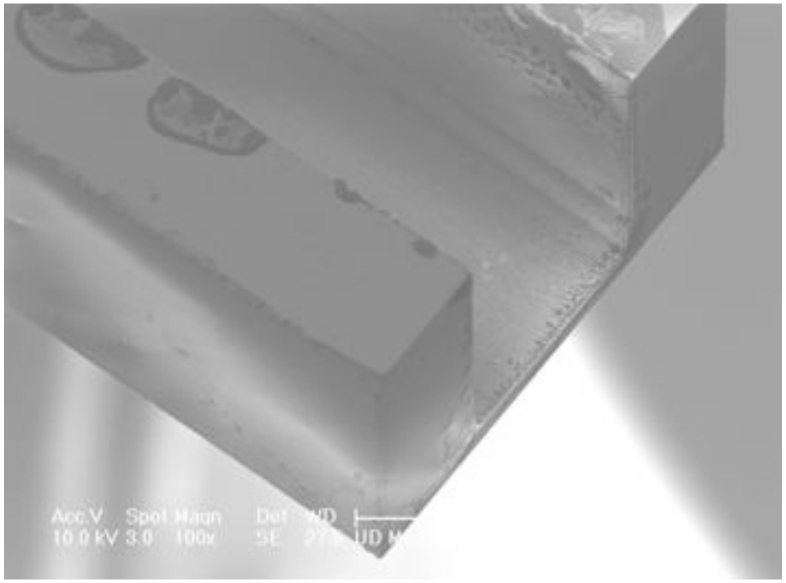

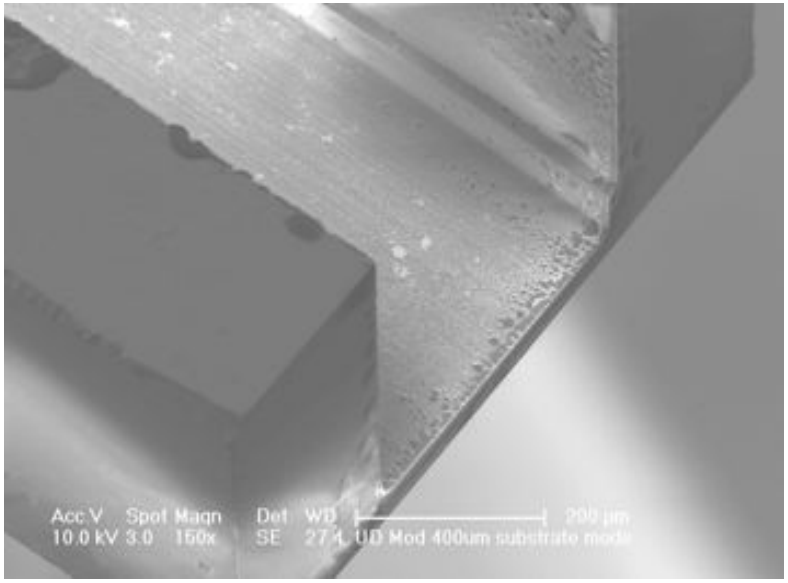

Setup for 220 GHz bandwidth measurements

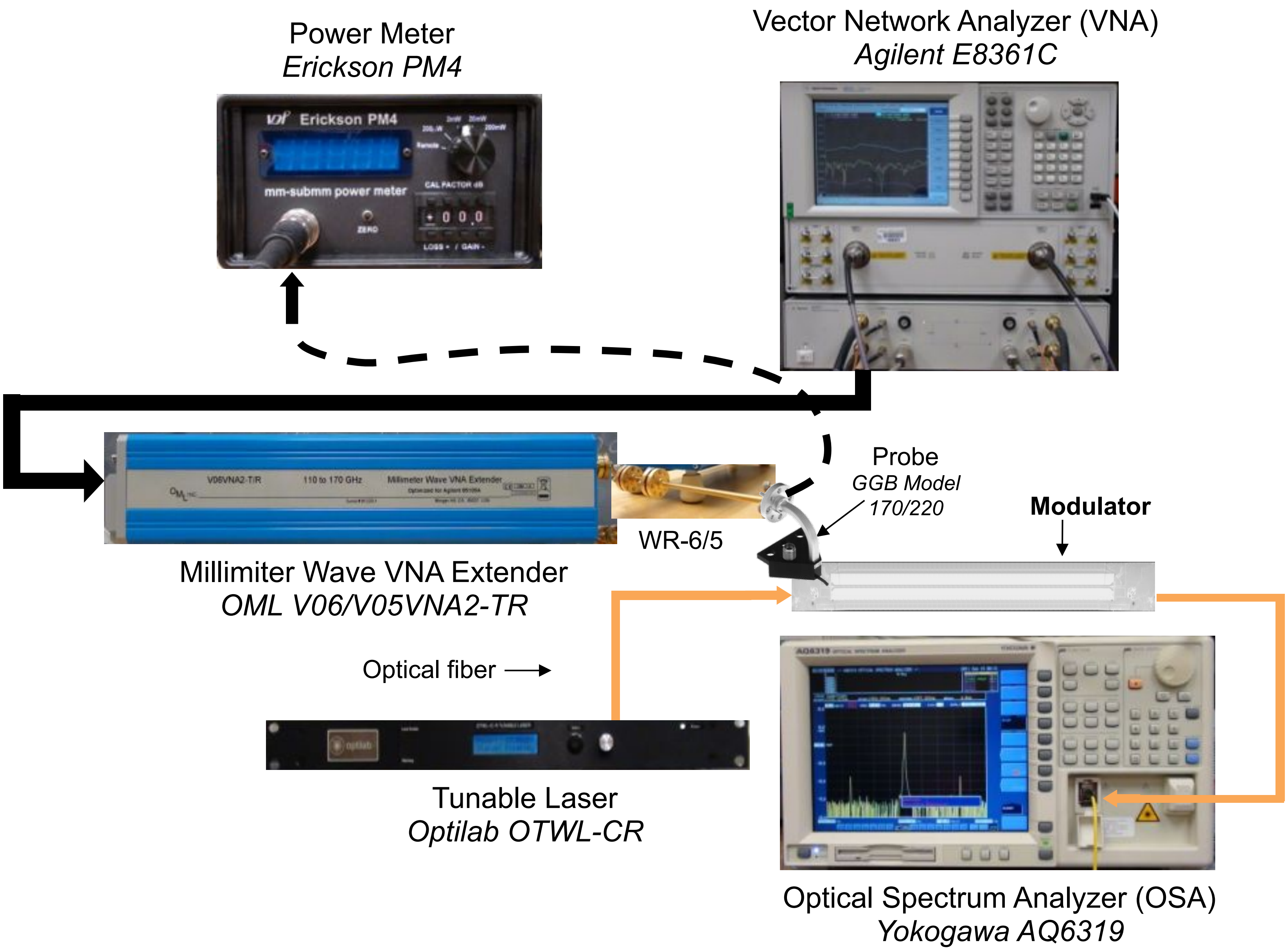

10-220 GHz Modulation Spectrum

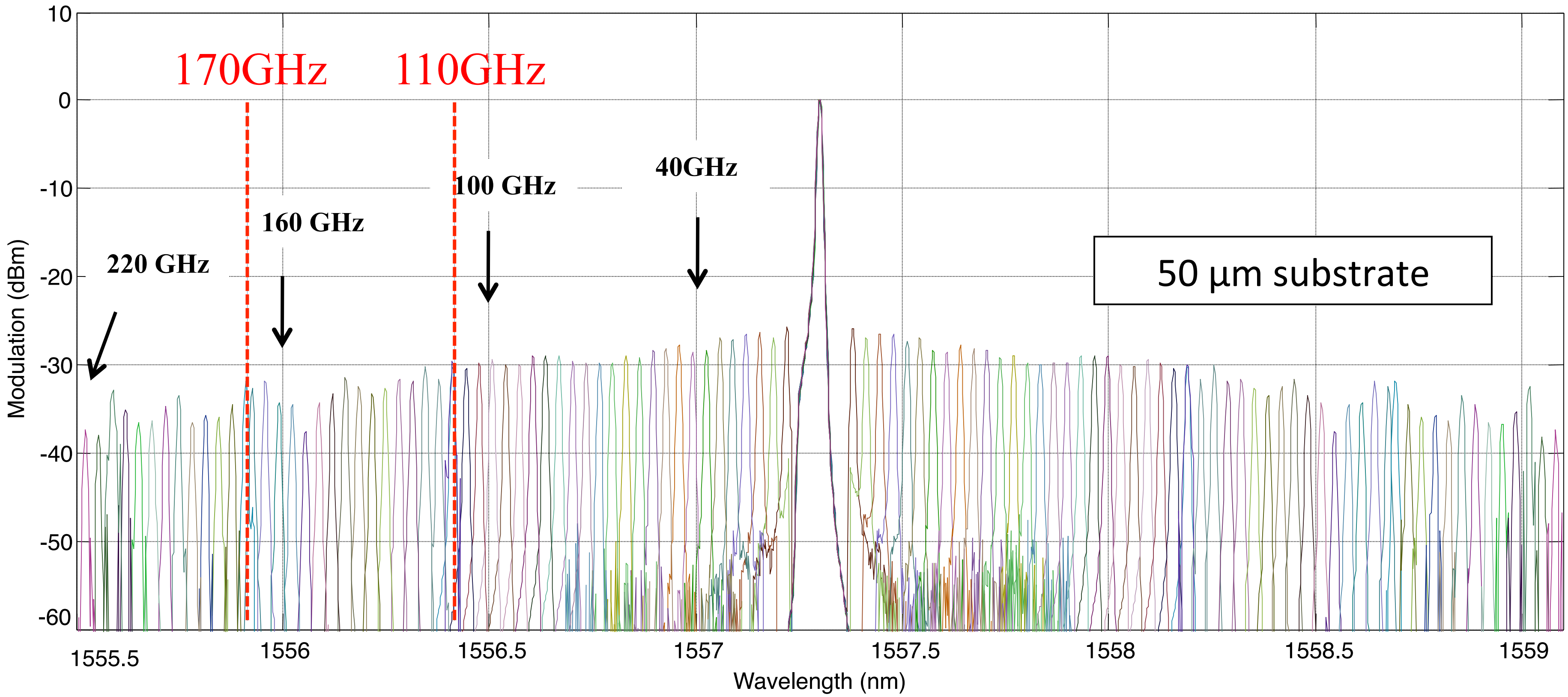

- Sidebands normalized to input power
- Only 3 dB attenuation between 10 GHz and 100 GHz
- Stronger attenuation above 110 GHz

Ultra-Wideband Frequency Synthesis

Why Optical Generation of RF Sources?

- Ultra-wide tuning range
  - Small tuning range in optical domain = huge tuning range in RF (200 GHz = 1.6 nm)
- RF distribution for remote LO sources, phased arrays
  - RF over fiber = transmit over km's with negligible loss/ dispersion
- Phase steering in optical domain, UWB
  - Phase is preserved in optical-to-RF conversion = fast, low-power, wide-BW, low-dispersion phase steering in optical domain

Coherent Optical Heterodyning for UWB IF Synthesis & Up/Down-conversion Receivers

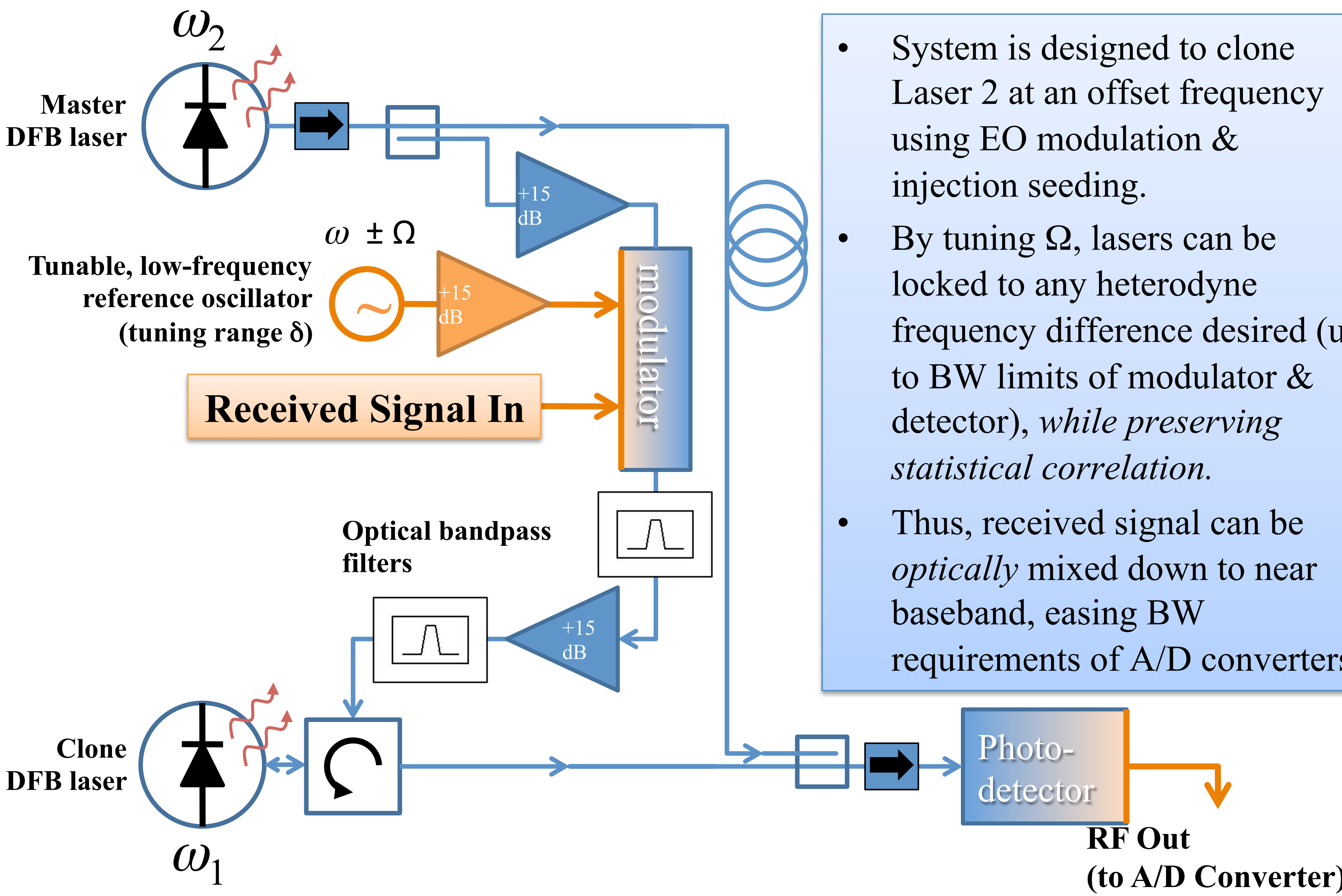

- System is designed to clone Laser 2 at an offset frequency using EO modulation & injection seeding.
- By tuning Ω, lasers can be locked to any heterodyne frequency difference desired (up to BW limits of modulator & detector), *while preserving statistical correlation.*
- Thus, received signal can be *optically* mixed down to near baseband, easing BW requirements of A/D converters.

Narrow-line Widely Tunable RF Generation System

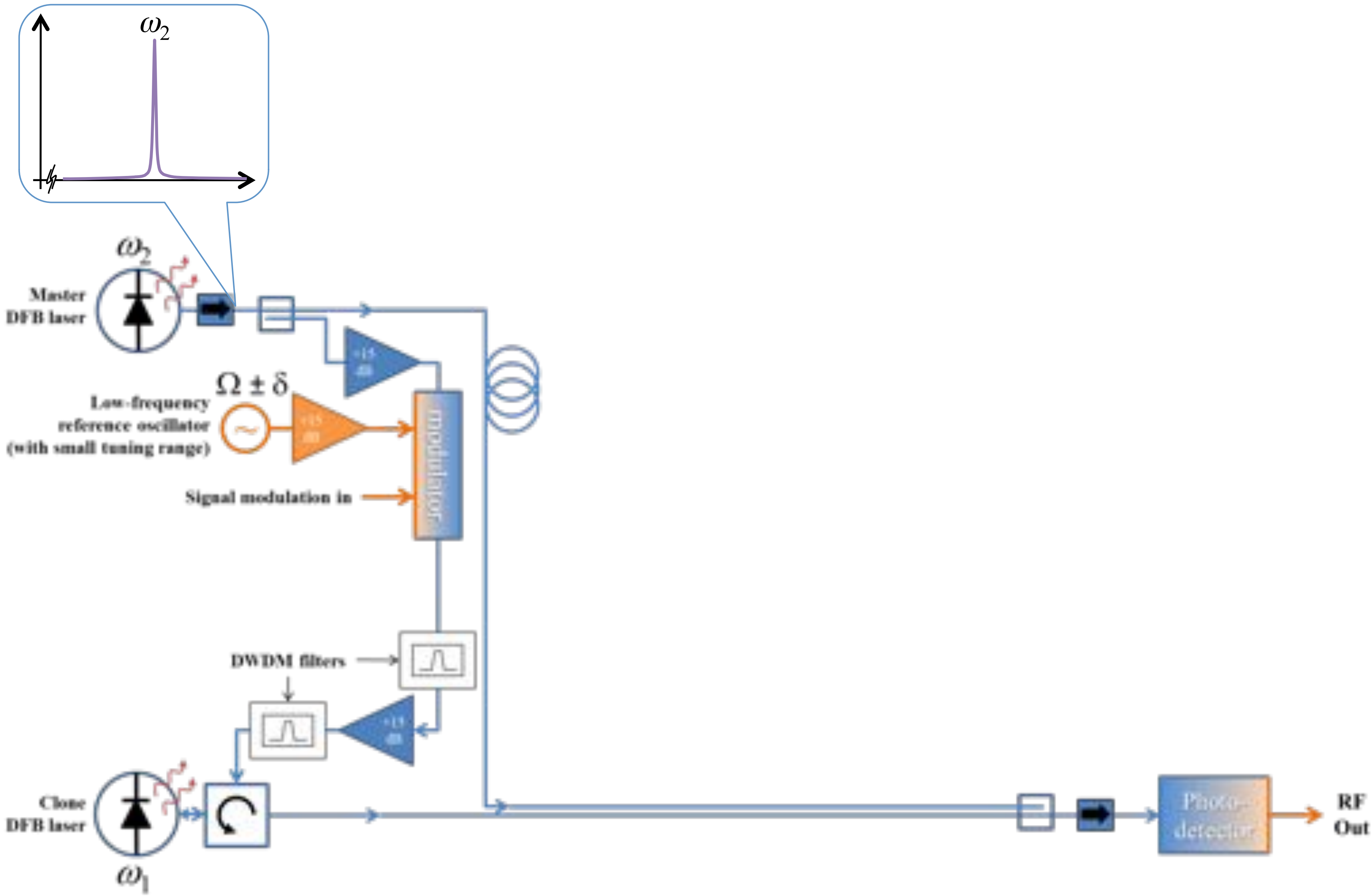

Narrow-line Widely Tunable RF Generation System

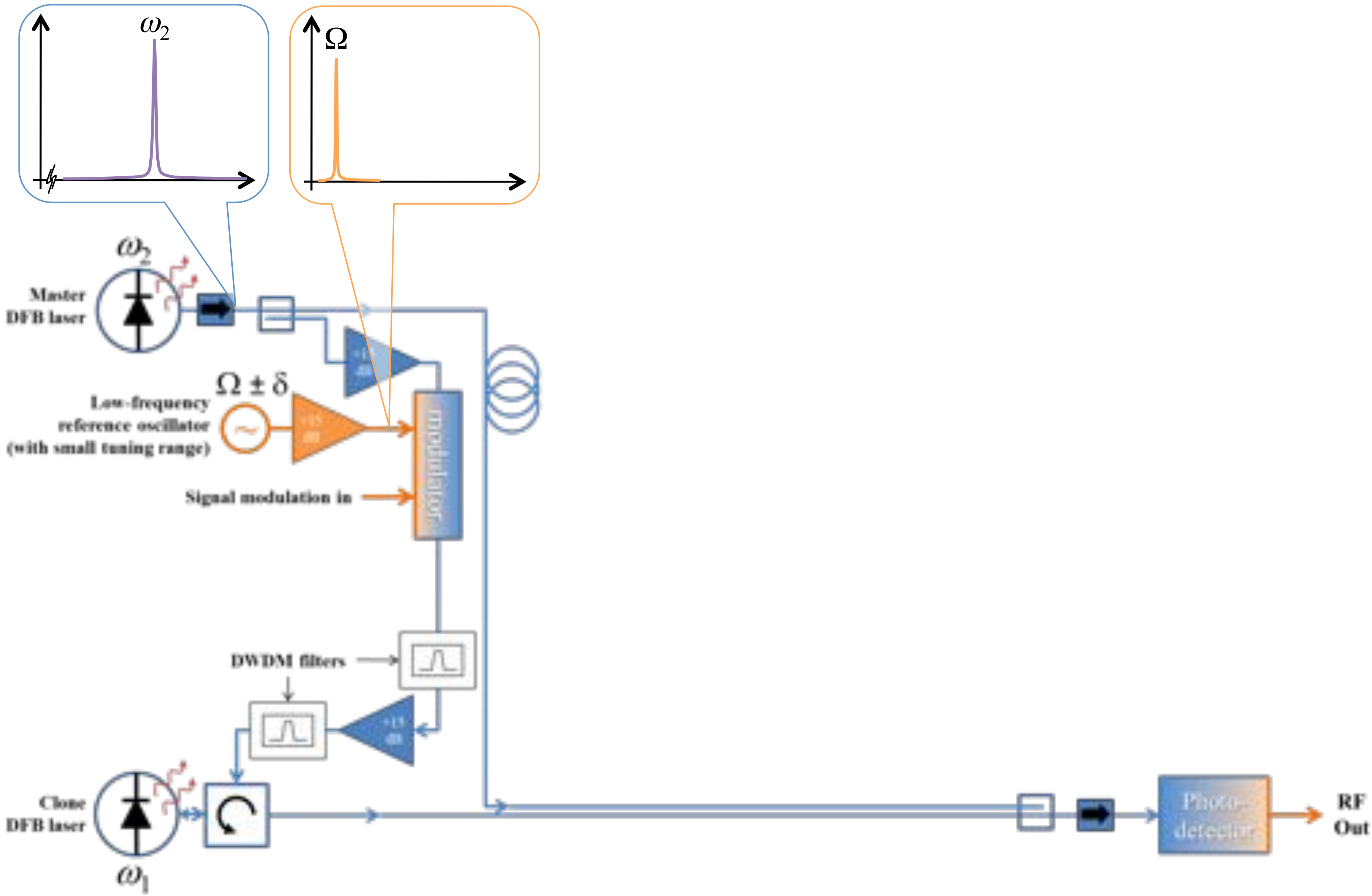

Narrow-line Widely Tunable RF Generation System

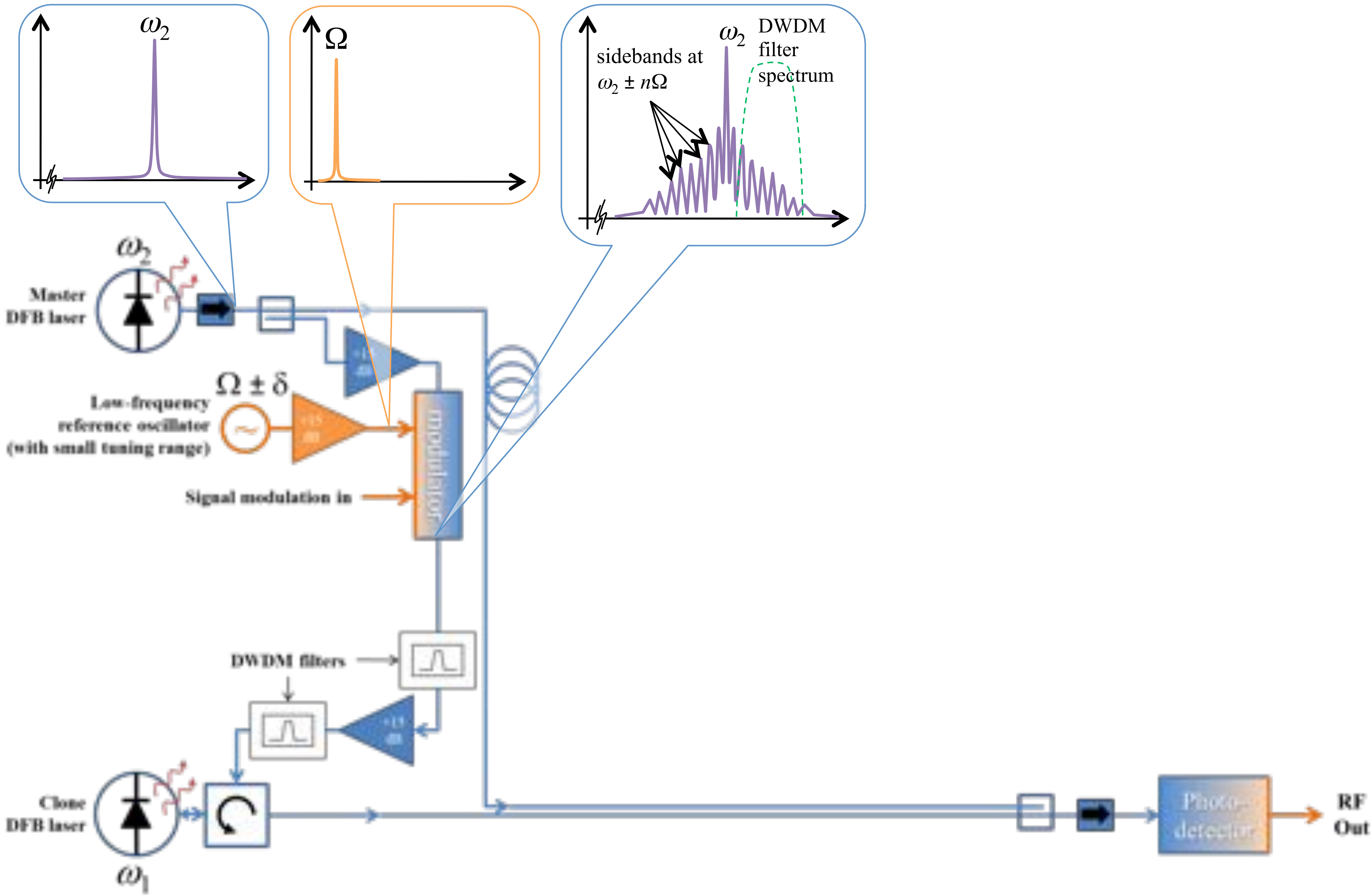

Narrow-line Widely Tunable RF Generation System

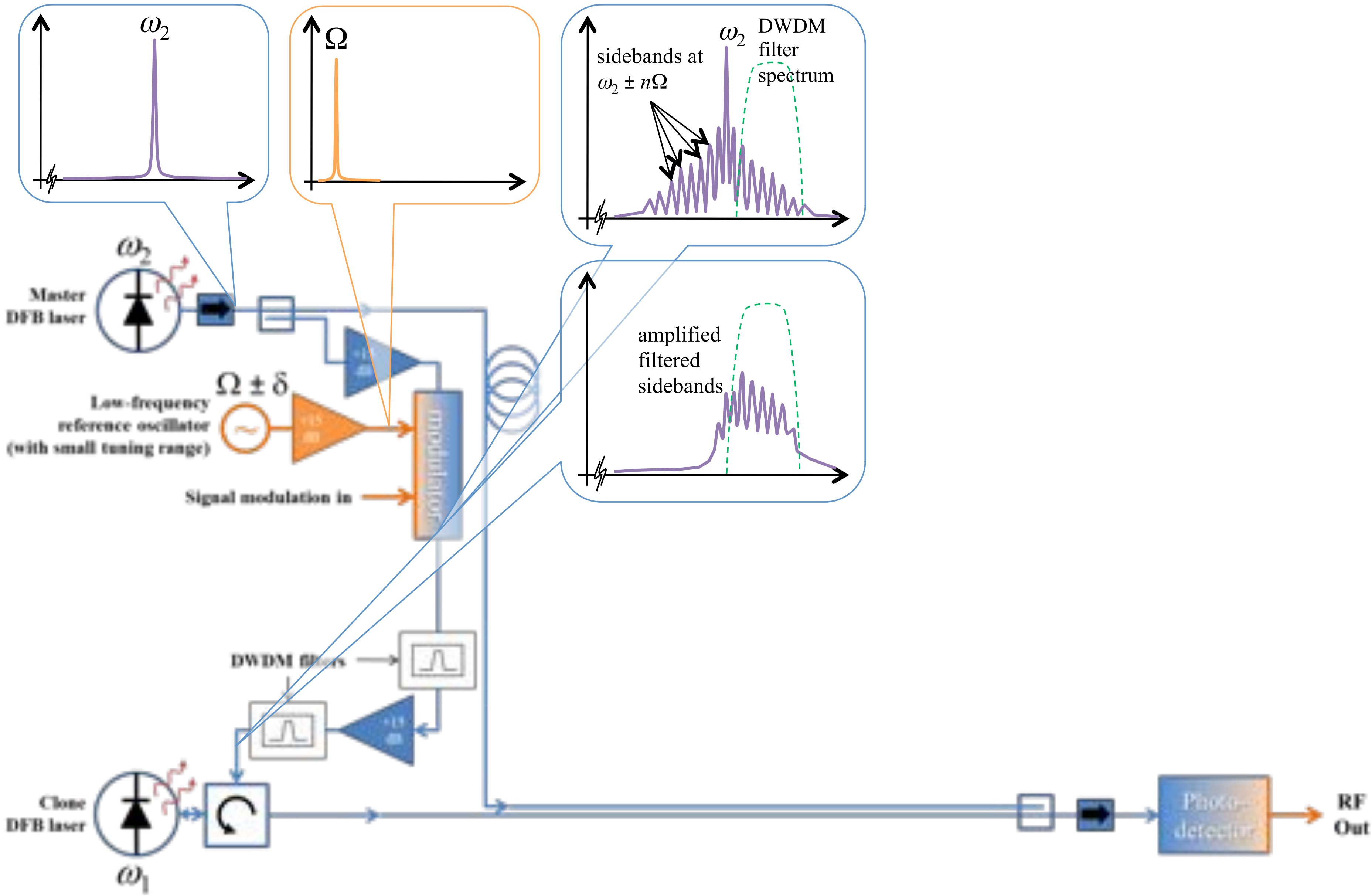

Narrow-line Widely Tunable RF Generation System

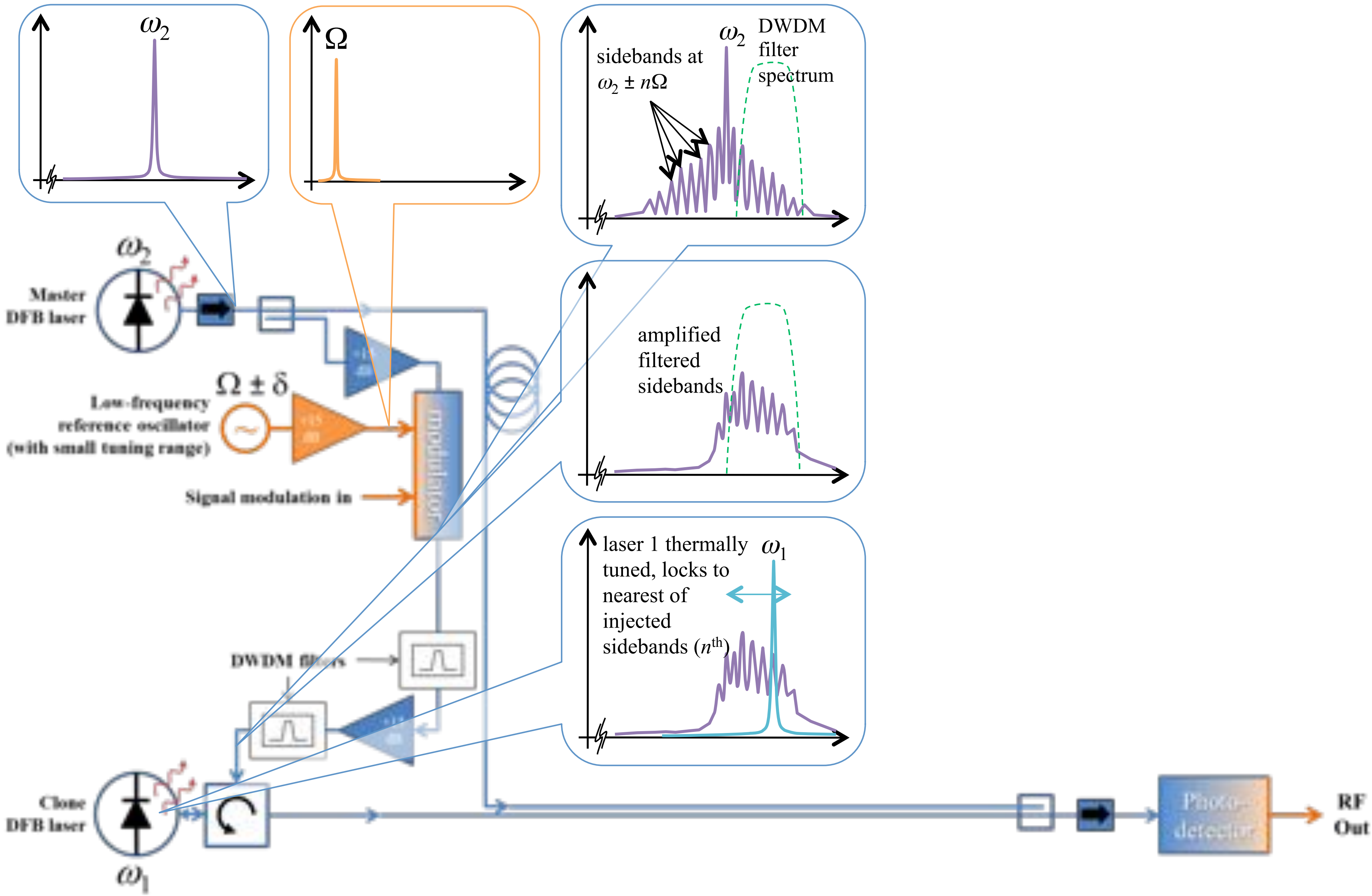

Narrow-line Widely Tunable RF Generation System

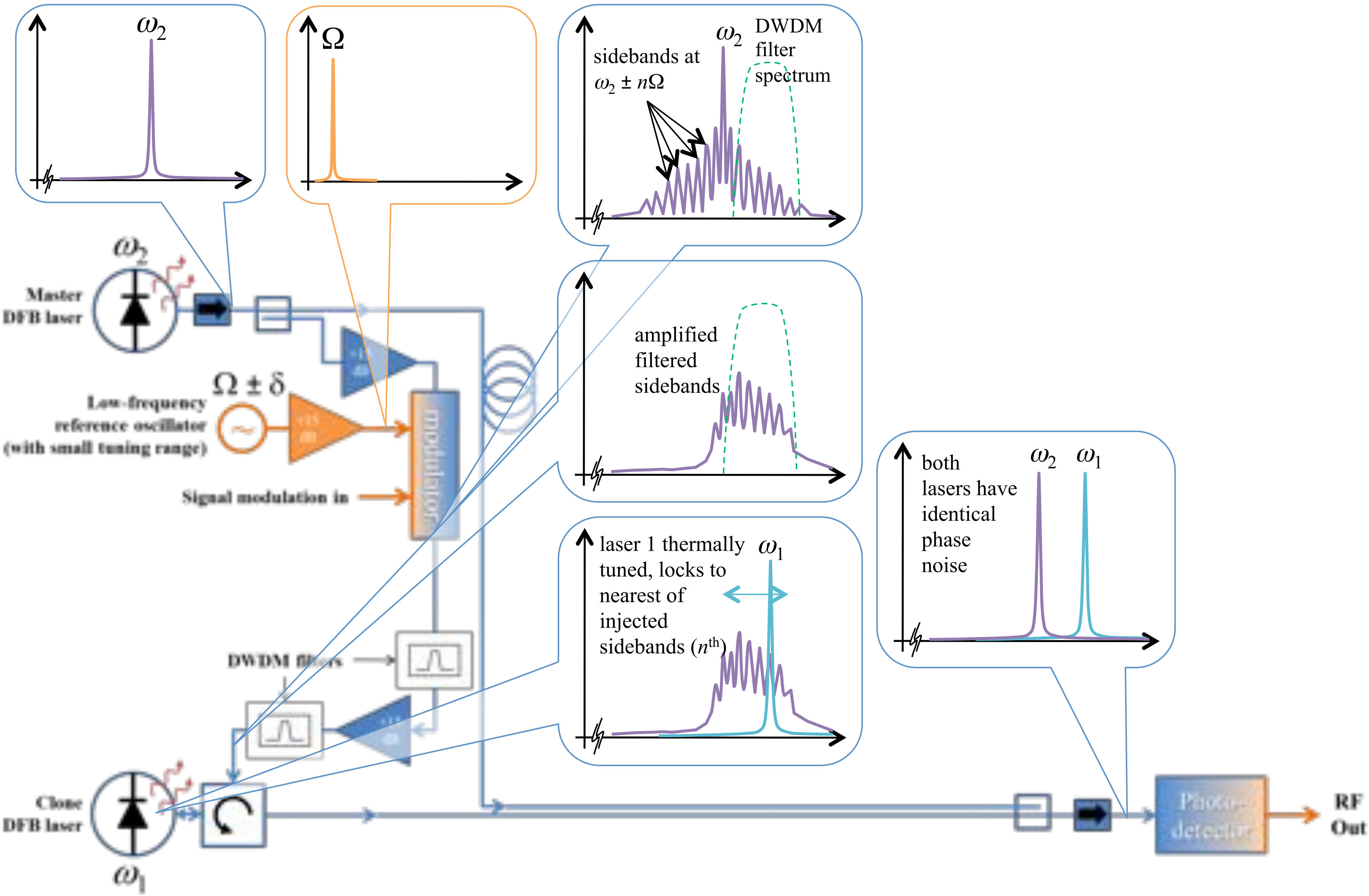

Narrow-line Widely Tunable RF Generation System

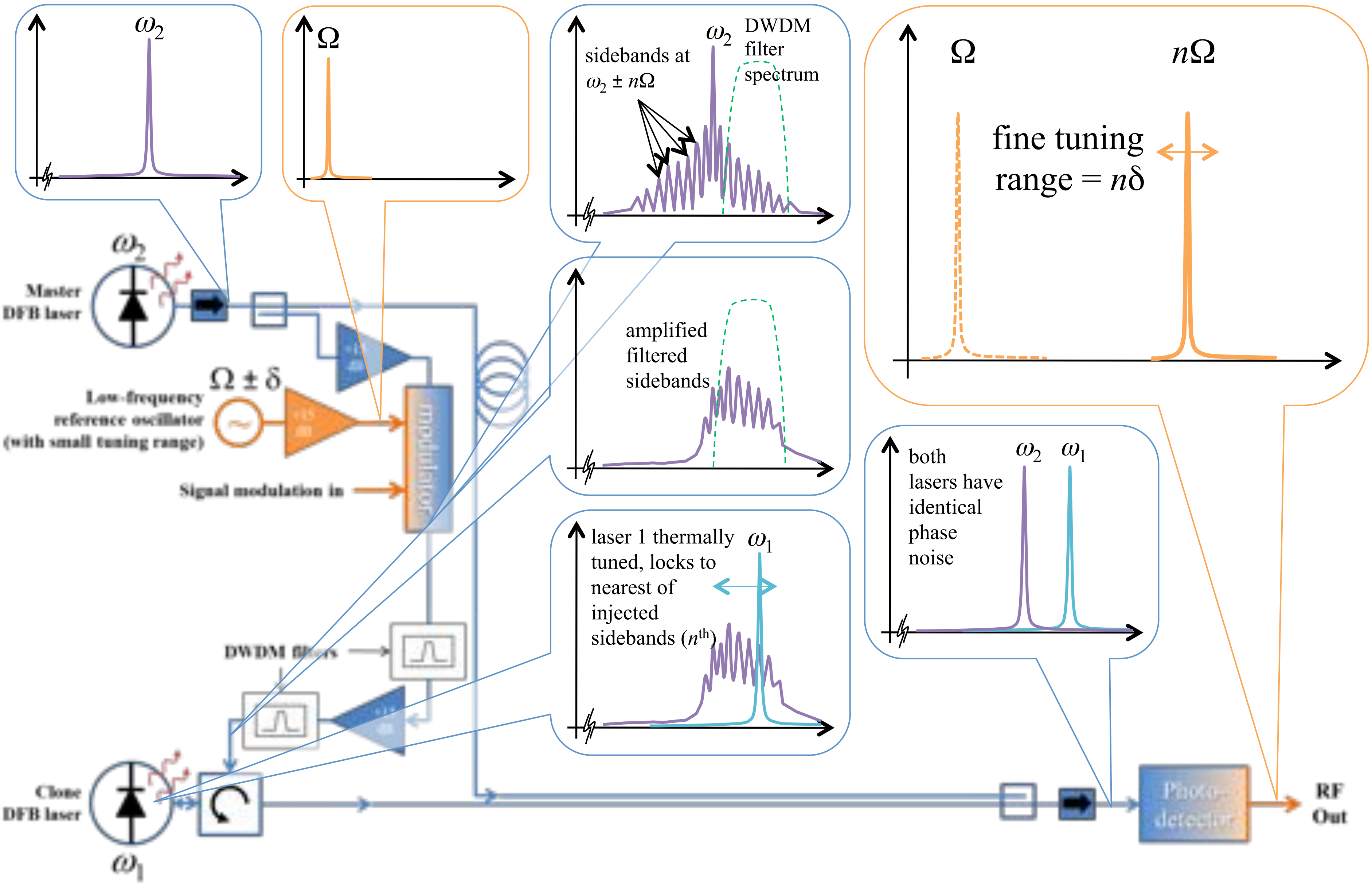

Demonstration of Narrow-line, Widely Tunable IF Synthesis

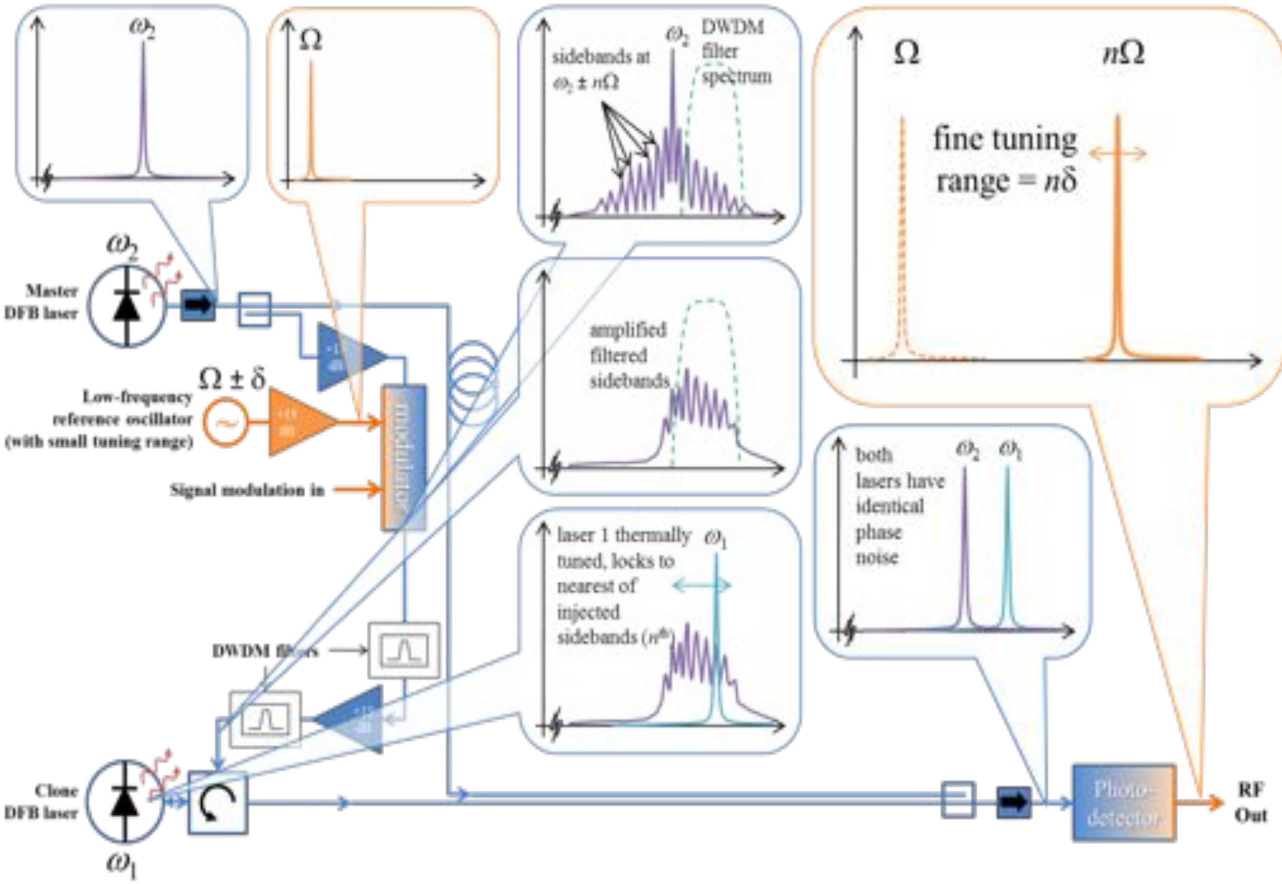

Demonstration Experiment Setup

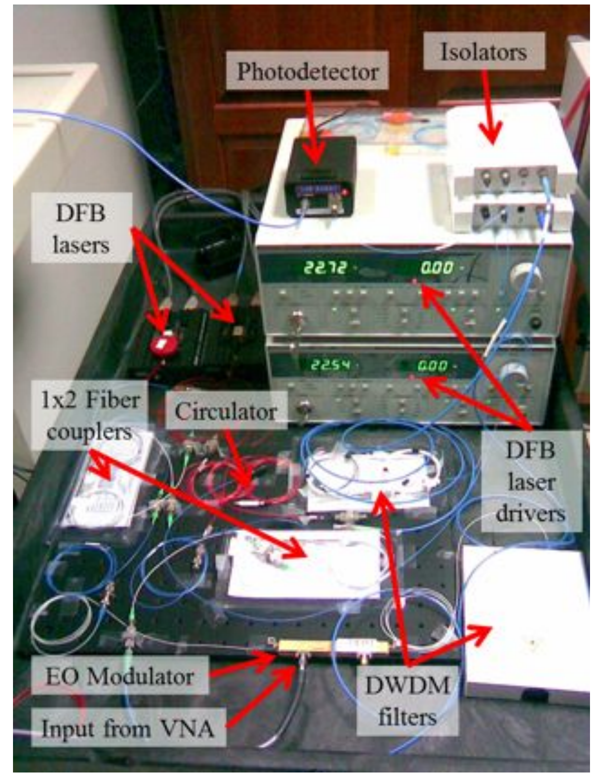

- System is designed to "clone" Laser 2 at an offset frequency using EO modulation & injection seeding, upconvert the received signal with the same modulator, then beat the Master and Clone together on a fast photodetector
  - ***Lasers' phases/linewidths cancel out, leaving only spectrally pure RF carrier + received signal!***
- Phase modulation generates many harmonics of the reference oscillator, providing ultra-wide tuning range
  - ***Clone laser can be thermally tuned, will lock to nearest of the injected harmonics***

Coherent Optical Heterodyne Receivers: Summary of Accomplishments

- **Linewidth of 1-2 Hz** has been demonstrated over a range from *0.6-49 GHz* (upper limit is photodetector bandwidth)
- **Thermally tuned DFB grating in clone laser provides built-in filtering** which allows locking to single sideband when injecting of a comb of harmonics derived from a common reference
- **Lasers can be locked to harmonics of the reference-oscillator frequency**—locking has been demonstrated with 2nd through 10th harmonics, *demonstrating wide tunability of RF from a single, low-frequency reference, while preserving the optical phase-noise cancellation from injection locking*

Measured RF Spectra from Locked Lasers

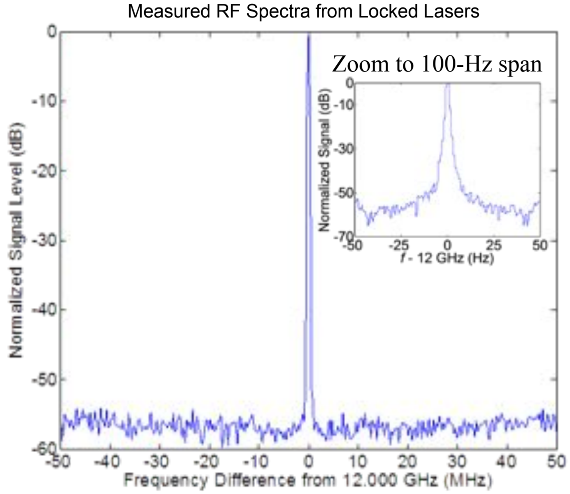

12-GHz Carrier Modulated by 8-GHz Sine Wave

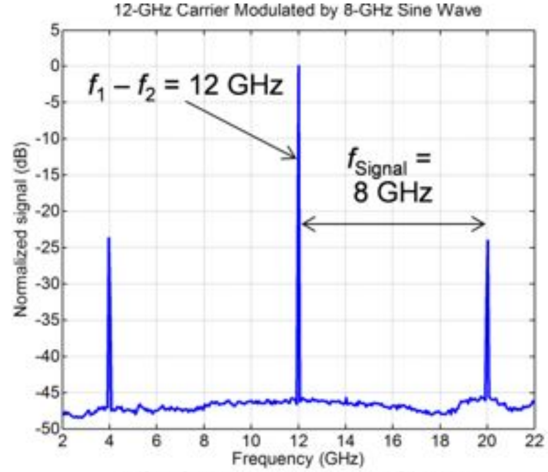

Phase noise of RF signal from locked lasers at several carrier frequencies.

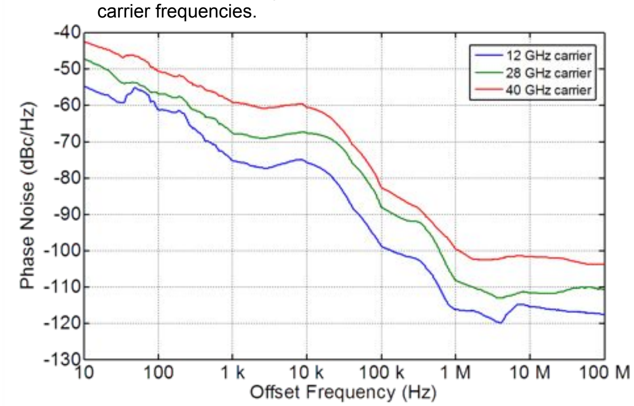

RF spectra when modulating a 12-GHz carrier with various 2-MHz waveforms

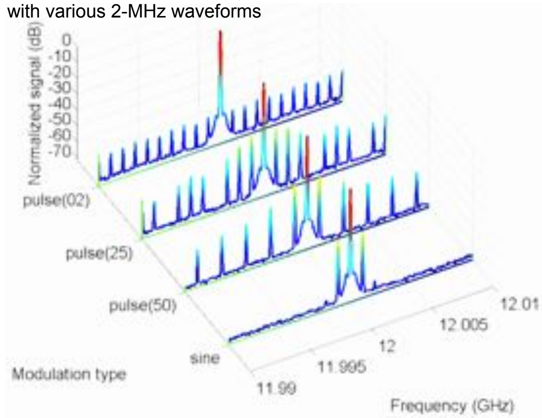

12-GHz Carrier Modulated by 1-kHz Sine Wave

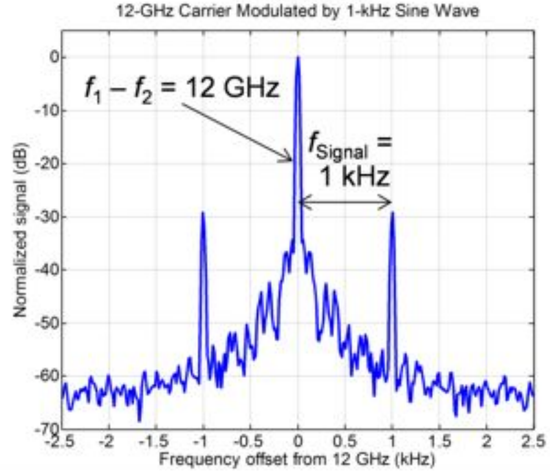

Phase noise at 24 GHz using various combinations of reference frequency and harmonic number

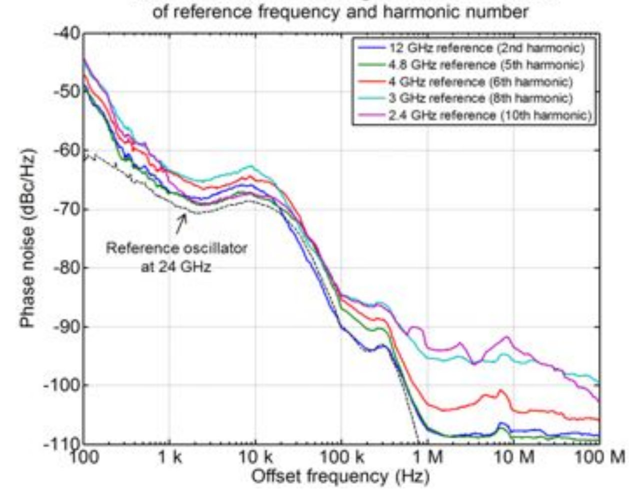

Example Signal: 2-MHz Sine Wave AM Modulated by 1-kHz Square Wave

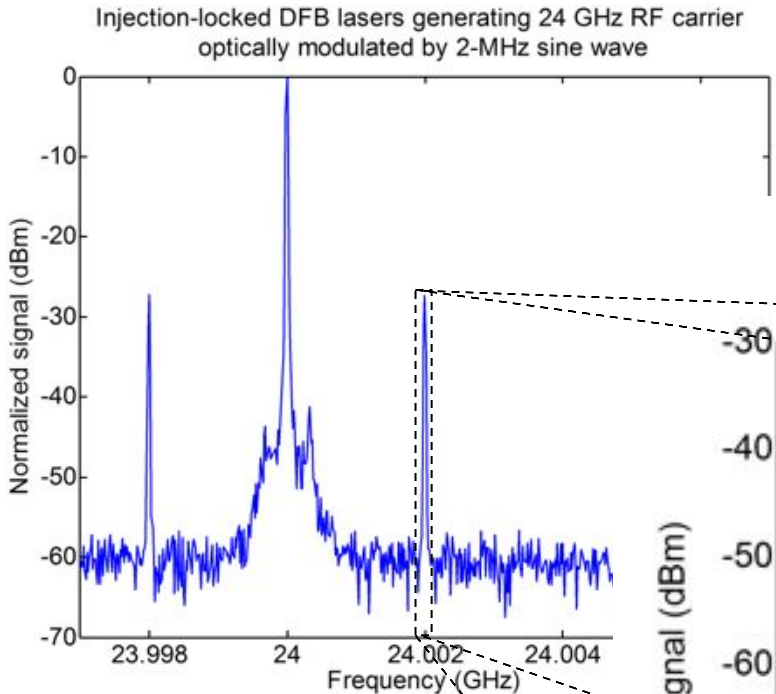

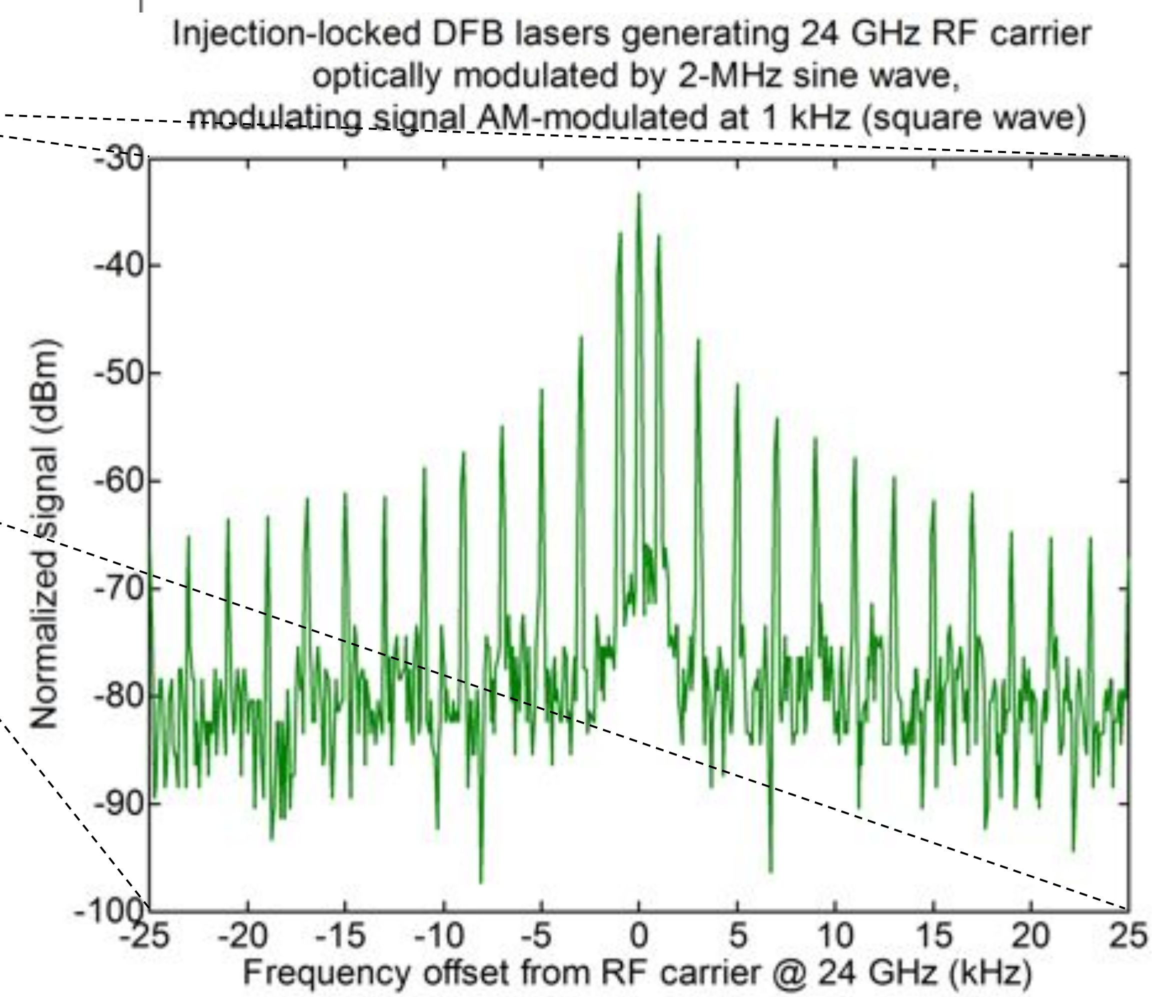

- Over 20 harmonics of 1-kHz square-wave modulation signal can be recovered with >10 dB SNR, and **each with ~1-Hz linewidth!**

Integrated DC-40GHz Photodiode Circuit

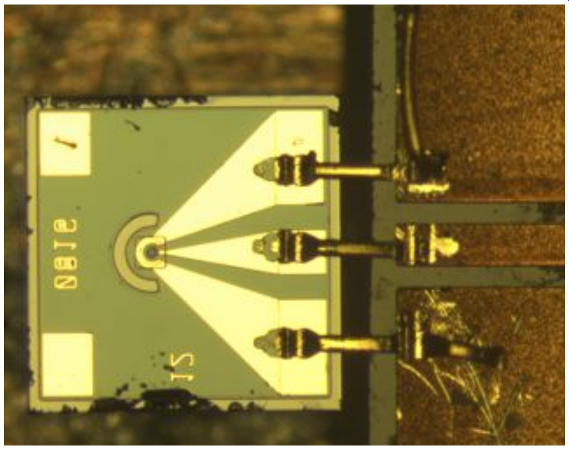

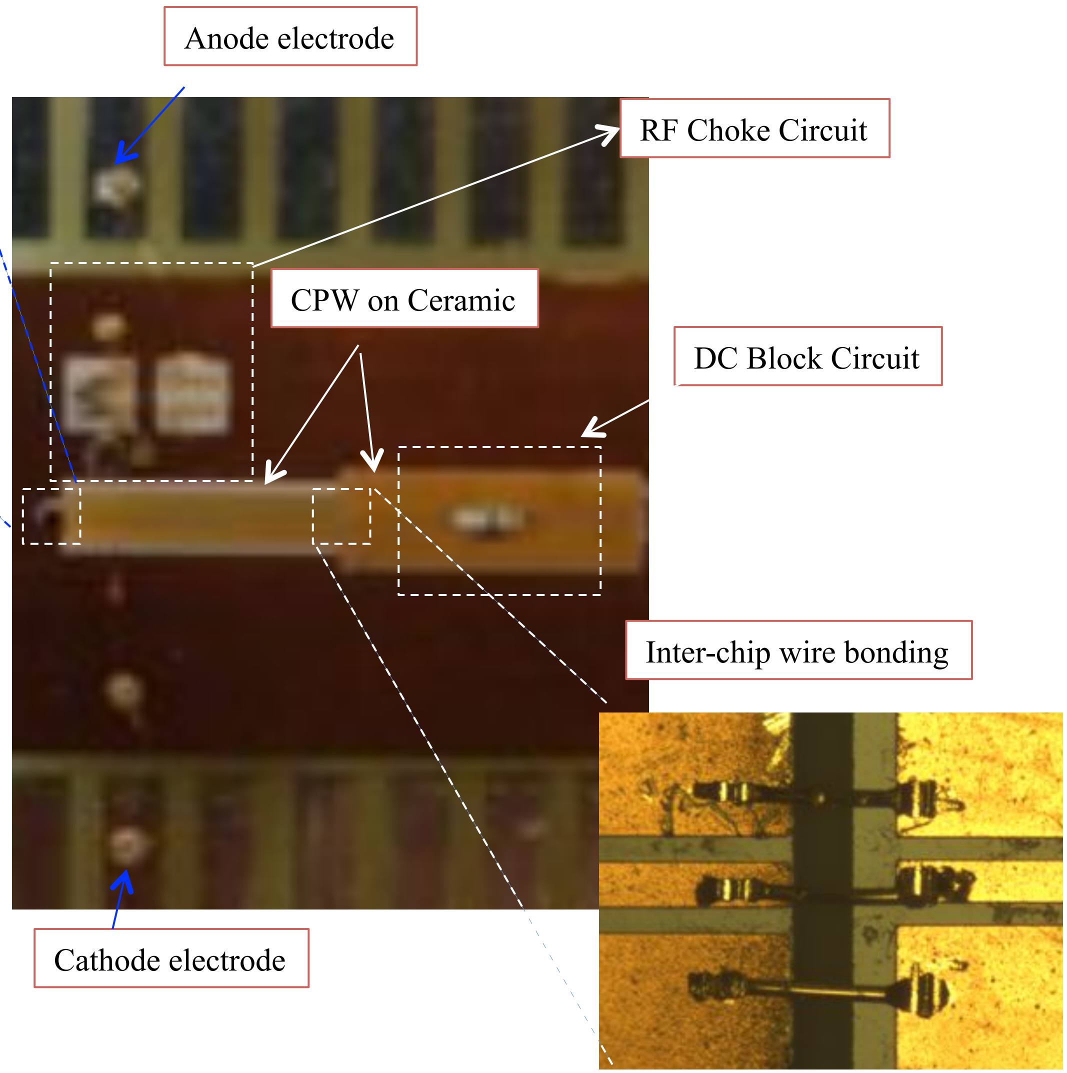

Photo-diode Chip Data:

- Bandwidth: DC-40 GHz
- Max CW Optical Power: 5 mW
- DC Responsivity: 0.55
- Output RF: 50 ohm CPW

Ultra-wideband Integrated Power Amplifier

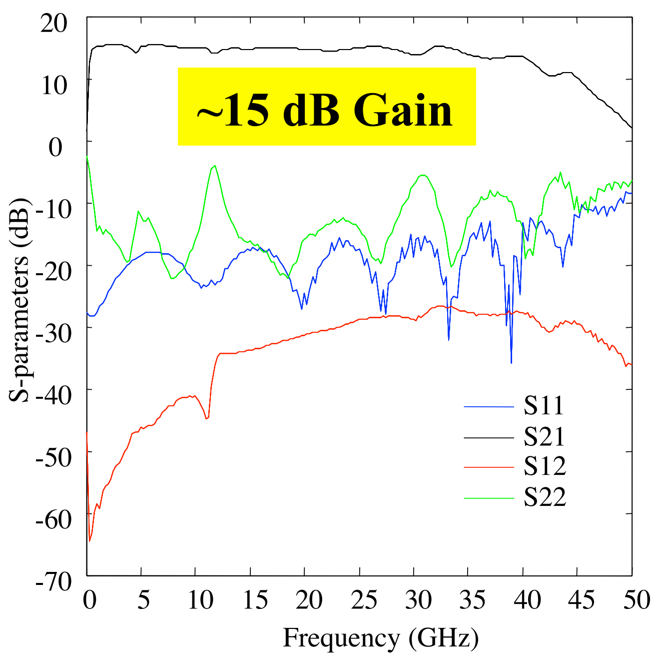

Measured Phase

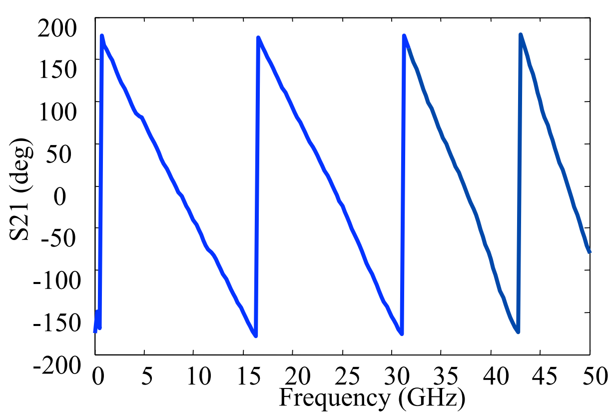

Characterization setup

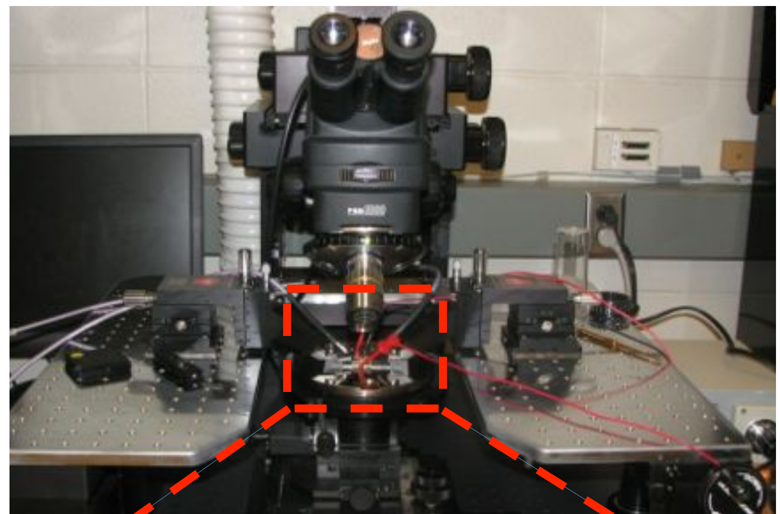

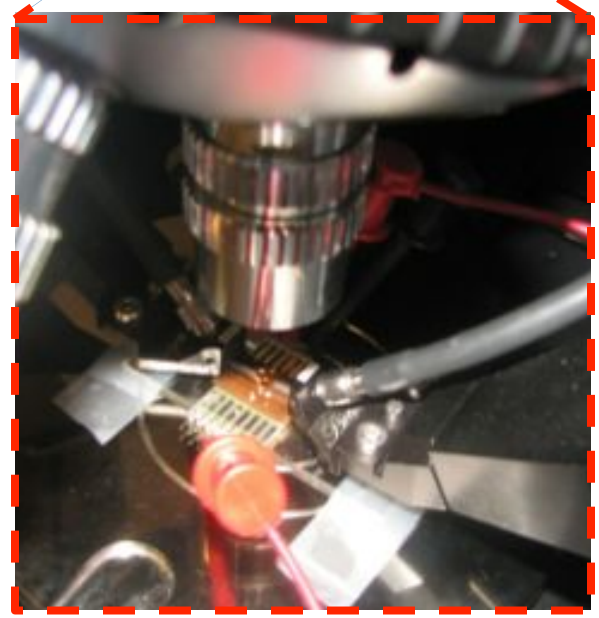

Experiment Setup

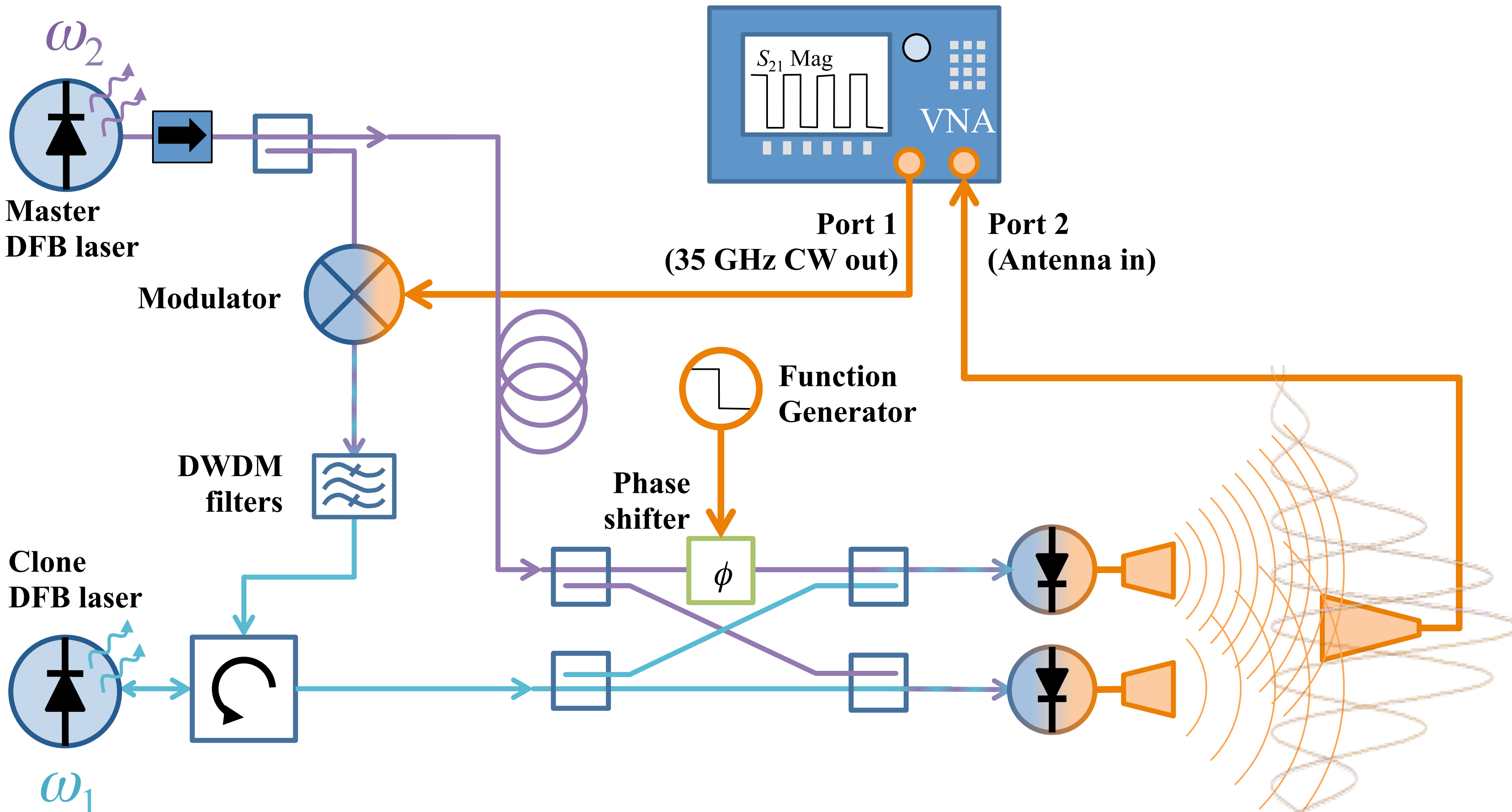

- Optical phase shift applied to one laser causes RF interference pattern to shift by the same amount

Optically-fed Phased Array Demonstration

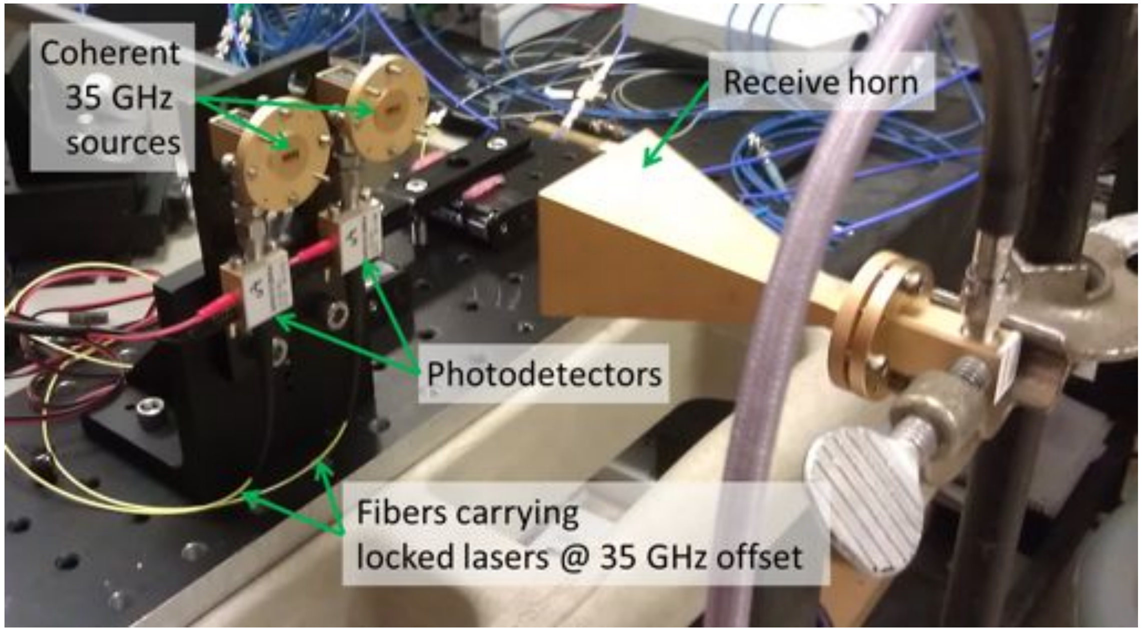

Top view

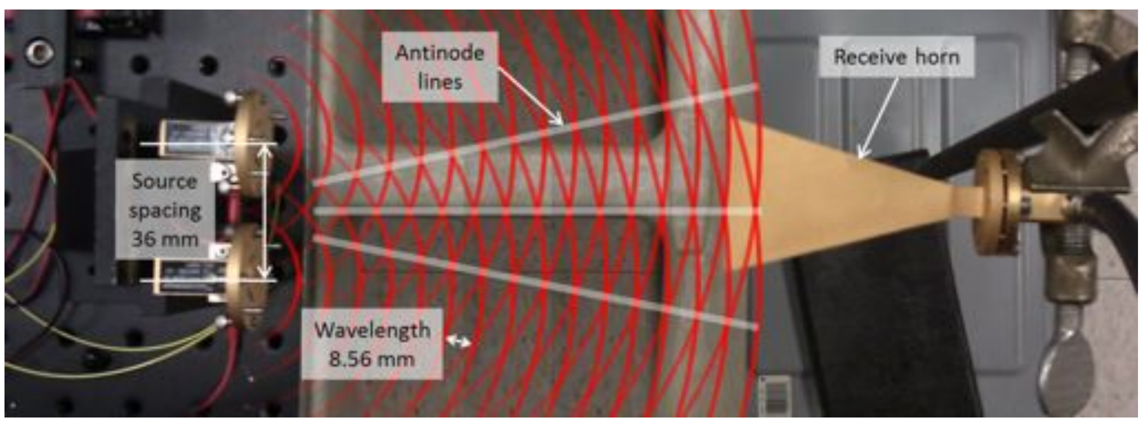

Results: Square-wave Modulation

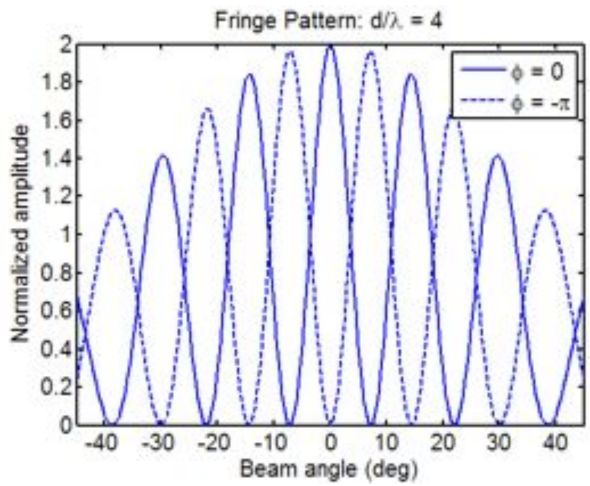

- Total phase between RF sources is $\phi = \phi_0$ + modulation phase
- Antenna position kept constant, modulation phase varies between $-\pi/2$ and $+\pi/2$ with modulation frequency of ~400 Hz

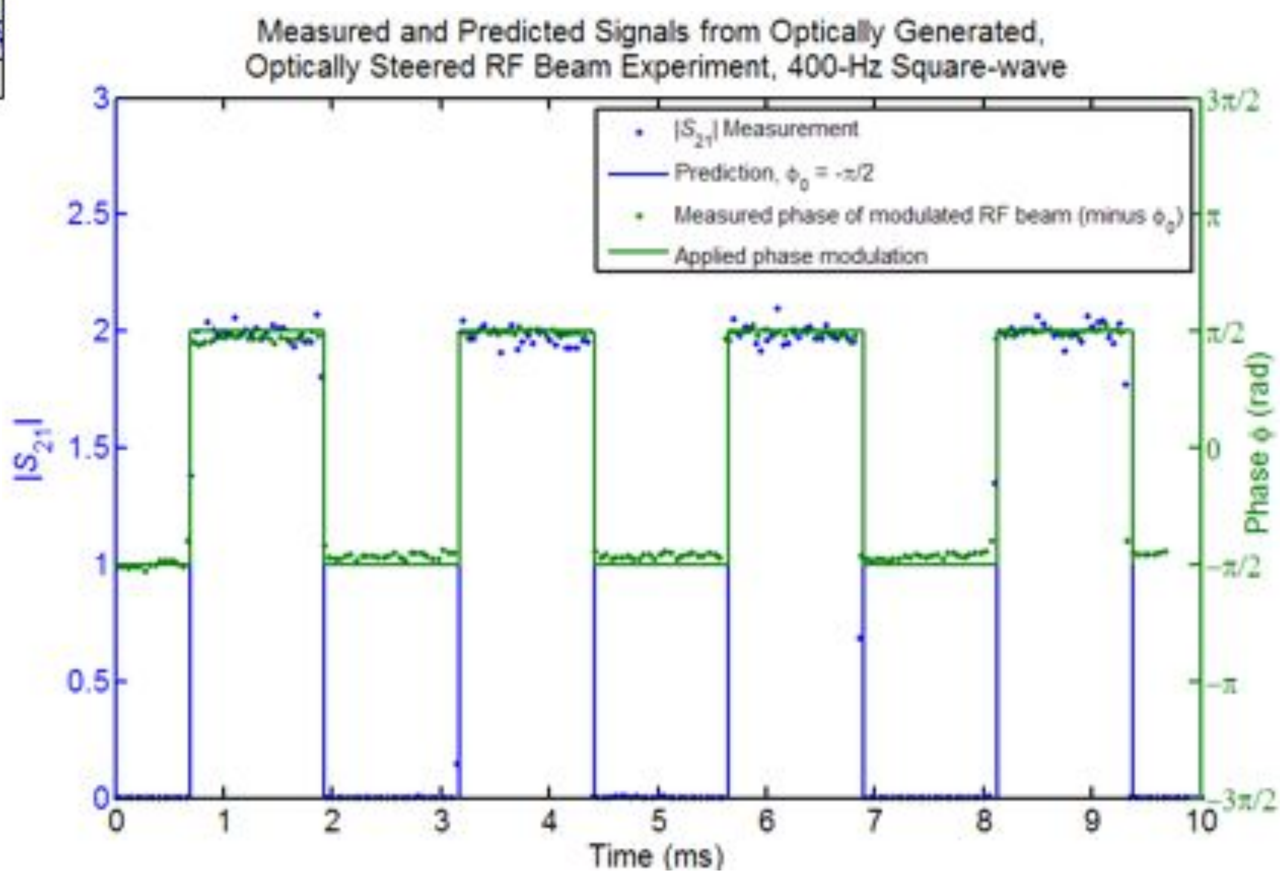

Integrated Silicon RF Photonics

Integrated RF-Photonic Module

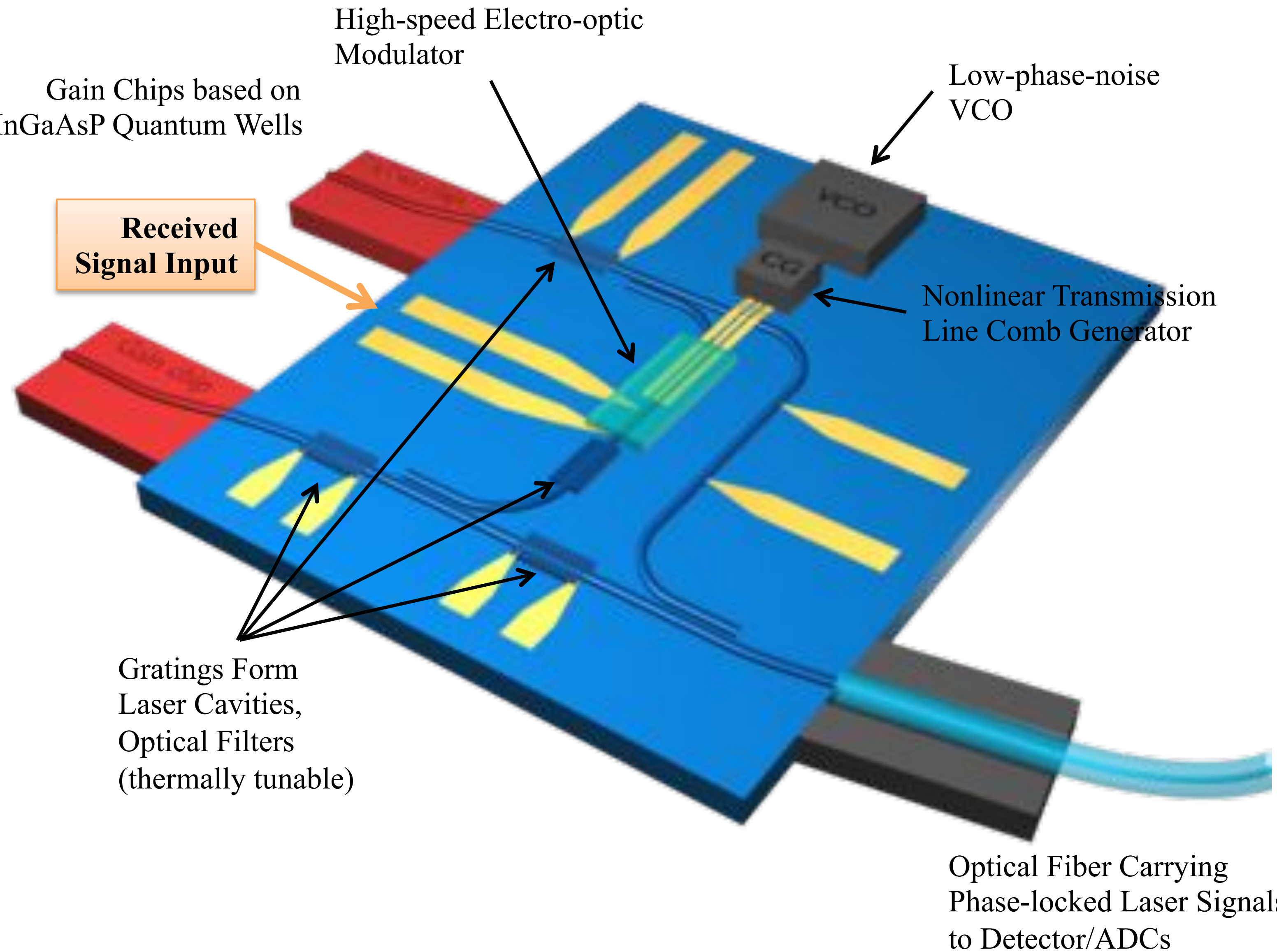

Future Integrated Device

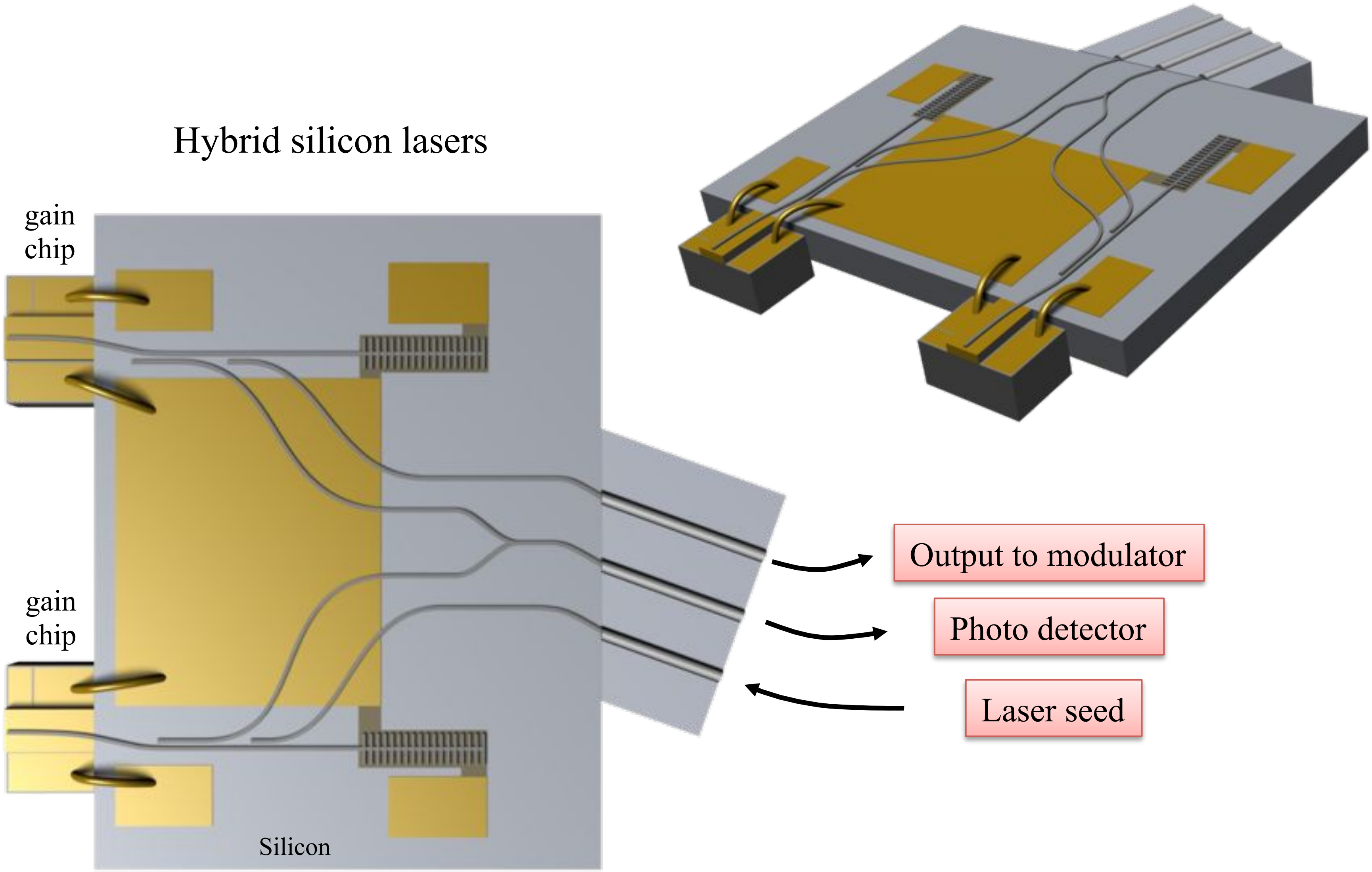

Gain Chip Alignment with Silicon Cavity

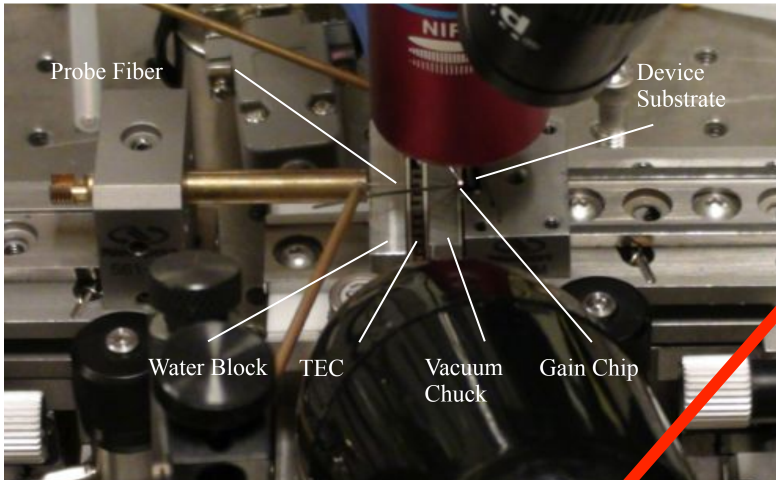

Macro view of alignment stage intended to be used to attach the gain chips to the substrate while monitoring output characteristics

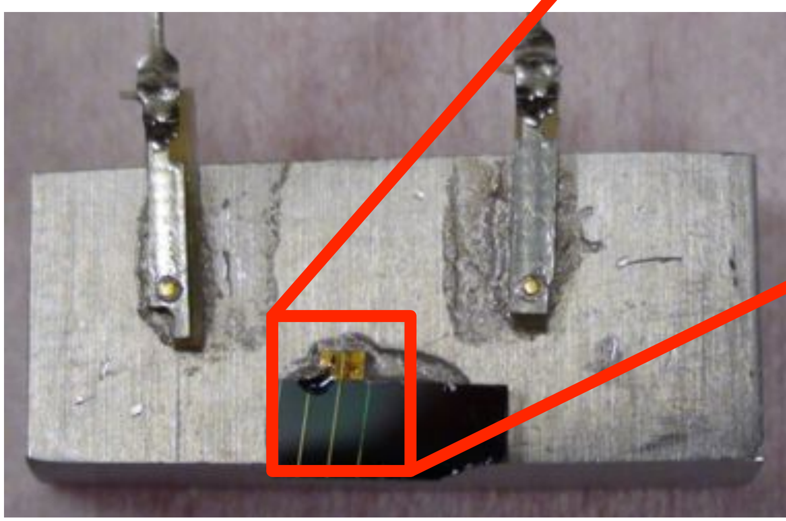

Integrated Silicon Laser for RF Generation

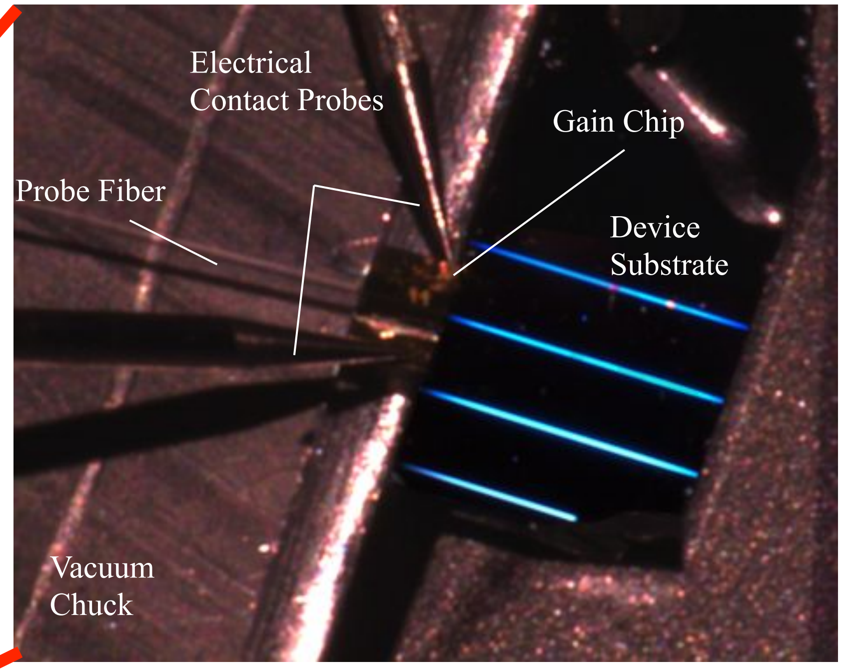

Close up of gain chip aligned to waveguide on substrate

Process Refining and Calibration

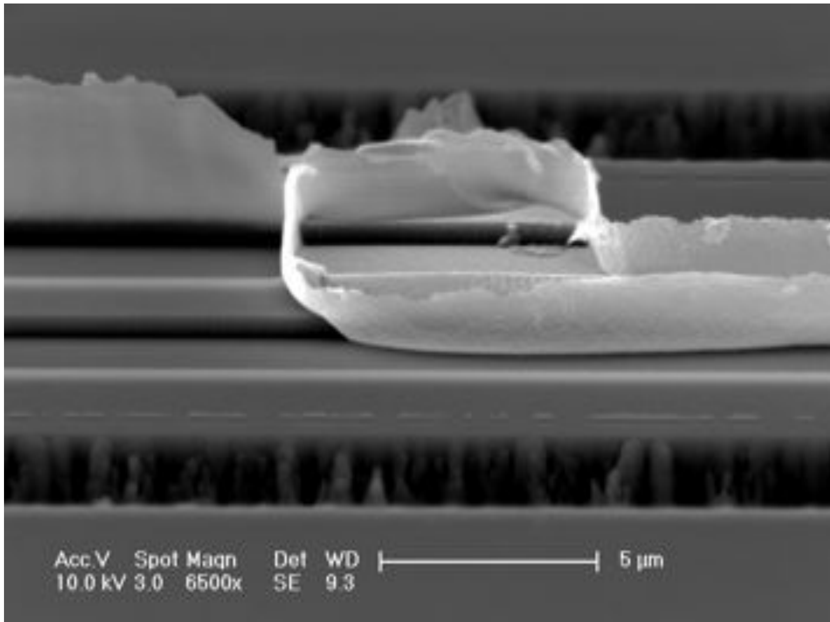

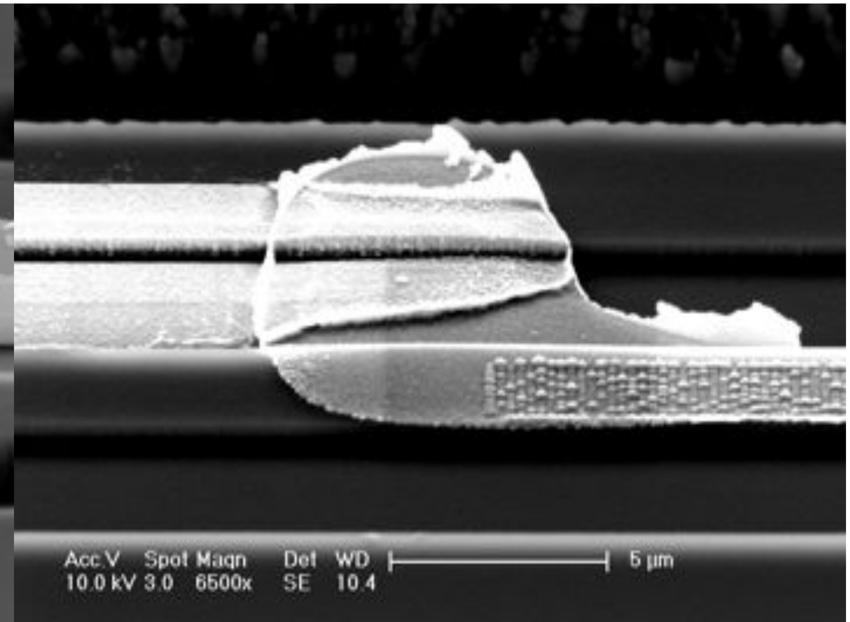

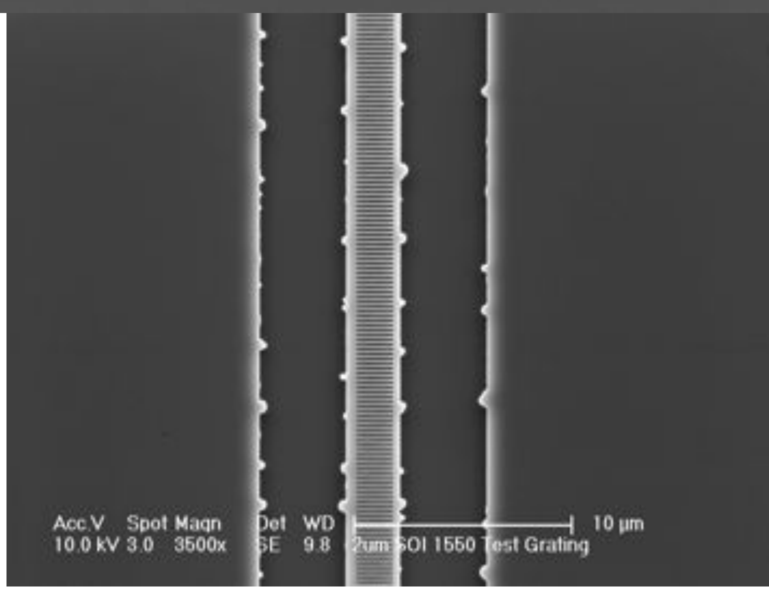

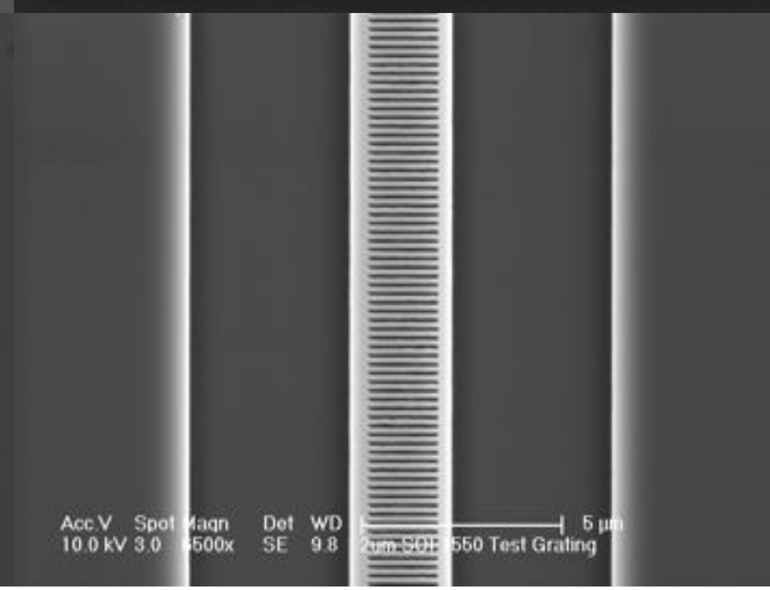

Testing Setup

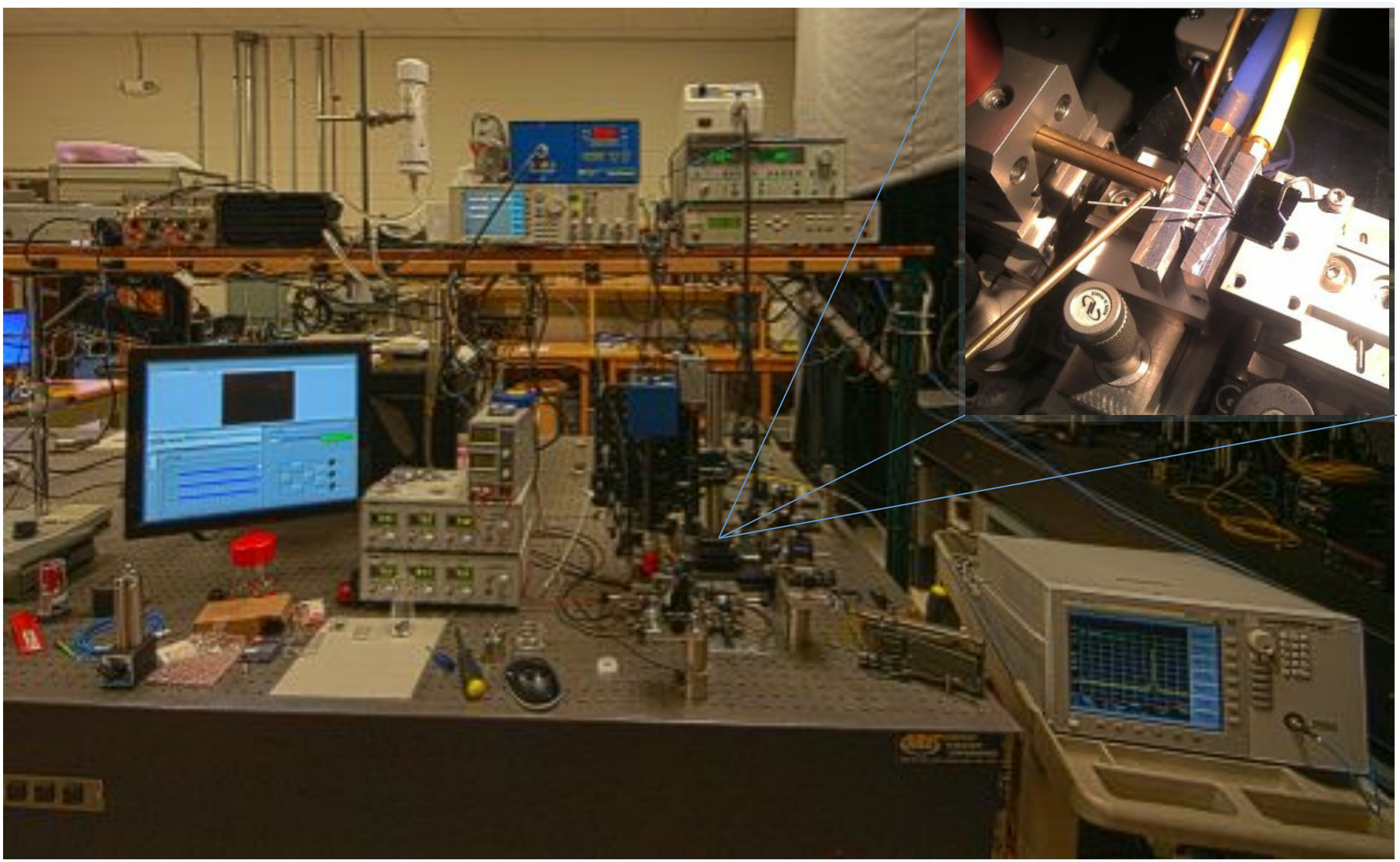

Tuning Distributed Bragg reflector (DBR)

- Tunes at approximately 0.09 nm/ºC

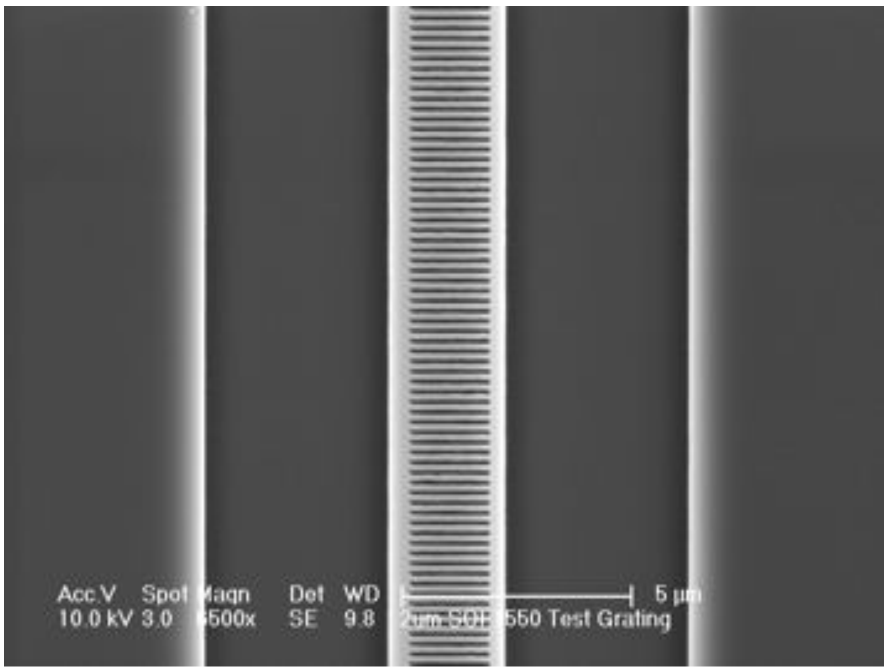

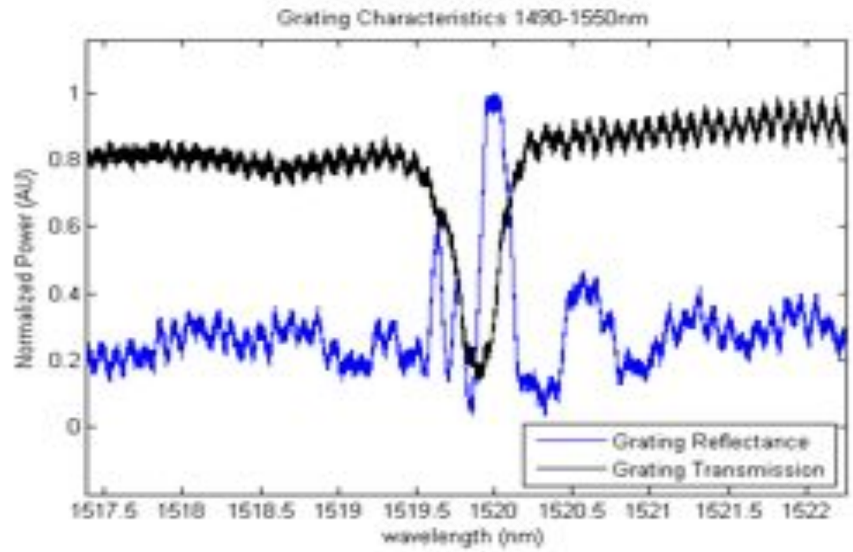

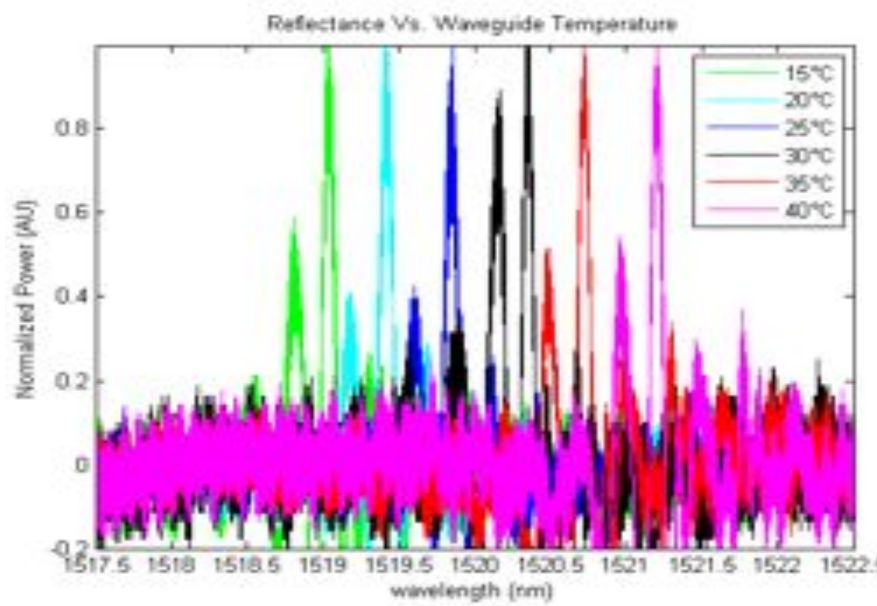

Integrated III-V and Silicon Photonic Laser

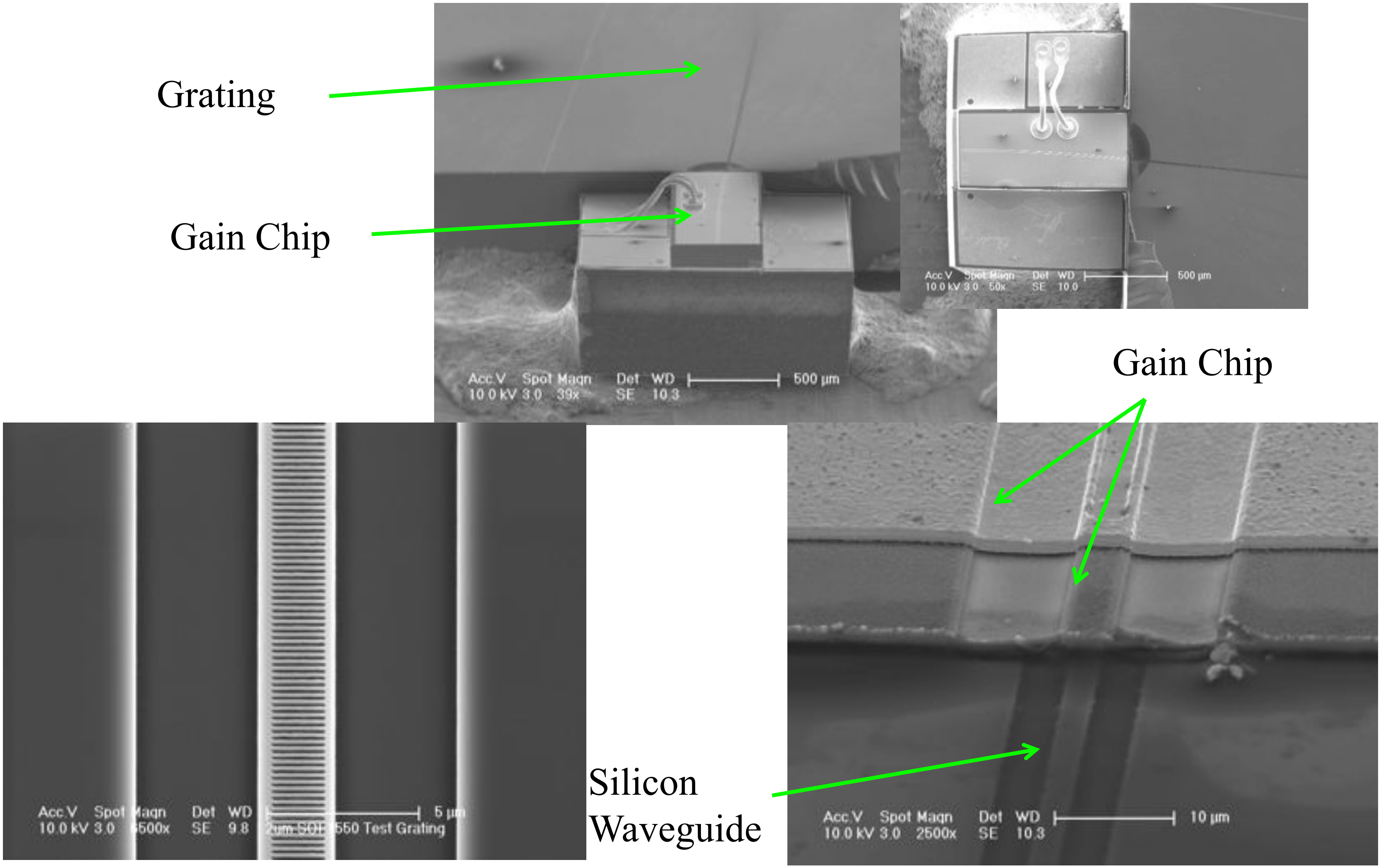

Hybrid III-V - Silicon Laser

ept

Realization

Characterization

Gain Chip

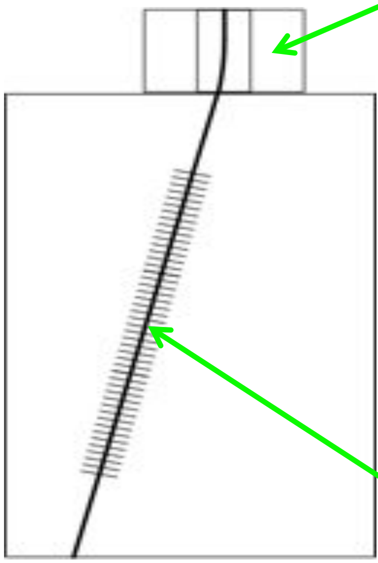

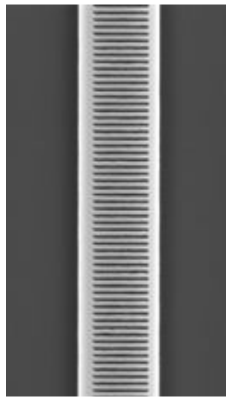

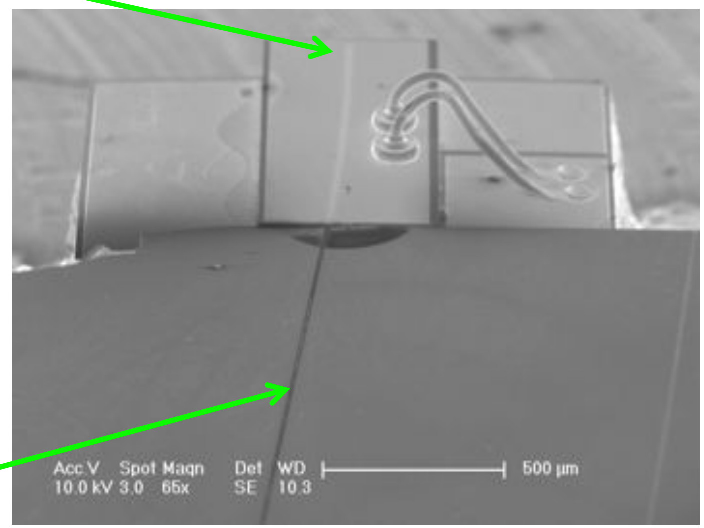

Grating

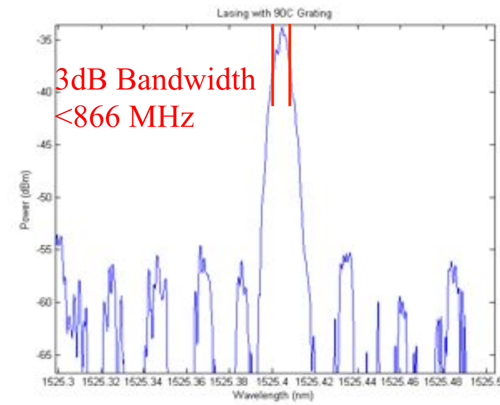

Evolution

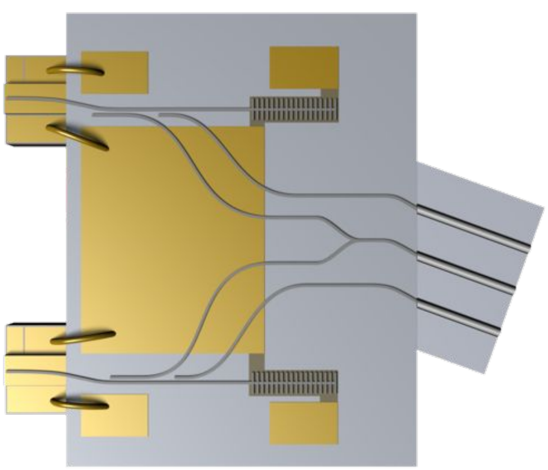

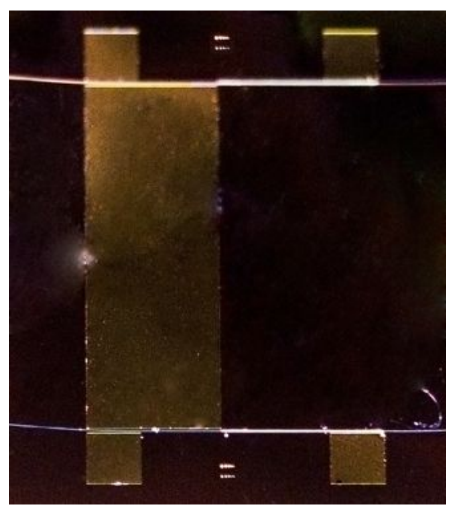

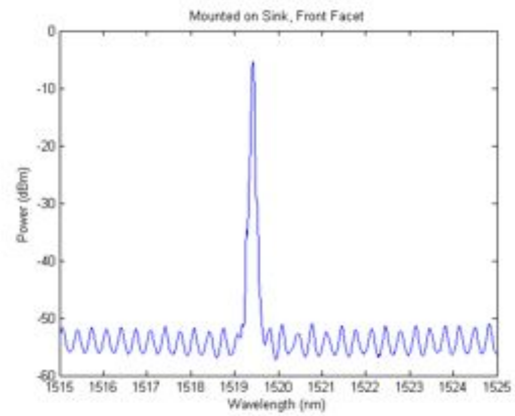

Dual Laser Design

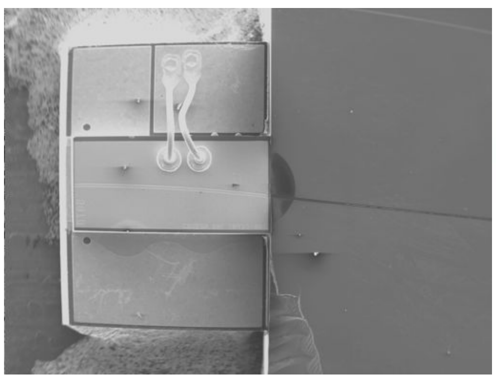

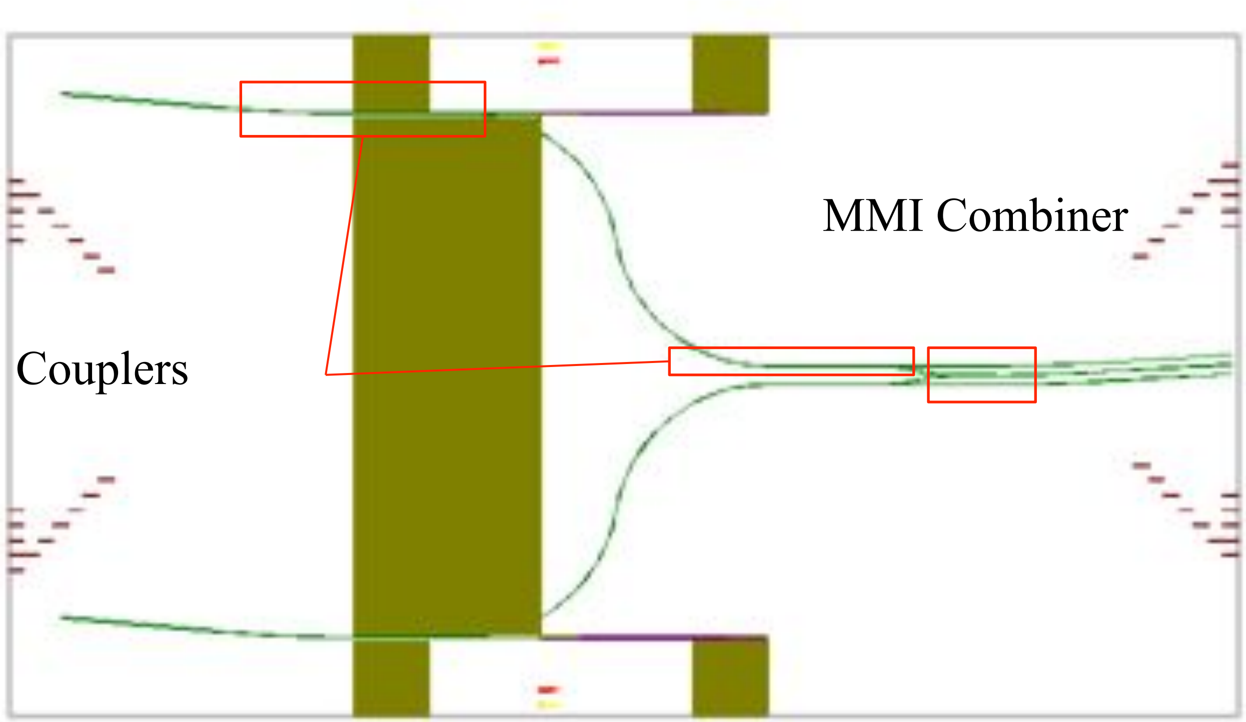

Dual Laser Integration

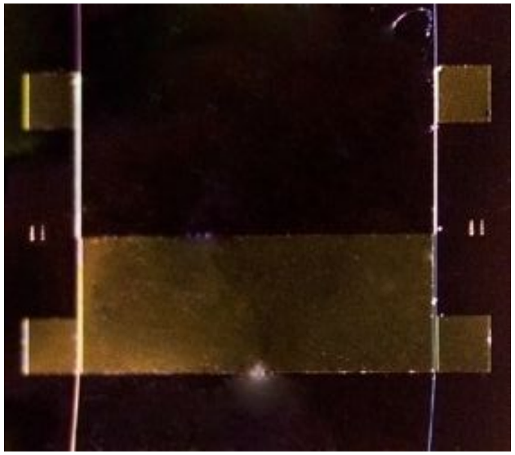

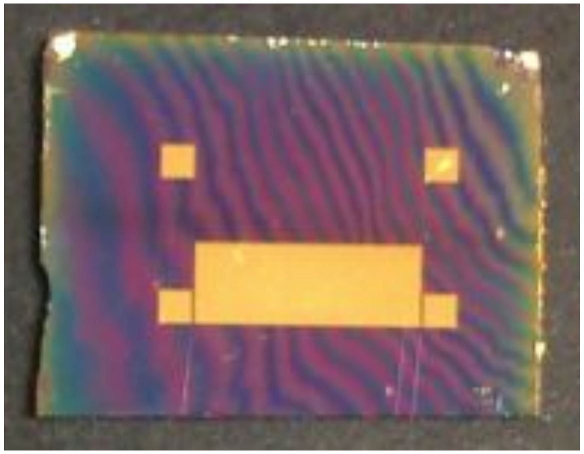

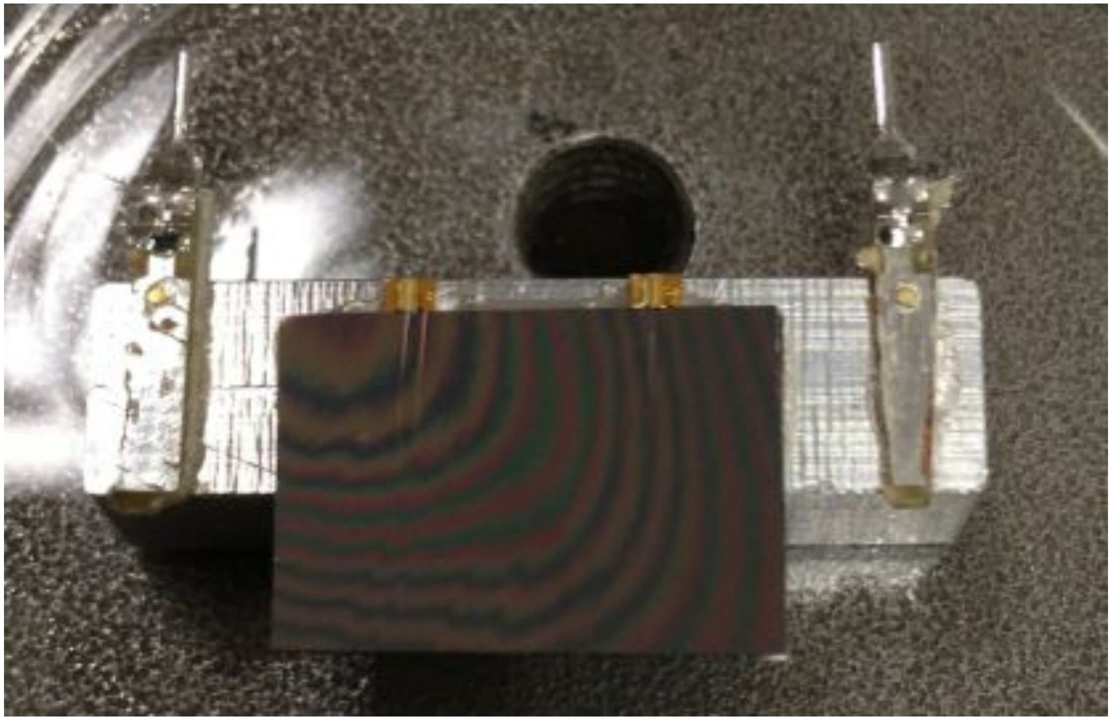

2 Functioning Lasers

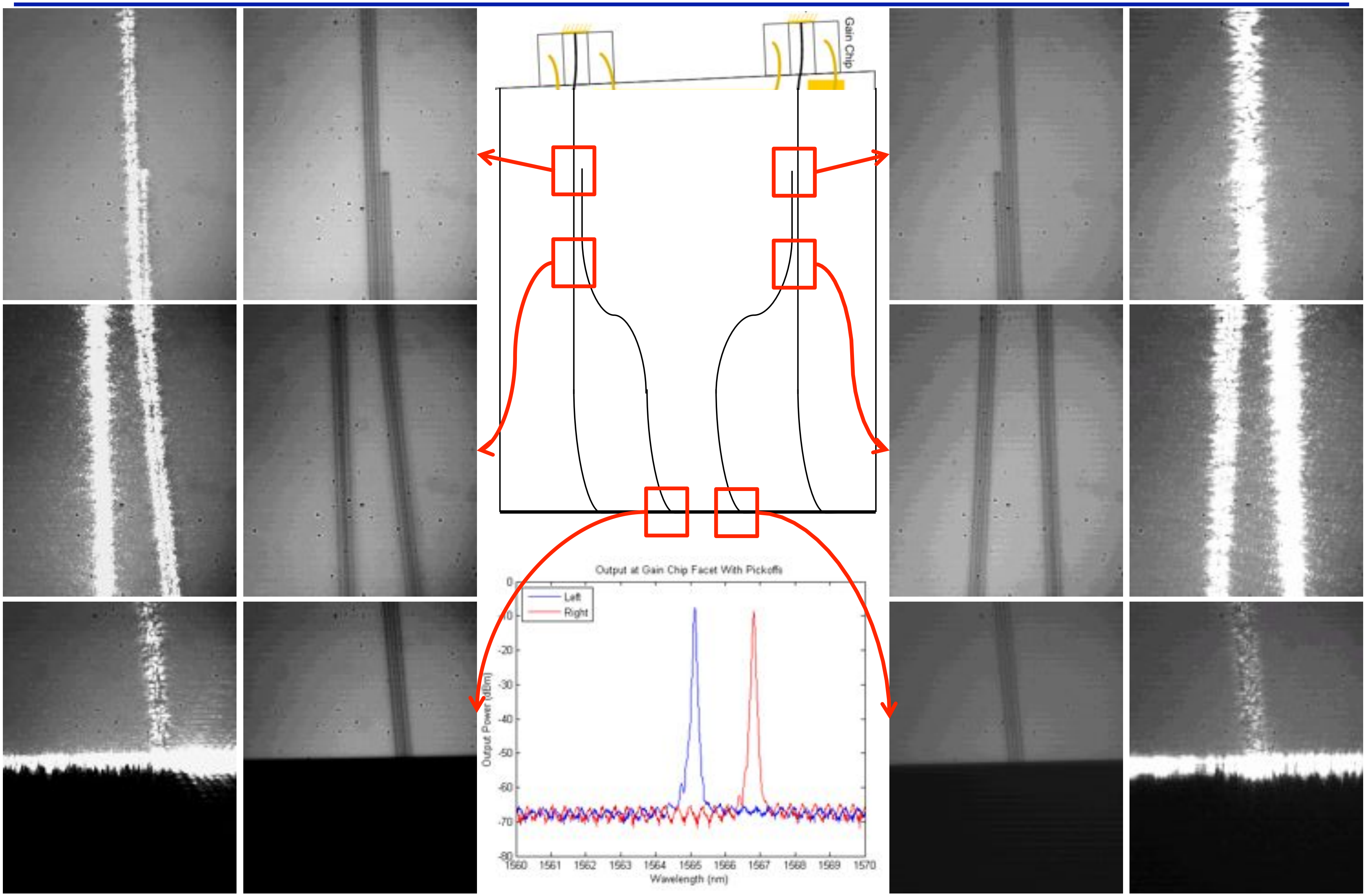

Two Lasers on a Chip

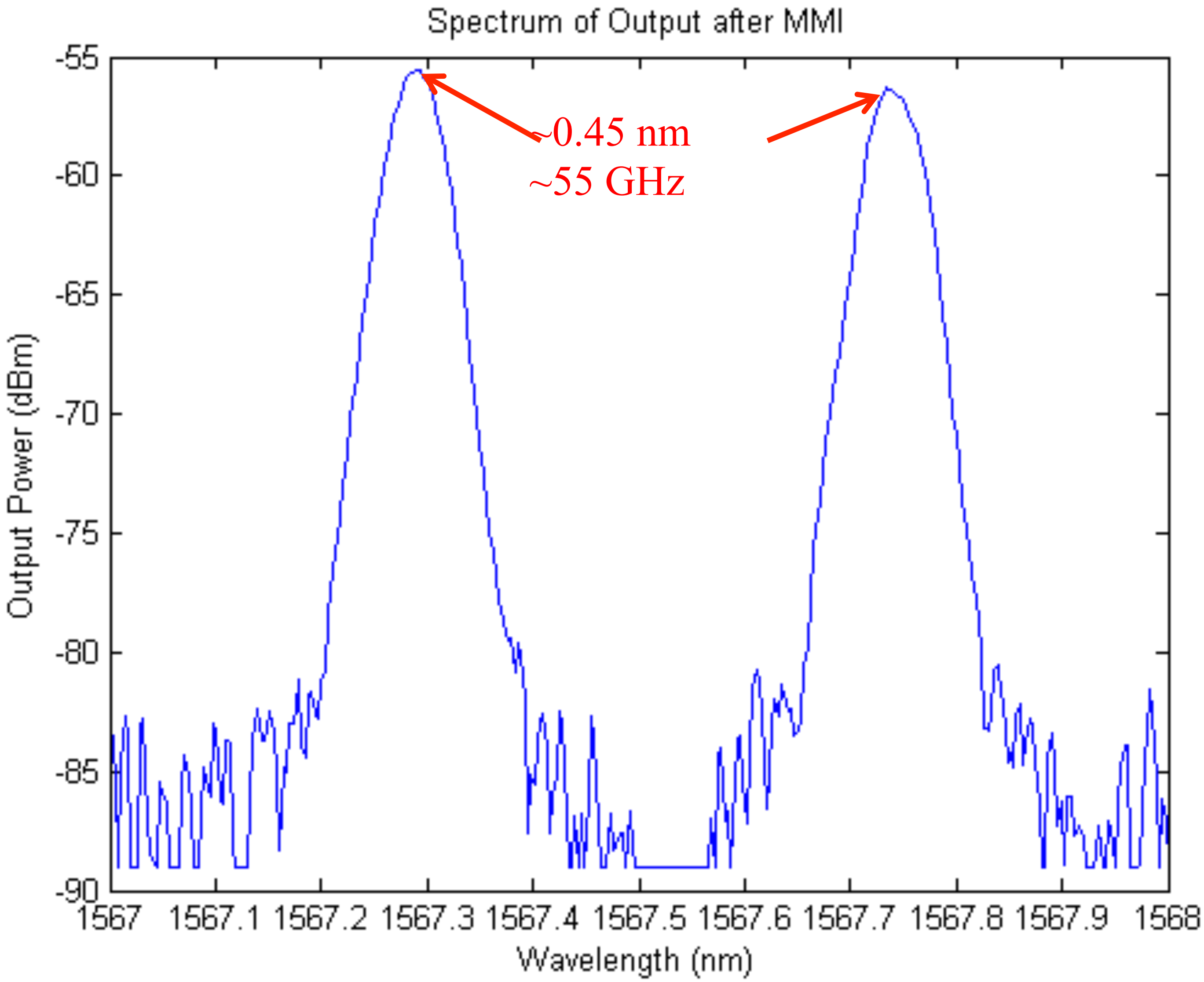

Silicon Nanomembrane 3D Integration for RF Signal Routing

UNIVERSITY OF DELAWARE

1743

UNIVERSITY OF DELAWARE

Si-NM Released from SOI Substrate

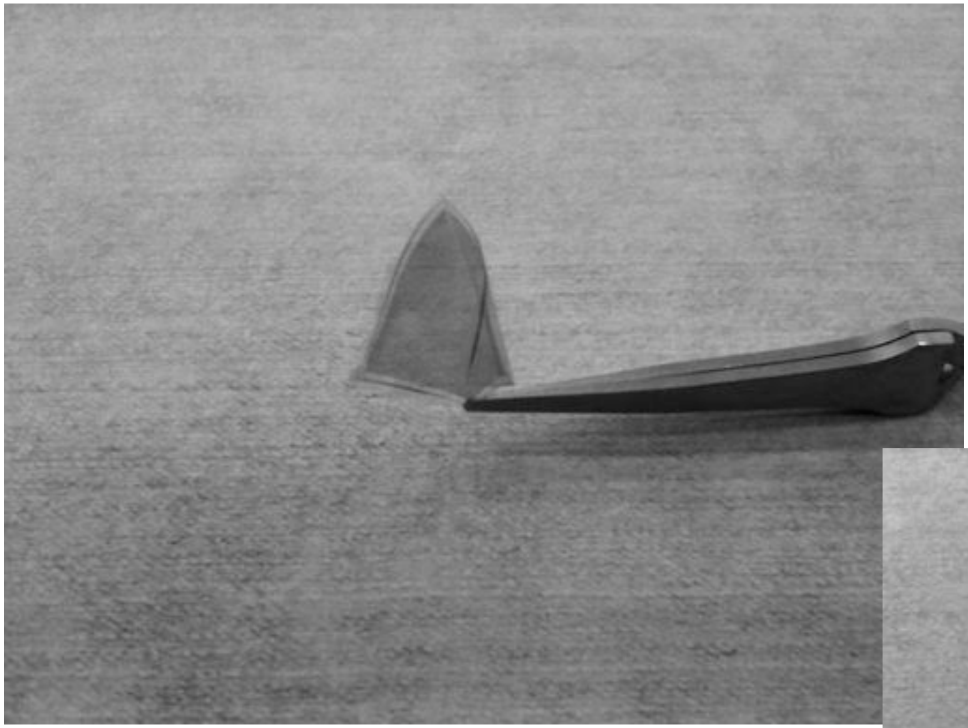

Single crystalline silicon device layers do not need to be associated with bulky rigid substrates

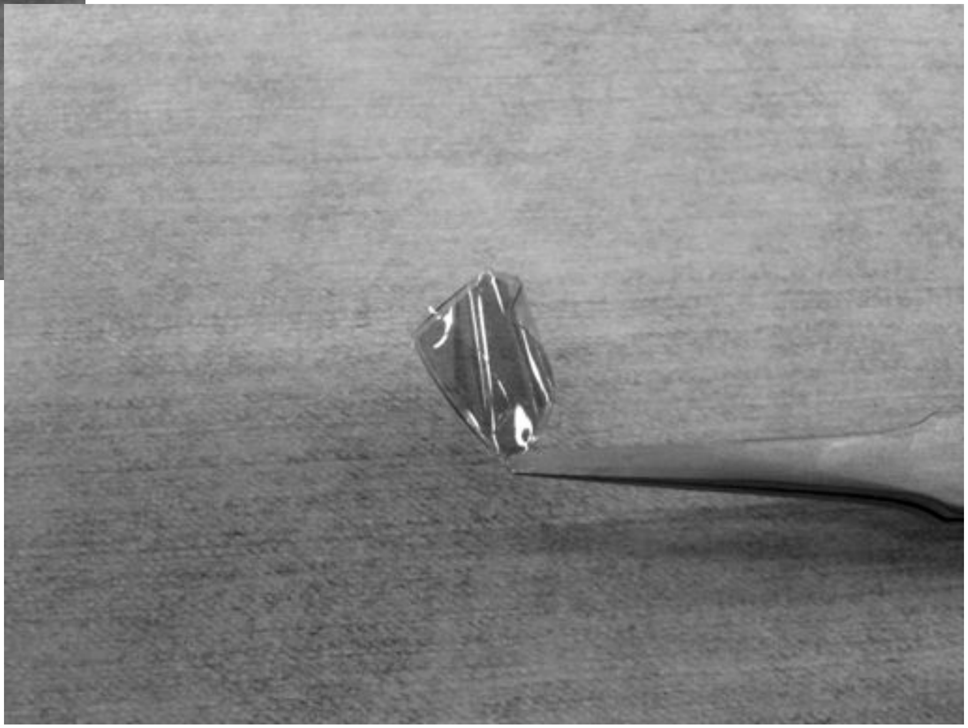

A 260nm SiNM with 20µm SU-8 substrate

WDM Si-NM Spectral Response

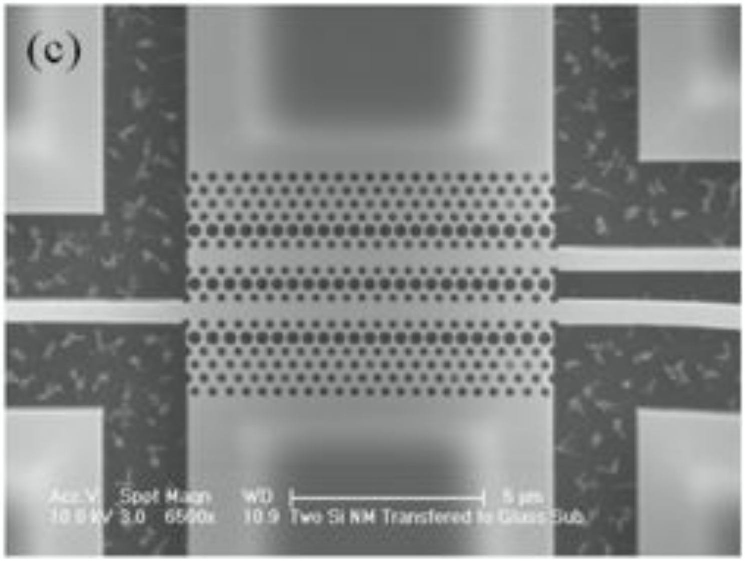

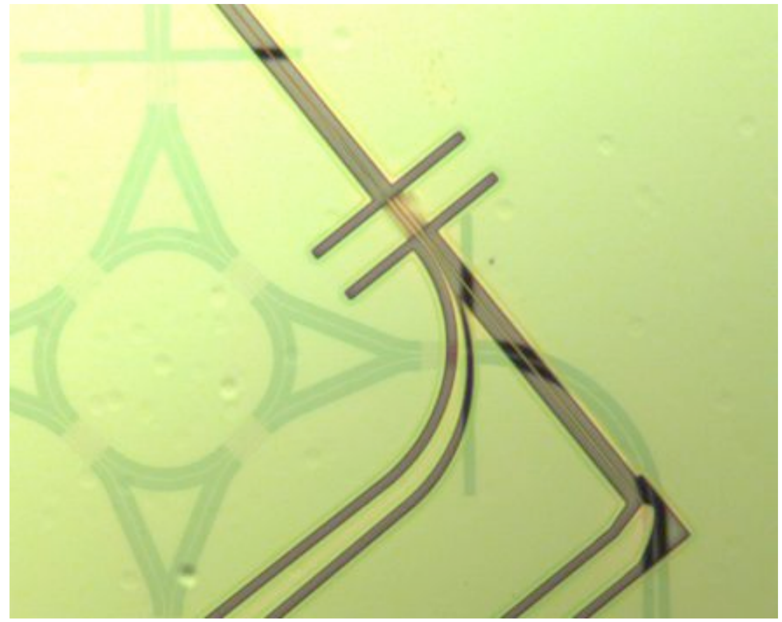

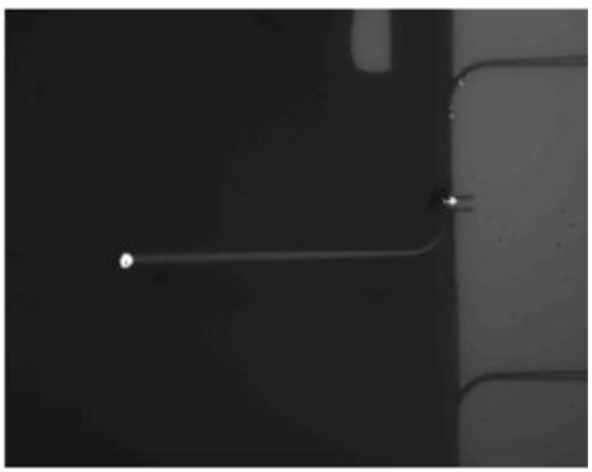

λ = 1550.0 nm

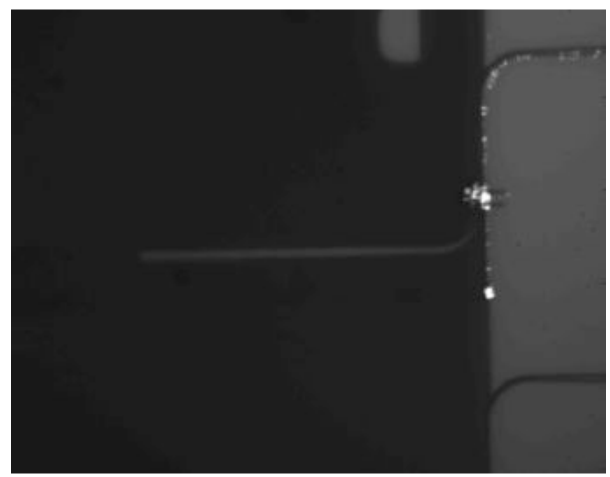

λ = 1558.0 nm

Photonic Crystal Routing Elements

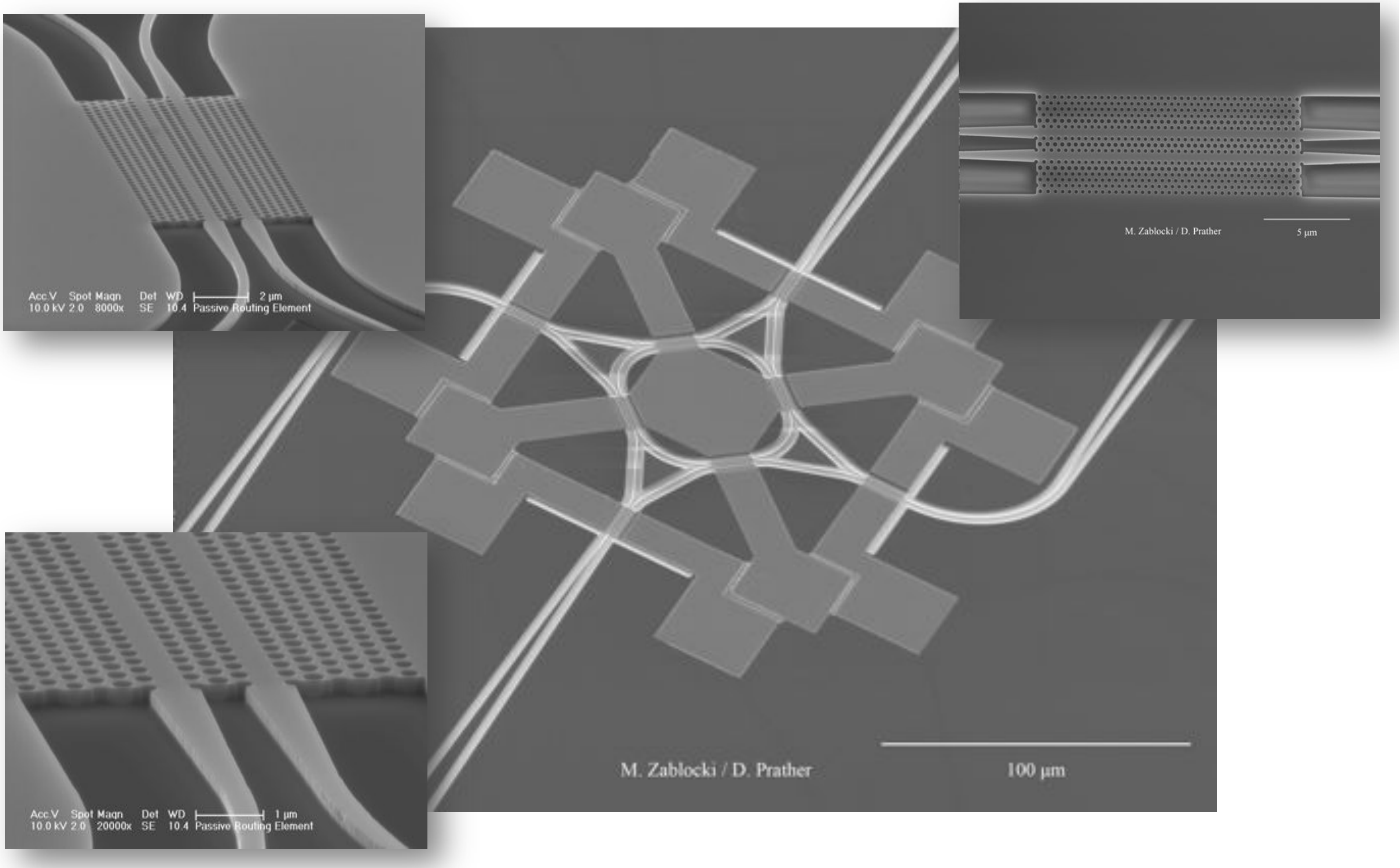

8-Port Router

The switch voltage is 1.2V with 2mA of current

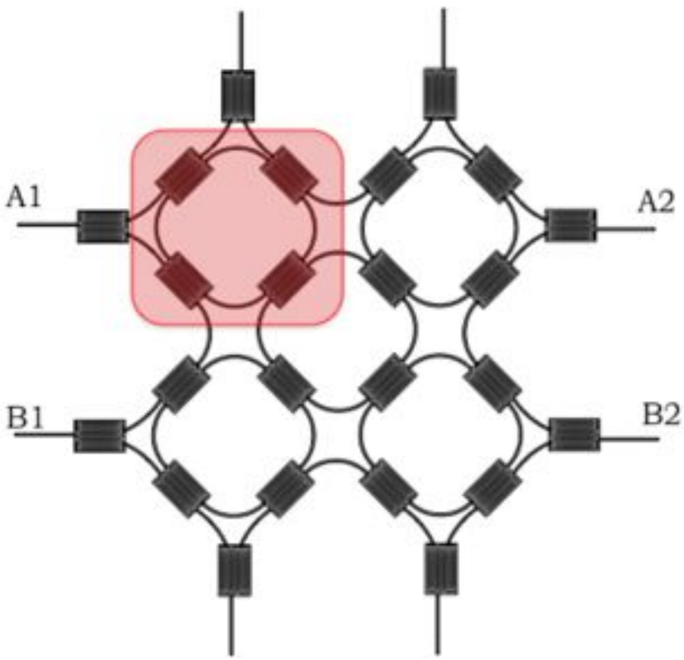

Routing Table

	A2	B2
A1	4	6
B1	6	4

Switching Table

	A2	B2
A1	0	2
B1	2	0

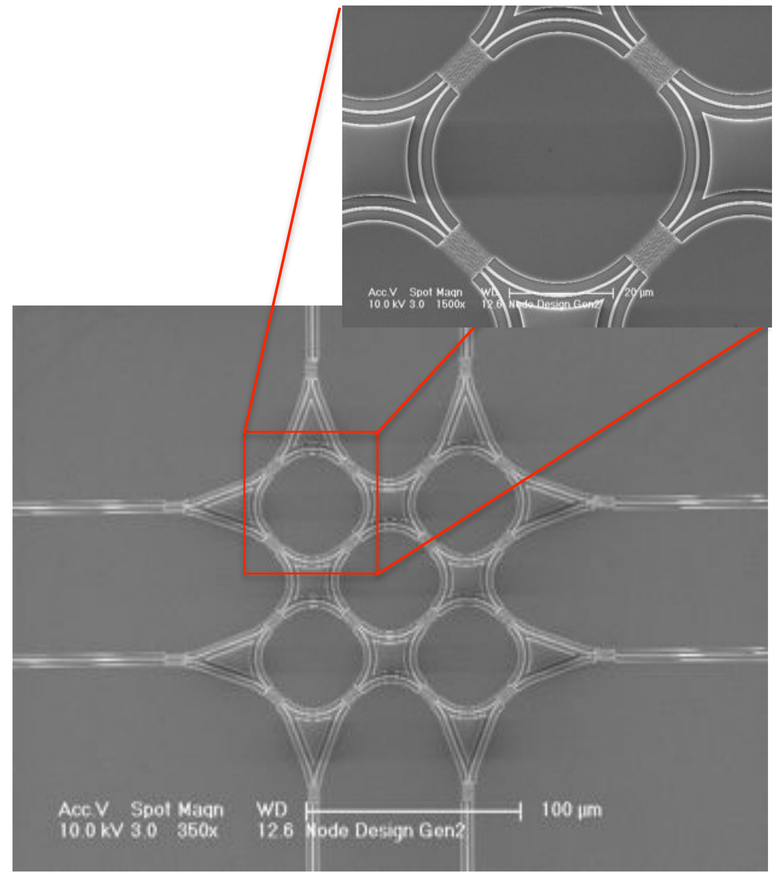

Propagation loss

	A2	B2
A1	0.16dB	0.24dB
B1	0.24dB	0.16dB

Switching Power

	A2	B2
A1	0	2mW
B1	2mW	0

Testing at Texas A&M Univ. Cyclotron

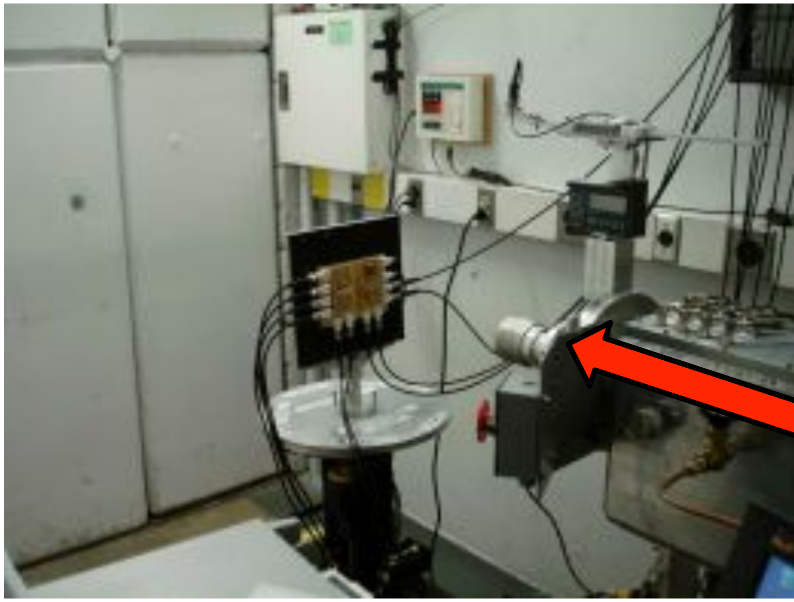

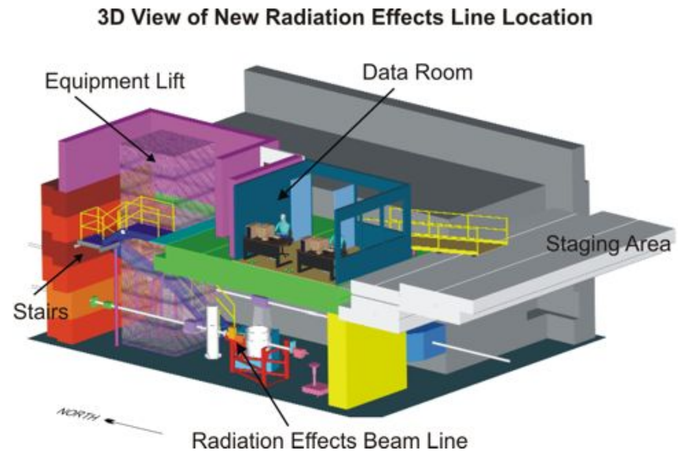

http://cyclotron.tamu.edu/ref/data_room.php

Beam Line (Proton, N, Kr)

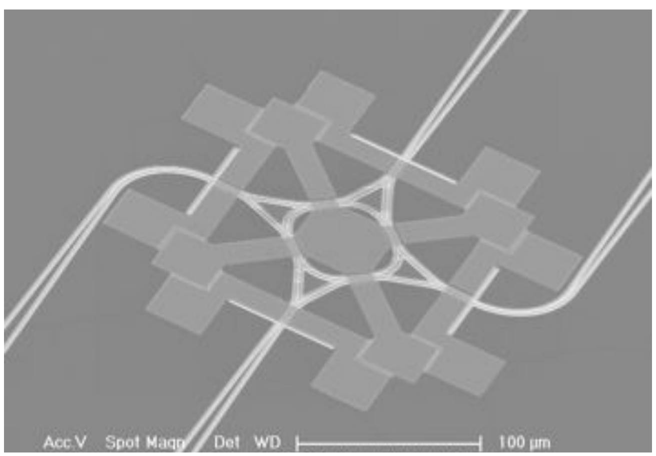

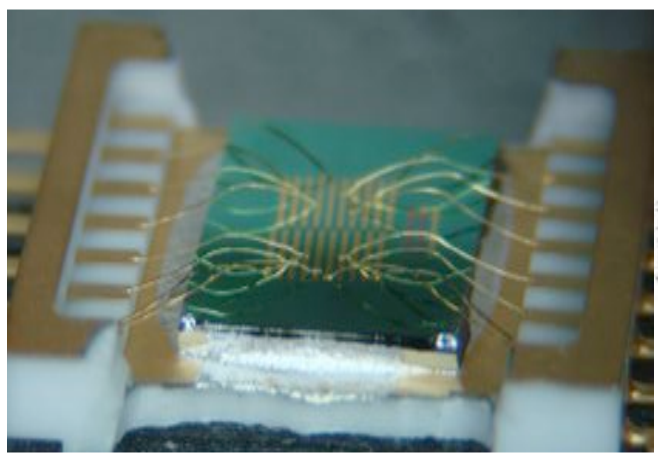

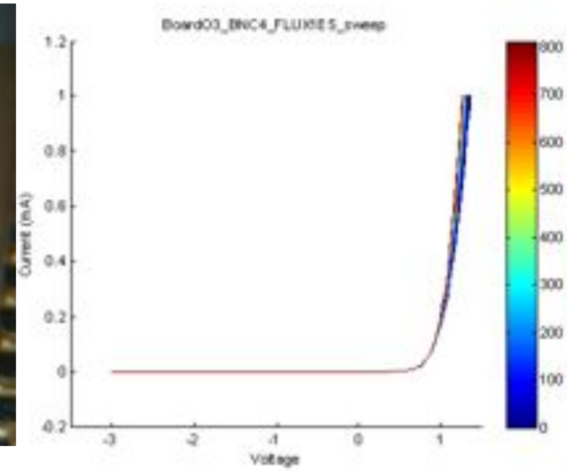

- Dosage: ^{14}N and ^{84}Kr ions at15 MeV with 6x10^{6} ions/cm^{2} Flux with total doses of 20 krad
- Minimal increase in current with set voltage exposed to LET radiation
- ~ 1% decrease in current with set voltage during sample relaxation after ion beam removed

Summary

- Presented an overview of passive RF imaging and the driving needs for advanced systems
- Discussed the realization of ultra high bandwidth optical phase modulators
- Looked at the application of ultra-wideband RF frequency synthesis and linear RF detection
- Discussed nanomembrane integration an RF signal router for multi-functional RF systems
- Thank You!